

# A theory for the zeros of Riemann $\zeta$ and other $L$ -functions (updated)

Guilherme Franca\* and André LeClair†

*Cornell University, Physics Department, Ithaca, New York 14850 USA*

In these lectures we first review the important properties of the Riemann  $\zeta$ -function that are necessary to understand the nature and importance of the Riemann hypothesis (RH). In particular this first part describes the analytic continuation, the functional equation, trivial zeros, the Euler product formula, Riemann's main result relating the zeros on the critical strip to the distribution of primes, the exact counting formula for the number of zeros on the strip  $N(T)$ , and the GUE statistics of the zeros on the critical line. We then turn to presenting some new results obtained in the past year and describe several strategies towards proving the RH. First we describe an electrostatic analogy and argue that if the electric potential along the line  $\Re(z) = 1$  is a regular alternating function, the RH would follow. The main new result is that the zeros on the critical line are in one-to-one correspondence with the zeros of the cosine function, and this leads to a transcendental equation for the  $n$ -th zero on the critical line that depends only on  $n$ . If there is a unique solution to this equation for every  $n$ , denoting  $N_0(T)$  the number of zeros on the critical line, then  $N_0(T) = N(T)$ , i.e. all zeros are on the critical line. These results are generalized to two infinite classes of functions, Dirichlet  $L$ -functions and  $L$ -functions based on modular forms. We present extensive numerical analysis of the solutions of these equations. We apply these methods to the Davenport-Heilbronn  $L$ -function, which is known to have zeros off of the line, and explain why the RH fails in this case. We also present a new approximation to the  $\zeta$ -function that is analogous to the Stirling approximation to the  $\Gamma$ -function.

In this updated version of these lectures, we removed some incorrect comments concerning  $\arg \zeta(\frac{1}{2} + iy)$ , and added references to subsequent publications, the most recent in 2024 which made some progress on some open questions posed in the previous version from 10 years ago.

Lectures delivered by A. LeClair at Riemann Master School on  $\zeta$ eta Functions  
Riemann Center, Hanover, Germany, June 10-14, 2014

---

Original version: July 2014; Updated version: August 2024

\* guifranca@gmail.com

† andre.leclair@cornell.edu

## CONTENTS

I. Introduction	4
II. Riemann $\zeta$ in quantum statistical mechanics and physics based approaches	7
A. The quantum theory of light: physical derivation of the functional equation	8
B. Bose-Einstein condensation and the pole of $\zeta$	11
III. Important properties of $\zeta$	11
A. Series representation	11
B. Convergence	13
C. The golden key: Euler product formula	13
D. The Dirichlet $\eta$ -function	14
E. Analytic continuation	15
F. Functional equation	17
G. Trivial zeros and specific values	19
IV. Gauss and the prime number theorem	21
V. Riemann zeros and the primes	22
A. Riemann's main result	22
B. $\psi(x)$ and the Riemann zeros	24
C. $\pi(x)$ and the Riemann zeros	26
VI. An electrostatic analogy	27
A. The electric field	27
B. The electric potential $\Phi$	30
C. Analysis	33
VII. Transcendental equations for zeros of the $\zeta$ -function	34
A. Asymptotic equation satisfied by the $n$ -th zero on the critical line	34
B. Exact equation satisfied by the $n$ -th zero on the critical line	38
C. A more general equation	40
D. On possible zeros off of the line	42
E. Further remarks	43
VIII. The argument of the Riemann $\zeta$ -function	44
IX. Zeros of Dirichlet $L$ -functions	49
A. Some properties of Dirichlet $L$ -functions	49
B. Exact equation for the $n$ -th zero	52
C. Asymptotic equation for the $n$ -th zero	54

	3
D. Counting formulas	54
X. Zeros of $L$ -functions based on modular forms	56
XI. The Lambert $W$ -function	58
XII. Approximate zeros in terms of the Lambert $W$ -function	61
A. Explicit formula	61
B. Further remarks	63
XIII. Numerical analysis: $\zeta$ -function	64
XIV. GUE statistics	66
XV. Prime number counting function revisited	68
XVI. Solutions to the exact equation	69
XVII. Numerical analysis: Dirichlet $L$ -functions	70
XVIII. Modular $L$ -function based on Ramanujan $\tau$	72
A. Definition of the function	73
B. Numerical analysis	74
XIX. Counterexample of Davenport-Heilbronn	75
XX. Saddle point approximation	79
XXI. Discussion and open problems	82
Acknowledgments	84
A. The Perron formula	85
B. Counting formula on the entire critical strip	85
C. Mathematica code	88
References	90

## I. INTRODUCTION

Riemann's zeta function  $\zeta(z)$  plays a central role in many areas of mathematics and physics. It was present at the birth of Quantum Mechanics, where the energy density of photons at finite temperature is proportional to  $\zeta(4)$  [1]. In mathematics, it is at the foundations of analytic number theory.

Riemann's major contribution to number theory was an explicit formula for the arithmetic function  $\pi(x)$ , which counts the number of primes less than  $x$ , in terms of an infinite sum over the non-trivial zeros of the  $\zeta(z)$  function, i.e. roots  $\rho$  of the equation  $\zeta(z) = 0$  on the *critical strip*  $0 \leq \Re(z) \leq 1$  [2]. It was later proven by Hadamard and de la Vallée Poussin that there are no zeros on the line  $\Re(z) = 1$ , which in turn proved the prime number theorem  $\pi(x) \sim \text{Li}(x)$ ; see section XV for a review. Hardy proved that there are an infinite number of zeros on the *critical line*  $\Re(z) = \frac{1}{2}$ . The *Riemann hypothesis* (RH) was his statement, in 1859, that all zeros on the critical strip have  $\Re(\rho) = \frac{1}{2}$ . Despite strong numerical evidence of its validity, it remains unproven to this day. Some excellent introductions to the RH are [3–5]. In this context, the common convention is that the argument of  $\zeta$  is  $s = \sigma + it$ . Throughout these lectures, the argument of  $\zeta$  will instead be denoted as  $z = x + iy$ , zeros will be denoted as  $\rho$ , and zeros on the positive critical line will be denoted as  $\rho_n = \frac{1}{2} + iy_n$  for  $n = 1, 2, \dots$ .

The aim of these lectures is clear from the Table of Contents. Not all the material was actually lectured on, since the topics in some of the first sections were covered by other lecturers in the school. There are two main components. Section II reviews the most important applications of  $\zeta$  to quantum statistical mechanics, and discusses other physics-based approaches, but is not necessary for understanding the rest of the lectures. The following three sections review the most important properties of Riemann's zeta function. This introduction to  $\zeta$  is self-contained, and describes all the necessary ingredients to understand the importance of the Riemann zeros and the nature of the Riemann hypothesis, and may perhaps be more accessible to mathematical physicists than the more advanced mathematics literature. The remaining sections present new work carried out over the past year. Sections VI–IX are based on the published works [6, 7]. The main new result is a transcendental equation satisfied by individual zeros of  $\zeta$  and other  $L$ -functions. These equations provide a novel characterization of the zeros, hence the title “A theory for the zeros of Riemann  $\zeta$  and other  $L$ -functions”. Sections VIII, XIX and XX contain additional results that have not been previously published.

Let us summarize some of the main points of the material presented in the second half of these lectures. It is difficult to visualize a complex function since it is a hypersurface in a 4-dimensional space. We present one way to visualize the RH based on an electrostatic analogy. From the real and imaginary parts of the function  $\xi(z)$  defined in (94) we construct a 2-dimensional vector field  $\vec{E}$  in section VI. By virtue of the Cauchy-Riemann equations, this field satisfies the conditions of an electrostatic field with no sources. It can be written as the

gradient of an electric potential  $\Phi(x, y)$ , and visualization is reduced to one real function over the 2-dimensional complex plane. We argue that if the real potential  $\Phi$  along the line  $\Re(z) = 1$  alternates between positive and negative values in the most regular manner possible, then the RH would appear to be true. Asymptotically one can analytically understand this regular alternating behavior, however the asymptotic expansion is not controlled enough to rule out zeros off the critical line.

The primary new result is described in section VII. There we present the equation (138) which is a transcendental equation for the ordinate of the  $n$ -th zero on the critical line.<sup>1</sup> These zeros are in one-to-one correspondence with the zeros of the cosine function. This equation involves two terms, a smooth one from  $\log \Gamma$  and a small fluctuating term involving  $\arg \zeta\left(\frac{1}{2} + iy\right)$ , i.e. the function commonly referred to as  $S(y)$  (125). If the small term  $S(y)$  is neglected, then there is a solution to the equation for every  $n$  which can be expressed explicitly in terms of the Lambert  $W$ -function (see section XII). The equation with the  $S(y)$  term can be solved numerically to calculate zeros to very high accuracy, 1000 digits or more.

More importantly, there is a clear strategy for proving the RH based on the França-LeClair equation. It is easily stated: if there is a unique solution to (138) for each  $n$ , then the zeros can be counted along the critical line since they are enumerated by the integer  $n$ . Specifically, one can determine  $N_0(T)$  which is the number of zeros on the critical line with  $0 < y < T$  (see eq. (140)). On the other hand, there is a known expression for  $N(T)$  which counts the zeros in the entire critical strip due to Backlund; the asymptotic expansion of  $N(T)$  was known to Riemann.<sup>2</sup> We find that  $N_0(T) = N(T)$ , which indicates that all zeros are on the critical line. The proof is not complete mainly because we cannot establish that there is a unique solution to (138) for every positive integer  $n$  due to the fluctuating behavior of the function  $S(y)$ . Nevertheless, we argue that the  $\delta \rightarrow 0^+$  prescription smooths out the discontinuities of  $S(y)$  sufficiently such that there are unique solutions for every  $n$ . There is extensive numerical evidence that this is indeed the case, presented in sections XIII, XIV, and XVI.

Understanding the properties of  $\arg \zeta\left(\frac{1}{2} + iy\right)$  is crucial to our construction, and section VIII is devoted to it.

$L$ -functions are generalizations of the Riemann  $\zeta$ -function, the latter being the trivial case [8]. It is straightforward to extend the results for  $\zeta$  to two infinite classes of important  $L$ -functions, the Dirichlet  $L$ -functions and  $L$ -functions associated with cusp (modular) forms. The former have applications primarily in multiplicative number theory, whereas the latter in additive number theory. These functions can be analytically continued to the entire (upper half) complex plane. The *Generalized Riemann Hypothesis* and *Grand Riemann Hypothesis* refers to these classes of functions. These would also follow if there were a unique solution for each  $n$  of the appropriate transcendental equation, which we present below.

---

<sup>1</sup>*Note added:* We will sometimes refer to this equation as the França-LeClair equation [7].

<sup>2</sup>Riemann only presented the asymptotic limit of  $N(T)$  as  $T \rightarrow \infty$ , but must have known the exact formula eventually written by Backlund.

There is a well-known counterexample to the RH which is based on the Davenport-Heilbronn function. It is an  $L$ -series that is a linear combination of two Dirichlet  $L$ -series, that also satisfies a functional equation. It has an infinite number of zeros on the critical line, but also zeros off of it, thus violating the RH. It is therefore interesting to apply our construction to this function. One finds that the zeros on the line do satisfy a transcendental equation, where again the solutions are enumerated by an integer  $n$ . However for some  $n$  there is no solution, and this happens precisely where there are zeros off of the line. This can be traced to the behavior of the analog of  $S(y)$ , which changes branch at these points. Nevertheless the zeros off the line continue to satisfy our general equation (148).

The final topic concerns a new approximation for  $\zeta$ . Stirling's approximation to  $n!$  is extremely useful; much of statistical mechanics would be impossible without it. Stirling's approximation to  $\Gamma(n) = (n - 1)!$  is a saddle point approximation, or steepest decent approximation, to the integral representation for  $\Gamma$  when  $n$  is real and positive. However since  $\Gamma(z)$  is an analytic function of the complex variable  $z$ , Stirling's approximation extends to the entire complex plane for  $z$  large. We describe essentially the same kind of analysis for the  $\zeta$  function. Solutions to the saddle point equation are explicit in terms of the Lambert  $W$ -function. The main complication compared to  $\Gamma$  is that one must sum over more than one branch of the  $W$ -function, however the approximation is quite good.

**Note added 1.** Since these are unpublished lectures, we took the liberty to update them now 10 years later. We removed some incorrect comments about the behavior of the argument of  $\zeta(\frac{1}{2} + iy)$ , the notorious “ $S(t)$ ”, about which we were somewhat naive at the time due to our limited background in Analytic Number Theory.<sup>3</sup> This is the only significant modification of the original content, which is in section VIII, apart from some corrected typos. The more important changes are additional remarks concerning work done by us subsequent to the 2014 lectures [9], and some followup work done in collaboration with Giuseppe Mussardo [10–15]. The latest articles [14, 15] only appeared this year of 2024. The latter works are progresses on some of the open questions raised in this original lectures from 2014. However, we do not review these new works in any detail in this update, but rather comment on them mostly in the final discussion section XXI. These additional remarks are highlighted throughout such that the reader can easily spot them.<sup>4</sup> ▲

---

<sup>3</sup>We originally thought that our  $\arg \zeta(\frac{1}{2} + iy)$  on the zeros was not identical to the standard definition of  $S(t = y)$  from piecewise integration. Furthermore, we were misled by numerical studies that that did not go high enough up the critical line to observe the extremely slow growth of  $\arg \zeta(\frac{1}{2} + iy)$ , which is roughly  $\log \log y$ .

<sup>4</sup>Additional references can be found in the published versions of these articles and others mentioned in this updated version of the lectures.

## II. RIEMANN $\zeta$ IN QUANTUM STATISTICAL MECHANICS AND PHYSICS BASED APPROACHES

In this section we describe some significant occurrences of Riemann's zeta function in the quantum statistical mechanics of free gases. We also discuss approaches to the RH based on Brownian Motion in one spatial dimension, or Random Walks. For other interesting connections of the RH to physics see [16, 17] (and references therein). One prominent idea is the Hilbert-Pólya conjecture, where they suggested that for zeros expressed in the form  $\rho_n = \frac{1}{2} + iy_n$ , the  $y_n$  are the real eigenvalues of a hermitian operator, perhaps an unknown quantum mechanical Hamiltonian. Most of this literature are variations of Berry-Keating's Hamiltonian  $H = xp$  [18, 19], and we do not include these ideas in these review lectures. We refer the reader to various reviews such as [17]. But it is fair to say that such a Hamiltonian has remained elusive in its specifics, and it is not at all clear if it exists as a bound state problem in Quantum Mechanics.

**Note added 2.** Recently we proposed that the Riemann zeros arise as quantized energies of a scattering problem in Quantum Mechanics, rather than a bound state problem. Although this is not what was presumably envisioned by Hilbert-Pólya, it is in a similar spirit and we believe is the proper version of the Hilbert-Pólya conjecture. We defined a model of particles scattering about a circle of impurities [14], where each impurity is associated with a scattering phase such that the S-matrix is unitary. This relates to the Hilbert-Pólya conjecture since roughly speaking  $S = e^{-iH}$ , where  $H$  is a hermitian Hamiltonian, thus  $S^\dagger S = 1$ .<sup>5</sup> In this model the Riemann zeros on the critical line arise from a Bethe-ansatz equation which is readily solved for the *exact* Riemann zeros. The spectral flow for these eigen-energies was studied in [15], where it was argued that the scattering problem necessarily has real eigenvalues since the S-matrix is unitary, and this would imply the Riemann Hypothesis is true. Further remarks are in the last discussion section XXI. ▲

**Note added 3.** Another approach to proving the RH based on physical ideas involves Brownian Motion or Random Walks [9, 11–13]. There it was argued that certain sums of non-principal Dirichlet characters over prime numbers behave like Brownian motion in one spatial dimension. Namely they behave as independent, identically distributed random variables, hence the central limit theorem applies. In this approach, the significance of the critical line  $\Re(z) = \frac{1}{2}$  is identical to the universal critical exponent 1/2 for the standard deviation  $N^{1/2}$  for  $N$  steps.<sup>6</sup> If this is the case, then the Euler product converges to the right of the critical line and this would also establish the validity of the RH for these  $L$ -functions. In this approach the random matrix (GUE) statistics reviewed below is intimately related to this Brownian motion. These Brownian motion arguments also extend to  $L$ -functions based on

<sup>5</sup>This is an over-simplification since one actually needs to consider a time-ordered exponential.

<sup>6</sup> $\frac{1}{2} = 1/2!$  However this by itself is not very meaningful since the  $L$  functions can easily be redefined to shift the critical line, whereas the random walk exponent 1/2 is universal. For instance, for  $L$ -functions based on cusp forms of weight  $k$ , the critical line is  $\Re(z) = k/2$ .

cuspidal forms [9]. For the principal Dirichlet  $L$  functions, such as  $\zeta(z)$  itself, these random walk ideas also apply [13] when one considers Möbius inversion for  $1/\zeta(z)$ . An extensive battery of statistical tests on such series were performed in [13] and rather convincing evidence was presented that non-principal Dirichlet characters  $\chi(p)$  where  $p$  is prime, or Möbius  $\mu$  over the integers, can out-perform current random number generators. The main obstruction for proving the RH is that pseudo-randomness of the primes is difficult to formulate rigorously, except perhaps along the lines just stated based on the Dirichlet characters. Assuming the particular series involved are indeed random walks, then the Riemann Hypothesis can only be proven *almost surely* in probability theory, namely with probability equal to 1, and this is somewhat of a brick wall toward proving that it is *surely true*. ▲

### A. The quantum theory of light: physical derivation of the functional equation

Perhaps the most important application of Riemann's zeta function in physics occurs in quantum statistical mechanics. One may argue that Quantum Mechanics was born in Planck's seminal paper on black body radiation [1], and  $\zeta$  was present at this birth; in fact his study led to the first determination of the fundamental Planck constant  $h$ , or more commonly  $\hbar = h/2\pi$ .

In order to explain discrepancies between the spectrum of radiation in a cavity at temperature  $T$  and the prediction of classical statistical mechanics, Planck proposed that the energy of radiation was "quantized", i.e. took on only the discrete values  $\hbar\omega_{\mathbf{k}}$ , where  $\mathbf{k}$  is the wave-vector, or momentum, and  $\omega_{\mathbf{k}} = |\mathbf{k}|$ . It is now well understood that these quantized energies are those of real light particles called photons. The following integral, related to the energy density of photons, appears in Planck's paper:

$$\frac{8\pi h}{c^3} \int_0^\infty \frac{\nu^3 d\nu}{e^{h\nu/k} - 1} = \frac{8\pi h}{c^3} \int_0^\infty \nu^3 (e^{-h\nu/k} + e^{-2h\nu/k} + e^{-3h\nu/k} + \dots) d\nu. \quad (1)$$

He then proceeds to evaluate this expression by termwise integration and writes

$$\frac{8\pi h}{c^3} \int_0^\infty \frac{\nu^3 d\nu}{e^{h\nu/k} - 1} = \frac{8\pi h}{c^3} \cdot 6 \left(\frac{k}{h}\right)^4 \left(1 + \frac{1}{2^4} + \frac{1}{3^4} + \frac{1}{4^4} \dots\right). \quad (2)$$

It is not clear whether Planck knew that the above sum was  $\zeta(4)$ , since he simply writes that it is approximately 1.0823 since it converges rapidly. Due to Euler, it was already known at the time that  $\zeta(4) = \pi^4/90$ .

The quantum statistical mechanics of photons leads to a physical demonstration of the most important functional equation satisfied by  $\zeta(z)$ . Consider a free quantum field theory of massless bosonic particles in  $d + 1$  spacetime dimensions with Euclidean action  $S = \int d^{d+1}x (\partial\Phi)^2$ . The geometry of Euclidean spacetime is taken to be  $S^1 \times \mathbb{R}^d$  where the circumference of the circle  $S^1$  is  $\beta$ . We will refer to the  $S^1$  direction as  $\hat{x}$ . Endow the flat



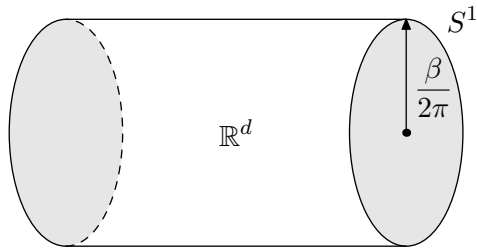


FIG. 1. Spacetime geometry for the partition function in (3).

space  $\mathbb{R}^d$  with a large but finite volume as follows. Let us refer to one of the directions perpendicular to  $\hat{x}$  as  $\hat{y}$  with length  $L$  and let the remaining  $d-1$  directions have volume  $A$ .

Let us first view the  $\hat{x}$  direction as compactified Euclidean time, so that we are dealing with finite temperature  $T = 1/\beta$  (see Figure 1). As a quantum statistical mechanical system, the partition function in the limit  $L, A \rightarrow \infty$  is

$$Z = e^{-\beta V \mathcal{F}(\beta)} \quad (3)$$

where  $V = L \cdot A$  and  $\mathcal{F}$  is the free energy density. Standard results give:

$$\mathcal{F}(\beta) = \frac{1}{\beta} \int \frac{d^d \mathbf{k}}{(2\pi)^d} \log(1 - e^{-\beta k}). \quad (4)$$

The Euclidean rotational symmetry allows one to view the above system with time now along the  $\hat{y}$  direction. In  $1d$ , interchanging the role of  $\hat{x}$  and  $\hat{y}$  is a special case of a modular transformation of the torus. In this version, the problem is a zero temperature quantum mechanical system with a finite size  $\beta$  in one direction, and the total volume of the system is  $V' = \beta \cdot A$ . The quantum mechanical path integral leads to

$$Z = e^{-L E_0(A, \beta)} \quad (5)$$

where  $E_0$  is the ground state energy. Let  $\mathcal{E}_0 = E_0/V'$  denote the ground state energy per volume. Comparing the two “channels”, their equivalence requires  $\mathcal{E}_0(\beta) = \mathcal{F}(\beta)$ . In this finite-size channel, the modes of the field in the  $\hat{x}$  direction are quantized with wave-vector  $k_x = 2\pi n/\beta$ , and the calculation of  $\mathcal{E}_0$  is as in the Casimir effect (see below):

$$\mathcal{E}_0 = \frac{1}{2\beta} \sum_{n \in \mathbb{Z}} \int \frac{d^{d-1} \mathbf{k}}{(2\pi)^{d-1}} (\mathbf{k}^2 + (2\pi n/\beta)^2)^{1/2}. \quad (6)$$

The free energy density  $\mathcal{F}$  can be calculated using

$$\int d^d \mathbf{k} = \frac{2\pi^{d/2}}{\Gamma(d/2)} \int d|\mathbf{k}| |\mathbf{k}|^{d-1}. \quad (7)$$

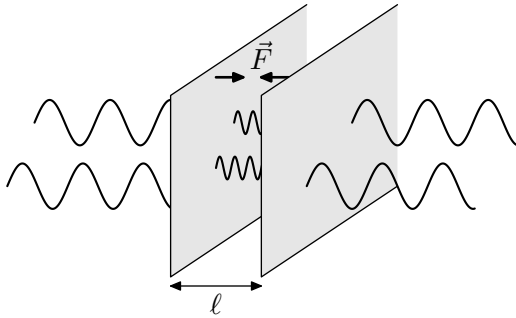


FIG. 2. Geometry of the Casimir effect.

For  $d > 0$  the integral is convergent and one finds

$$\mathcal{F} = -\frac{1}{\beta^{d+1}} \frac{\Gamma(d+1) \zeta(d+1)}{2^{d-1} \pi^{d/2} d \Gamma(d/2)}. \quad (8)$$

For the Casimir energy, after performing the  $\mathbf{k}$  integral,  $\mathcal{E}_0$  involves  $\sum_{n \in \mathbb{Z}} |n|^d$  which must be regularized. As is usually done, let us regularize this as  $2 \zeta(-d)$ . Then

$$\mathcal{E}_0 = -\frac{1}{\beta^{d+1}} \pi^{d/2} \Gamma(-d/2) \zeta(-d). \quad (9)$$

Let us analytically continue in  $d$  and define the function

$$\chi(z) \equiv \pi^{-z/2} \Gamma(z/2) \zeta(z). \quad (10)$$

Then the equality  $\mathcal{E}_0 = \mathcal{F}$  requires the identity

$$\chi(z) = \chi(1-z). \quad (11)$$

The above relation is a known functional identity that was proven by Riemann using complex analysis. It will play an essential role in the rest of these lectures.

The above calculations show that  $\zeta$ -function regularization of the ground state energy  $\mathcal{E}_0$  is consistent with a modular transformation to the finite-temperature channel. Our calculations can thus be viewed as a proof of the identity (11) based on physical consistency.

For spatial dimension  $d = 3$ , the ground state energy  $\mathcal{E}_0$  is closely related to the measurable Casimir effect, the difference only being in the boundary conditions. In the Casimir effect one measures the ground state energy of the electromagnetic field between two plates by measuring the force as one varies their separation, as illustrated in Figure 2.

There is a simple relation between the vacuum energy densities  $\rho$  in the cylindrical geometry above, and that of the usual Casimir effect:

$$\rho_{\text{vac}}^{\text{casimir}}(\ell) = 2\rho_{\text{vac}}^{\text{cylinder}}(\beta = 2\ell) = -\frac{\pi^2}{720\ell^4}. \quad (12)$$

It is remarkable that since the Casimir effect has been measured in the laboratory, such a measurement verifies

$$\zeta(-3) = 1 + 2^3 + 3^3 + 4^3 + \dots = \frac{1}{120}. \quad (13)$$

Of course the above equation is non-sense on its own. It only makes sense after analytically continuing  $\zeta(z)$  from  $\Re(z) > 1$  to the rest of the complex plane.

### B. Bose-Einstein condensation and the pole of $\zeta$

It is known that  $\zeta(z)$  has only one pole, a simple one at  $z = 1$ . This property is also related to some basic physics. In the phenomenon of Bose-Einstein condensation, below a critical temperature  $T$  all of the bosonic particles occupy the lowest energy single particle state. This critical temperature depends on the density  $n$ . In  $d$  spatial dimensions the formula reads

$$n = \int \frac{d^d \mathbf{k}}{(2\pi)^d} \frac{1}{e^{\omega_{\mathbf{k}}/T} - 1} = \left( \frac{mT}{2\pi} \right)^{d/2} \zeta(d/2). \quad (14)$$

The Coleman-Mermin-Wagner theorem in statistical physics says that Bose-Einstein condensation is impossible in  $d = 2$  spatial dimensions. This is manifest in the above formula since  $\zeta(1) = \infty$ .

## III. IMPORTANT PROPERTIES OF $\zeta$

After having discussed some applications of  $\zeta$  in physics, let us now focus on its most basic mathematical properties as a complex analytic function.

### A. Series representation

The  $\zeta$ -function is defined for  $\Re(z) > 1$  through the series

$$\zeta(z) = \sum_{n=1}^{\infty} \frac{1}{n^z}. \quad (15)$$

The first appearance of  $\zeta(z)$  was in the so called ‘‘Basel problem’’ posed by Pietro Mengoli in 1644. This problem consists in finding the precise sum of the infinite series of squares of natural numbers:

$$\zeta(2) = \sum_{n=1}^{\infty} \frac{1}{n^2} = \frac{1}{1^2} + \frac{1}{2^2} + \frac{1}{3^2} + \dots = ? \quad (16)$$

The leading mathematicians of that time, like the Bernoulli family, attempted the problem unsuccessfully. It was only in 1735 that Euler, only 28 years old, solved the problem claiming that such sum is equal to  $\pi^2/6$ , and was brought to fame. Nevertheless, his arguments were

not fully justified, as he manipulated infinite series with abandon, and it was only in 1741 that Euler could provide a formal proof. Even such a proof had to wait 100 years until all the steps could be rigorously justified by the Weierstrass factorization theorem. Just out of curiosity let us reproduce Euler's steps. From the Taylor series of  $\sin z$  we have

$$\frac{\sin \pi z}{\pi z} = 1 - \frac{(\pi z)^2}{3!} + \frac{(\pi z)^4}{5!} + \dots . \quad (17)$$

From the Weierstrass product formula for the  $\Gamma(z)$  function it is possible to obtain the product formula for  $\sin z$  which reads

$$\frac{\sin \pi z}{\pi z} = \prod_{n=1}^{\infty} \left( 1 - \left( \frac{z}{n} \right)^2 \right). \quad (18)$$

Now collecting terms of powers of  $z$  in (18) one finds

$$\frac{\sin \pi z}{\pi z} = 1 - z^2 \sum_{n=1}^{\infty} \frac{1}{n^2} + z^4 \sum_{\substack{n,m=1 \\ m>n}}^{\infty} \frac{1}{n^2 m^2} + \dots . \quad (19)$$

Comparing the  $z^2$  coefficient of (19) and (17) we immediately obtain Euler's result,

$$\zeta(2) = \sum_{n=1}^{\infty} \frac{1}{n^2} = \frac{\pi^2}{6}. \quad (20)$$

Comparing the  $z^4$  coefficients we have

$$\sum_{\substack{n,m=1 \\ m>n}}^{\infty} \frac{1}{n^2 m^2} = \frac{\pi^4}{5!}. \quad (21)$$

Now consider the full range sum

$$\sum_{n,m=1}^{\infty} \frac{1}{n^2 m^2} = \sum_{n=1}^{\infty} \frac{1}{n^4} + \sum_{\substack{n,m=1 \\ m>n}}^{\infty} \frac{1}{n^2 m^2} + \sum_{\substack{n,m=1 \\ m<n}}^{\infty} \frac{1}{n^2 m^2}. \quad (22)$$

The LHS is nothing but  $\zeta^2(2)$ . The first term in the RHS is  $\zeta(4)$  and the two other terms are both equal to (21). Therefore we have

$$\zeta(4) = \sum_{n=1}^{\infty} \frac{1}{n^4} = \frac{\pi^4}{90}. \quad (23)$$

Considering the other powers  $z^{2n}$  we can obtain  $\zeta(2n)$  for even integers. We will see later a better approach to compute these values through an interesting relation with the Bernoulli numbers. For positive odd integer  $n$ ,  $\zeta(n)$  has no such simple expression, and this is related to its pole at  $n = 1$ .

## B. Convergence

Let us now analyze the domain of convergence of the series (15). Absolute convergence implies convergence, therefore it is enough to consider

$$\sum_{n=1}^{\infty} \frac{1}{|n^z|} = \sum_{n=1}^{\infty} \frac{1}{n^x}, \quad (24)$$

where  $z = x + iy$ . Let  $x = 1 + \delta$  with  $\delta > 0$ . By the integral test we have

$$\int_1^{\infty} \frac{1}{u^{1+\delta}} du = -\frac{1}{\delta u^{\delta}} \Big|_1^{\infty} = \frac{1}{\delta}. \quad (25)$$

If  $\delta > 0$  the above integral is finite, therefore the series is absolutely convergent for  $\Re(z) > 1$  and  $\zeta(z)$  is an analytic function on this region. Note that if  $\delta = 0$  the above integral diverges as  $\log(\infty)$ . If  $\delta \leq -1$  the integral also diverges. Therefore, the series representation given by (15) is defined only for  $\Re(z) > 1$ .

## C. The golden key: Euler product formula

The importance of the  $\zeta$ -function in number theory is mainly because of its relation to prime numbers. The first one to realize this connection was again Euler. To see this, let us consider the following product

$$\prod_{i=1}^{\infty} \left(1 - \frac{1}{p_i^z}\right)^{-1} \quad (26)$$

where  $p_i$  denotes a prime number, i.e.  $p_1 = 2$ ,  $p_2 = 3$  and so on. We know that  $(1 - z)^{-1} = \sum_{n=0}^{\infty} z^n$  for  $|z| < 1$ , thus (26) is equal to

$$\prod_{i=1}^{\infty} \sum_{n=0}^{\infty} \frac{1}{p_i^{nz}} = \left(1 + \frac{1}{p_1^z} + \frac{1}{p_1^{2z}} + \dots\right) \times \left(1 + \frac{1}{p_2^z} + \frac{1}{p_2^{2z}} + \dots\right) \times \dots \quad (27)$$

If we open the product in (27) we have an infinite sum of terms, each one having the form

$$\left(p_1^{\alpha_1} p_2^{\alpha_2} \dots p_j^{\alpha_j}\right)^{-z} \quad \text{where } j = 1, 2, \dots \text{ and } \alpha_j = 0, 1, 2, \dots, \quad (28)$$

i.e. we have a finite product of primes raised to every possible power. From the fundamental theorem of arithmetic, also known as the unique prime factorization theorem, we know that every natural number can be expressed in exactly one way through a product of powers of primes;  $n = p_1^{\alpha_1} p_2^{\alpha_2} \dots p_j^{\alpha_j}$  where  $p_1 < p_2 < \dots < p_j$ . Therefore (27) involves a sum of all natural numbers, which is exactly the definition (15). Thus we have the very important result known as the *Euler product formula*

$$\zeta(z) = \sum_{n=1}^{\infty} \frac{1}{n^z} = \prod_{i=1}^{\infty} \left(1 - \frac{1}{p_i^z}\right)^{-1}. \quad (29)$$

This result is of course only valid for  $\Re(z) > 1$ . A simpler derivation of it is also given in section IV. From this formula we can easily see that there are no zeros in this region,

$$\zeta(z) \neq 0 \quad \text{for } \Re(z) > 1, \quad (30)$$

since each factor  $(1 - p_i^{-z})$  never diverges.

#### D. The Dirichlet $\eta$ -function

Instead of the  $\zeta$ -function defined in (15), let us consider its alternating version

$$\eta(z) = \sum_{n=1}^{\infty} \frac{(-1)^{n-1}}{n^z}. \quad (31)$$

This series is known as the *Dirichlet  $\eta$ -function*. For an alternating series  $\sum (-1)^{n-1} a_n$ , if  $\lim_{n \rightarrow \infty} a_n = 0$  and  $a_n > a_{n+1}$  then the series converges. We can see that both conditions are satisfied for (31) provided that  $\Re(z) > 0$ .

The  $\eta$ -function (31) has a negative sign at even naturals:

$$\eta(z) = 1 - \frac{1}{2^z} + \frac{1}{3^z} - \frac{1}{4^z} + \dots. \quad (32)$$

On the other hand the  $\zeta$ -function (15) has only positive signs, thus if we multiply it by  $2/2^z$  we double all the even naturals appearing in (32) but with a positive sign

$$\frac{2}{2^z} \zeta(z) = \frac{2}{2^z} + \frac{2}{4^z} + \frac{2}{6^z} + \dots. \quad (33)$$

Summing (32) and (33) we obtain  $\zeta(z)$  again, therefore

$$\zeta(z) = \frac{1}{1 - 2^{1-z}} \eta(z). \quad (34)$$

In obtaining this equality we had to assume  $\Re(z) > 1$ , nevertheless (31) is defined for  $\Re(z) > 0$ , thus (34) yields the analytic continuation of  $\zeta(z)$  in the region  $\Re(z) > 0$ .

### E. Analytic continuation

One of Riemann's main contributions is the analytic continuation of the  $\zeta$ -function to the entire complex plane (except for a simple pole at  $z = 1$ ). Actually, Riemann was the first one to consider the function (15) over a complex field. Following his steps, let us start from the integral definition of the  $\Gamma$ -function

$$\Gamma(z) = \int_0^{\infty} u^{z-1} e^{-u} du. \quad (35)$$

Replacing  $u \rightarrow nu$  and summing over  $n$  we have<sup>7</sup>

$$\Gamma(z) \sum_{n=1}^{\infty} \frac{1}{n^z} = \sum_{n=1}^{\infty} \int_0^{\infty} u^{z-1} e^{-nu} du. \quad (36)$$

If we are allowed to interchange the order of the sum with the integral, and noting that  $\sum_{n=1}^{\infty} e^{-nz} = (e^z - 1)^{-1}$ , then formally we have

$$\Gamma(z)\zeta(z) = \int_0^{\infty} \frac{u^{z-1}}{e^u - 1} du. \quad (37)$$

The integral in (36) converges for  $\Re(z) > 1$ . Under this condition it is possible to show that the integral (37) also converges. Thus the step in going from (36) to (37) is justified as long as we assume  $\Re(z) > 1$ .

Since the integrand in (37) diverges at  $u = 0$ , let us promote  $u$  to a complex variable and consider the following integral

$$\mathcal{J}(z) = \frac{1}{2\pi i} \int_{\mathcal{C}} \frac{u^z}{e^{-u} - 1} \frac{du}{u} \quad (38)$$

over the path  $\mathcal{C}$  illustrated in Figure 3, which excludes the origin through a circle of radius  $\delta < 2\pi$ , avoiding the pole of the integrand in (38).

On  $\mathcal{C}_1$  we choose  $u = re^{-i\pi}$  then

$$\frac{1}{2\pi i} \int_{\mathcal{C}_1} \frac{u^z}{e^{-u} - 1} \frac{du}{u} = -\frac{e^{-i\pi z}}{2\pi i} \int_{\delta}^{\infty} \frac{r^{z-1}}{e^r - 1} dr. \quad (39)$$

---

<sup>7</sup>According to Edwards book [2] this formula also appeared in one of Abel's paper and a similar one in a paper of Chebyshev. Riemann should probably be aware of this.

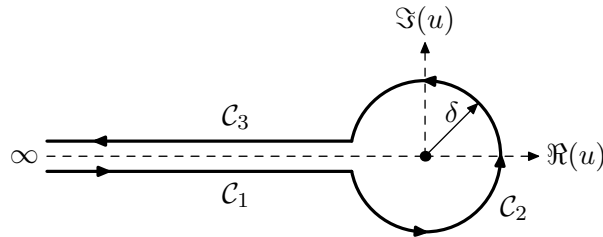


FIG. 3. Contour  $\mathcal{C} = \mathcal{C}_1 + \mathcal{C}_2 + \mathcal{C}_3$  excluding the origin.  $\mathcal{C}_2$  has radius  $\delta < 2\pi$ .

Analogously, on  $\mathcal{C}_3$  we choose  $w = re^{i\pi}$ , then we have

$$\lim_{\delta \rightarrow 0} \frac{1}{2\pi i} \left( \int_{\mathcal{C}_1} + \int_{\mathcal{C}_3} \right) \frac{u^z}{e^{-u} - 1} \frac{du}{u} = \frac{\sin \pi z}{\pi} \int_0^\infty \frac{r^{z-1}}{e^r - 1} dr. \quad (40)$$

For the integral over  $\mathcal{C}_2$  we have  $u = \delta e^{i\theta}$ , and since we are interested in  $\delta \rightarrow 0$  we obtain

$$\frac{1}{2\pi i} \int_{\mathcal{C}_2} \frac{u^z}{e^{-u} - 1} \frac{du}{u} = \frac{\delta^z}{2\pi} \int_{-\pi}^{\pi} \frac{e^{i\theta z}}{e^{-\delta e^{i\theta}} - 1} d\theta \approx -\frac{\delta^{z-1}}{2\pi} \int_{-\pi}^{\pi} e^{i\theta(z-1)} d\theta. \quad (41)$$

Thus we have

$$\left| \frac{1}{2\pi i} \int_{\mathcal{C}_2} \frac{u^z}{e^{-u} - 1} \frac{du}{u} \right| \leq \frac{\delta^{x-1}}{2\pi} \int_{-\pi}^{\pi} e^{-y\theta} d\theta = \delta^{x-1} \frac{\sinh \pi y}{\pi y}. \quad (42)$$

Since we are assuming  $x > 1$ , the above result vanishes when  $\delta \rightarrow 0$ . Therefore from (37) and (40) we conclude that

$$\zeta(z) = \frac{\pi \mathcal{J}(z)}{\Gamma(z) \sin(\pi z)}. \quad (43)$$

Using the well known identity

$$\Gamma(z)\Gamma(1-z) = \frac{\pi}{\sin(\pi z)} \quad (44)$$

we can further simplify (43) obtaining

$$\zeta(z) = \Gamma(1-z) \mathcal{J}(z). \quad (45)$$

Although in obtaining (45) we assumed  $\Re(z) > 1$ , the function  $\Gamma(z)$  and the integral (38) remains valid for every complex  $z$ . Thus we can define  $\zeta(z)$  through (45) on the whole complex plane (except at  $z = 1$  as will be shown below). Since (45) and (15) are the same on the half plane  $\Re(z) > 1$ , then (45) yields the analytic continuation of the  $\zeta$ -function to the entire complex plane. The function defined by (45) is known as the *Riemann  $\zeta$ -function*.

The integral (38) is an entire function of  $z$ , and  $\Gamma(1-z)$  has simple poles at  $z = 1, 2, \dots$ . Since  $\zeta(z)$  does not have zeros for  $\Re(z) > 1$  then  $\mathcal{J}(z)$  must vanish at  $z = 2, 3, \dots$ . In fact



it is easy to see this explicitly. Note that for  $z = n \in \mathbb{Z}$  the integral (38) over  $\mathcal{C}_1$  and  $\mathcal{C}_3$  cancel each other, thus it remains the integral over  $\mathcal{C}_2$  only. From Cauchy's integral formula we have

$$\mathcal{J}(n) = \lim_{u \rightarrow 0} \frac{u^n}{e^{-u} - 1} = 0 \quad (n = 2, 3, \dots). \quad (46)$$

Moreover, since  $\mathcal{J}(n) = 0$  for  $n \geq 2$ , cancelling the poles of  $\Gamma(1 - n)$ , the only possible pole of  $\zeta(z)$  occurs at  $z = 1$ . From (46) we have  $\mathcal{J}(1) = -1$ , showing that  $\zeta(z)$  indeed has a *simple pole* inherited from the simple pole of  $\Gamma(0)$ . Since this pole is simple, we can compute the residue of  $\zeta(1)$  through

$$\text{Res } \zeta(1) = \lim_{z \rightarrow 1} (z - 1) \zeta(z) = \lim_{z \rightarrow 1} (z - 1) \Gamma(1 - z) \mathcal{J}(z) = -\Gamma(1) \mathcal{J}(1) = 1, \quad (47)$$

where we have used (45) and the well known property  $\Gamma(z + 1) = z \Gamma(z)$ .

## F. Functional equation

The functional equation was already motivated by physical arguments in (11). Now we proceed to derive it mathematically. There are at least 7 different ways to do this [20]. We are going to present only one way, which we think is the simplest.

Let us now consider the following integral

$$\mathcal{J}_N(z) = \frac{1}{2\pi i} \oint_{\mathcal{C}_N} \frac{u^{z-1}}{e^{-u} - 1} du \quad (48)$$

with the path of integration  $\mathcal{C}_N$  as shown in Figure 4. Note that the integrand has the poles  $u_n = 2\pi n i$  ( $n \in \mathbb{Z}$ ) along the imaginary axis. On this contour  $r < 2\pi$  and  $2\pi N i < R < (2N + 2)\pi i$ , thus the annular region encloses  $2N$  poles corresponding to  $n = \pm 1, \pm 2, \dots, \pm N$ .

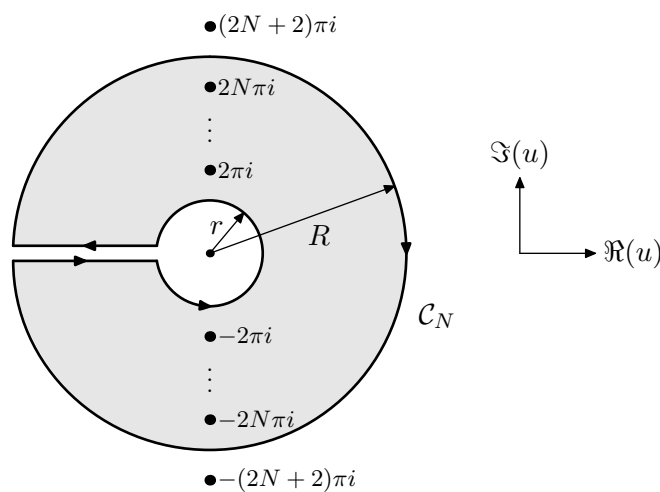


FIG. 4. Contour  $\mathcal{C}_N$  where  $r < 2\pi$  and  $2N\pi < R < (2N + 2)\pi$ . This contour encloses  $2N$  poles.

Let us first consider the integral (48) over the outer circle with radius  $R$ , i.e.  $u = Re^{i\theta}$ . Let  $g(u) = (e^{-u} - 1)^{-1}$ . The function  $g(u)$  is meromorphic, i.e. has only isolated singularities at  $u_n = 2\pi ni$ . Around the circle of radius  $R$  there are no singularities thus  $g(u)$  is bounded in this region, i.e.  $|g(u)| \leq M$ . We also have  $|u^{z-1}| = R^{x-1}e^{-\theta y} \leq R^{x-1}e^{|\theta|y}$ . Therefore

$$\left| \int_R \frac{u^{z-1}}{e^{-u} - 1} du \right| \leq \int_{-\pi}^{\pi} MR^{x-1}e^{|\theta|y} R d\theta = 2\pi MR^x e^{|\theta|y}. \quad (49)$$

Now if  $N \rightarrow \infty$  then  $R \rightarrow \infty$  and the above result goes to zero if  $x < 0$ . In this way the only contribution from the integral (48) is due to the smaller circle  $r$  and this is equal to the integral (38). Thus we conclude that

$$\lim_{N \rightarrow \infty} \mathcal{J}_N(z) = \mathcal{J}(z) \quad (\Re(z) < 0). \quad (50)$$

We can now evaluate the integral (48) through the residue theorem. The integrand is  $f(u) = u^{z-1}/(e^{-u} - 1)$ , then we have

$$\mathcal{J}_N(z) = - \sum_{n=1}^{N+1} (\text{Res}f(u_n) + \text{Res}f(u_{-n})), \quad (51)$$

where the minus sign is because the contour is traversed in the clockwise direction. The residue can be computed as follows:

$$\text{Res}f(u_n) = \lim_{u \rightarrow u_n} (u - u_n) f(u) = u_n^{z-1} \lim_{u \rightarrow u_n} \frac{u - u_n}{e^{-u} - 1} = -(2\pi ni)^{z-1}. \quad (52)$$

Therefore,

$$\mathcal{J}_N(z) = \sum_{n=1}^{N+1} (2\pi n)^{z-1} (i^{z-1} + (-i)^{z-1}) = 2(2\pi)^{z-1} \cos(\pi(z-1)/2) \sum_{n=1}^{N+1} n^{z-1}. \quad (53)$$

Now the sum in (53) becomes particularly interesting if we replace  $z \rightarrow 1 - z$ , yielding the same term  $n^{-z}$  that appears in the series of the  $\zeta$ -function. In view of (50), now valid for  $\Re(z) > 1$ , we thus have

$$\lim_{N \rightarrow \infty} \mathcal{J}_N(1 - z) = \mathcal{J}(1 - z) = 2(2\pi)^{-z} \cos(\pi z/2) \zeta(z). \quad (54)$$

Using (45) we obtain

$$\zeta(1 - z) = 2(2\pi)^{-z} \cos(\pi z/2) \Gamma(z) \zeta(z), \quad (55)$$

which relates  $\zeta(z)$  to  $\zeta(1 - z)$ . This equality can be written in a much more symmetric form

using the following two well known properties of the  $\Gamma$ -function:

$$\Gamma(z)\Gamma(1-z) = \frac{\pi}{\sin(\pi z)}, \quad (56)$$

$$\Gamma(z)\Gamma(z+1/2) = 2^{1-2z}\sqrt{\pi}\Gamma(2z). \quad (57)$$

Replacing  $z \rightarrow (z+1)/2$  in (56) and substituting into (55) we have

$$\zeta(1-z) = \frac{2(2\pi)^{-z}\pi\Gamma(z)\zeta(z)}{\Gamma((z+1)/2)\Gamma((1-z)/2)}. \quad (58)$$

Now replacing  $z \rightarrow z/2$  in (57) and substituting the term  $\Gamma(z)/\Gamma((z+1)/2)$  into the above equation we obtain

$$\chi(z) = \chi(1-z), \quad \chi(z) \equiv \pi^{-z/2}\Gamma(z/2)\zeta(z). \quad (59)$$

This equality is known as the *functional equation* for the  $\zeta$ -function. This is an amazing relation, first discovered by Riemann. In deriving (59) we had to assume  $\Re(z) > 1$ , but through analytic continuation it is valid on the whole complex plane, except at  $z = 1$  where  $\zeta(z)$  has a simple pole. Note also that replacing  $z \rightarrow 1 + 2n$  for  $n = 1, 2, \dots$  into (55) we see that  $\zeta(-2n) = 0$ , corresponding to the zeros of  $\cos(\pi/2 + n\pi)$ .

### G. Trivial zeros and specific values

We already have seen that due to the Euler product formula (29)  $\zeta(z)$  has no zeros for  $\Re(z) > 1$ . We have also seen in connection with (45) that  $\zeta(z)$  has a simple pole at  $z = 1$ . It follows from this pole that there are an infinite number of prime numbers. Moreover, due to (55) we have  $\zeta(-2n) = 0$  for  $n = 1, 2, \dots$ . These are the so called *trivial zeros*. Since there are no zeros for  $\Re(z) > 1$ , the functional equation (59) implies that there are no other zeros for  $\Re(z) < 0$ .

The other possible zeros of  $\zeta(z)$  must therefore be inside the so-called *critical strip*,  $0 \leq \Re(z) \leq 1$ . These are called the *non-trivial zeros*, since they can be complex contrary to the trivial ones. Note that from (59), since  $\Gamma(z/2)$  has no zeros on the critical strip, then  $\zeta(z)$  and  $\chi(z)$  have the same zeros on this region. Moreover, these zeros are symmetric between the line  $\Re(z) = 1/2$ . Since  $(\chi(z))^* = \chi(z^*)$  if  $\rho$  is a zero so is its complex conjugate  $\rho^*$ . Thus zeros occur in a quadruple:  $\rho, \rho^*, 1 - \rho$  and  $1 - \rho^*$ . The exception are for zeros on the so called *critical line*  $\Re(z) = 1/2$ , where  $\rho$  and  $1 - \rho^*$  coincide. It is known that there are an infinite number of zeros on the critical line. It remains unknown whether they are all simple zeros. We will discuss these non-trivial zeros in more detail later.

Now let us consider special values of the  $\zeta$ -function. Let us start by considering the negative integers  $\zeta(-n)$ . From (45) we have  $\zeta(-n) = n! \mathcal{J}(-n)$ . The integral (38) at this

point can be computed through the residue theorem. Since the only pole is at  $z = 0$  we have

$$\zeta(-n) = n! \operatorname{Res} \left( \frac{u^{-n-1}}{e^{-u} - 1} \right) \Big|_{u=0}. \quad (60)$$

The Bernoulli polynomials  $B_n(x)$  are defined through the generating function

$$\frac{ue^{xu}}{e^u - 1} = \sum_{n=0}^{\infty} \frac{B_n(x)}{n!} u^n \quad (|u| < 2\pi). \quad (61)$$

The values  $B_n \equiv B_n(0)$  are called Bernoulli numbers and defined by setting  $x = 0$  in (61). Then using (61) into (60) we have

$$\zeta(-n) = n! \operatorname{Res} \left( -u^{-n-2} \sum_{m=0}^{\infty} \frac{B_m(1)}{m!} u^m \right) \Big|_{u=0} = -\frac{B_{n+1}(1)}{n+1}. \quad (62)$$

From the well known relation  $B_n(x+1) - B_n(x) = nx^{n-1}$  for  $n \geq 1$  we have  $B_n(1) = B_n(0)$  for  $n \geq 2$ . Thus we have

$$\zeta(-n) = -\frac{B_{n+1}}{n+1} \quad (n \geq 1). \quad (63)$$

The case  $\zeta(0)$  can be obtained from (62) since  $B_1(1) = 1/2$ , then  $\zeta(0) = -1/2$ . Also, since  $B_{2n+1} = 0$  we see once again that  $\zeta(-2n) = 0$  for  $n \geq 1$ .

Setting  $z = 2k$  in (55) we have  $\zeta(1 - 2k) = 2(2\pi)^{-2k} \cos(\pi k) \Gamma(2k) \zeta(2k)$ , but from (63) we have  $\zeta(1 - 2k) = -B_{2k}/2k$ , and thus we have  $\zeta(z)$  over the positive even integers,

$$\zeta(2k) = (-1)^{k+1} \frac{(2\pi)^{2k} B_{2k}}{2(2k)!} \quad (k \geq 1). \quad (64)$$

The previous results (20) and (23) are particular cases of the above formula.

A very interesting question concerns the values of  $\zeta(2k+1)$ . Setting  $z = 2k+1$  into (55) we get zero on both sides, and for  $z = -2k$  the poles of  $\Gamma(-2k)$  cancel with the zeros of  $\zeta(-2k)$  but this product is still undetermined, so we get no information about  $\zeta(2k+1)$ . No simple formula analogous to (64) is known for these values. It is known that  $\zeta(3)$  is irrational, this number is called *Apéry's constant* [21–24]. It is also known that there are infinite numbers in the form  $\zeta(2k+1)$  which are irrational [25]. Due to the unexpected nature of the result, when Apéry first showed his proof many mathematicians considered it as flawed, however, H. Cohen, H. Lenstra and A. van der Poorten confirmed that in fact Apéry was correct. It has been conjectured that  $\zeta(2k+1)/\pi^{2k+1}$  is transcendental [26]. A very interesting physical connection, providing a link between number theory and statistical mechanics, is that the most fundamental correlation function of the  $XXX$  spin-1/2 chain can be expressed in terms of  $\zeta(2k+1)$  [27].

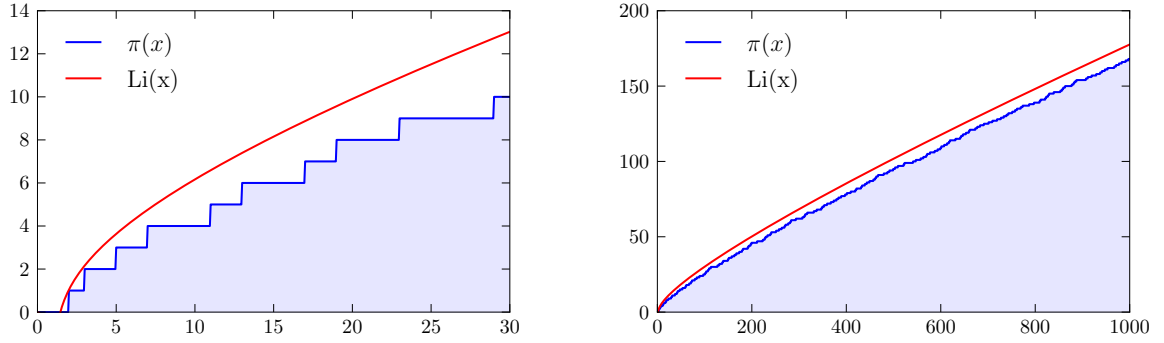


FIG. 5. The  $\text{Li}(x)$  approximation to the prime number counting function  $\pi(x)$ .

#### IV. GAUSS AND THE PRIME NUMBER THEOREM

Let  $\pi(x)$  denote the number of primes less than the positive real number  $x$ . It is a staircase function that jumps by one at each prime. In 1792, Gauss, when only 15 years old, based on examining data on the known primes, guessed that their density went as  $1/\log(x)$ . This leads to the approximation

$$\pi(x) = \sum_{p \leq x} 1 \approx \text{Li}(x) \quad (65)$$

where  $\text{Li}(x)$  is the log-integral function,

$$\text{Li}(x) = \int_0^x \frac{dt}{\log t}. \quad (66)$$

$\text{Li}(x)$  is a smooth function, and does indeed provide a smooth approximation to  $\pi(x)$  as Figure 5 shows.

The *Prime number theorem* (PNT) is the statement that  $\text{Li}(x)$  is the leading approximation to  $\pi(x)$ . It was only proven 100 years later using the main result of Riemann described in the next section. As we will explain later, the PNT follows if there are no Riemann zeros with  $\Re(z) = 1$ .

The key ingredient in Riemann's derivation of his result is the Euler product formula relating  $\zeta(z)$  to the prime numbers. A simple derivation of Euler's formula is based to the ancient "sieve" method for locating primes. One begins with a list of integers. First one removes all even integers, then all multiples of 3, then all multiples of 5, and so on. Eventually one ends up with the primes. We can describe this procedure analytically as follows. Begin with

$$\zeta(z) = 1 + \frac{1}{2^z} + \frac{1}{3^z} + \frac{1}{4^z} + \dots \quad (67)$$

One has

$$\frac{1}{2^z} \zeta(z) = \frac{1}{2^z} + \frac{1}{4^z} + \frac{1}{6^z} + \dots \quad (68)$$

thus

$$\left(1 - \frac{1}{2^z}\right) \zeta(z) = 1 + \frac{1}{3^z} + \frac{1}{5^z} + \dots \quad (69)$$

Repeating this process with powers of 3 we have

$$\left(1 - \frac{1}{3^z}\right) \left(1 - \frac{1}{2^z}\right) \zeta(z) = 1 + \frac{1}{5^z} + \frac{1}{7^z} + \dots \quad (70)$$

Continuing this process to infinity, the right hand side equals 1. Thus

$$\zeta(z) = \prod_p \frac{1}{1 - p^{-z}}. \quad (71)$$

Chebyshev tried to prove the PNT using  $\zeta(z)$  in 1850. It was finally proven in 1896 by Hadamard and de la Vallé Poussin by demonstrating that  $\zeta(z)$  indeed has no zeros with  $\Re(z) = 1$ .

## V. RIEMANN ZEROS AND THE PRIMES

### A. Riemann's main result

Riemann obtained an explicit and exact expression for  $\pi(x)$  in terms of the non-trivial zeros  $\rho$  of  $\zeta(z)$ . There are simpler but equivalent versions of the main result, based on the function  $\psi(x)$  below. However, let us present the main formula for  $\pi(x)$  itself, since it is historically more important. The derivation is given in the next subsection.

The function  $\pi(x)$  is related to another number-theoretic function  $J(x)$ , defined as

$$J(x) = \sum_{2 \leq n \leq x} \frac{\Lambda(n)}{\log n} \quad (72)$$

where  $\Lambda(n)$ , the von Mangoldt function, is defined by

$$\Lambda(n) = \begin{cases} \log p & \text{if } n = p^m \text{ for some prime } p \text{ and integer } m \geq 1, \\ 0 & \text{otherwise.} \end{cases} \quad (73)$$

For instance  $\Lambda(3) = \Lambda(9) = \log 3$ . The two functions  $\pi(x)$  and  $J(x)$  are related by Möbius inversion as follows:

$$\pi(x) = \sum_{n \geq 1} \frac{\mu(n)}{n} J(x^{1/n}). \quad (74)$$

Here  $\mu(n)$  is the Möbius function defined as follows. For  $n > 1$ , through the prime decomposition theorem we can write  $n = p_1^{\alpha_1} \cdots p_k^{\alpha_k}$ . Then

$$\mu(n) = \begin{cases} (-1)^k & \text{if } \alpha_1 = \alpha_2 = \cdots = \alpha_k = 1, \\ 0 & \text{otherwise.} \end{cases} \quad (75)$$

We also have  $\mu(1) = 1$ . Note that  $\mu(n) = 0$  if and only if  $n$  has a square factor  $> 1$ . The above expression (74) is actually a finite sum, since for large enough  $n$ ,  $x^{1/n} < 2$  and  $J = 0$ .

The main result of Riemann is a formula for  $J(x)$ , expressed as an infinite sum over non-trivial zeros  $\rho$ ,

$$J(x) = \text{Li}(x) - \sum_{\rho} \text{Li}(x^{\rho}) + \int_x^{\infty} \frac{dt}{\log t} \frac{1}{(t^2 - 1)t} - \log 2. \quad (76)$$

Riemann derived the result (76) starting from the Euler product formula and utilizing some insightful complex analysis that was sophisticated for the time. Some care must be taken in numerically evaluating  $\text{Li}(x^{\rho})$  since it has a branch point. It is more properly defined through the exponential integral function

$$\text{Li}(x) = \text{Ei}(\rho \log x), \quad \text{Ei}(z) = - \int_{-z}^{\infty} dt \frac{e^{-t}}{t}. \quad (77)$$

The sum in (76) is real because the  $\rho$ 's come in conjugate pairs. If there are no zeros on the line  $\Re(z) = 1$ , then the dominant term is the first one, i.e.  $J(x) \sim \text{Li}(x)$ , and this proves the PNT. The sum over  $\rho$  corrections to  $\text{Li}(x)$  deform it to the staircase function  $\pi(x)$  as Figure 6 shows. Thus, the complete knowledge of the primes is contained in the Riemann zeros.

Von Mangoldt provided a simpler formulation based on the function

$$\psi(x) = \sum_{n \leq x} \Lambda(n). \quad (78)$$

The function  $\psi(x)$  has a simpler expression in terms of Riemann zeros which reads

$$\psi(x) = x - \sum_{\rho} \frac{x^{\rho}}{\rho} - \log(2\pi) - \frac{1}{2} \log \left( 1 - \frac{1}{x^2} \right). \quad (79)$$

In this formulation, the PNT follows from the fact that the leading term is  $\psi(x) \sim x$ .

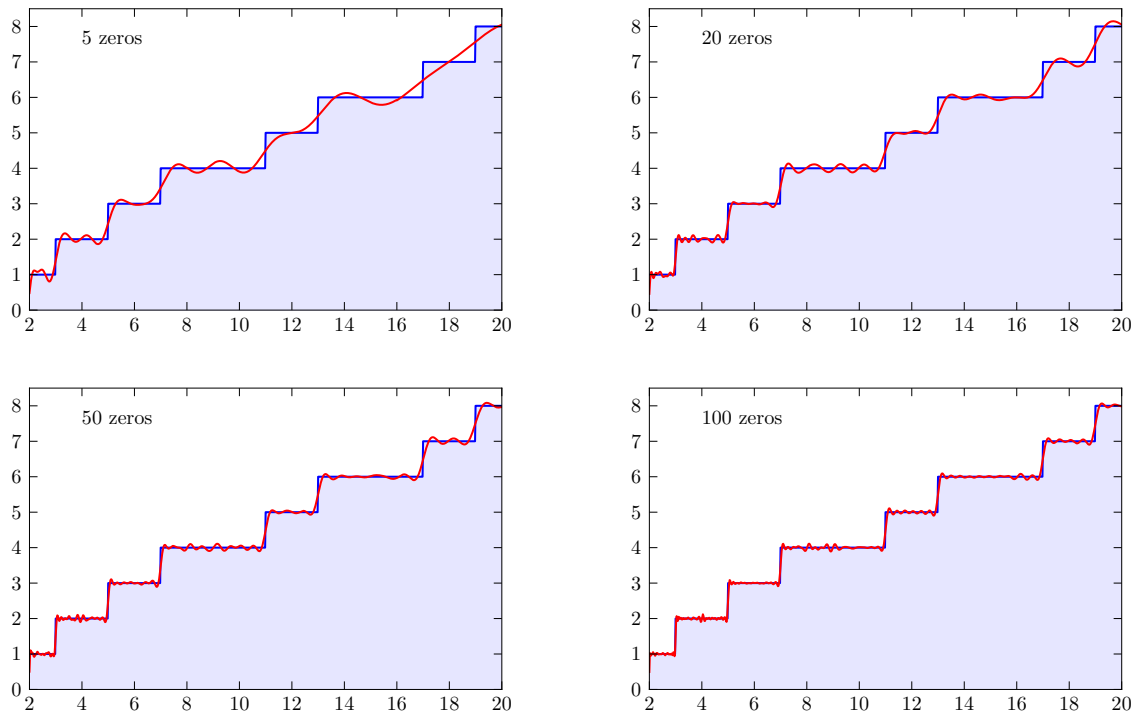


FIG. 6. The function  $\pi(x)$  as a sum of Riemann zeros from equations (74) and (76). The dashed (blue) region represents the exact  $\pi(x)$  while the (red) oscillating curve is (74), obtained with different number of zeros as indicated in the figures.

### B. $\psi(x)$ and the Riemann zeros

We first derive the formula (79). From the Euler product formula one has

$$\partial_z \log \zeta(z) = - \sum_p \partial_z \log (1 - p^{-z}) = - \sum_p \log p \frac{p^{-z}}{1 - p^{-z}}. \quad (80)$$

Taylor expanding the factor  $1/(1 - p^{-z})$  one obtains

$$\partial_z \log \zeta(z) = - \sum_p \sum_{m=1}^{\infty} \frac{\log p}{p^{mz}}. \quad (81)$$

For any arithmetic function  $a(n)$ , the Perron formula relates

$$A(x) = \sum'_{n \leq x} a(n) \quad (82)$$



to the poles of the Dirichlet series

$$g(z) = \sum_{n=1}^{\infty} \frac{a(n)}{n^z}. \quad (83)$$

In (82) the restriction on the sum is such that if  $x$  is an integer, then the last term of the sum must be multiplied by  $1/2$ . Now  $\zeta(z)$  can be factored in terms of its zeros,  $\zeta(z) \propto \prod_{\rho} (z - \rho)$ , thus  $\partial_z \log \zeta(z)$  has poles at each zero  $\rho$ . This implies that the Perron formula can be used to relate  $\psi(x)$  to the Riemann zeros.

The Perron formula is essentially an inverse Mellin transform. If the series for  $g(z)$  converges for  $\Re(z) > z_1$ , then

$$A(x) = \frac{1}{2\pi i} \int_{c-i\infty}^{c+i\infty} \frac{dz}{z} g(z) x^z \quad (84)$$

where the  $z$ -contour of integration is a straight vertical line from  $-\infty$  to  $+\infty$  with  $c > z_1$ . For completeness, we present a derivation of this formula in Appendix A.

Let us apply the Perron formula to  $\psi(x)$ ,

$$\psi(x) = \frac{1}{2\pi i} \int_{c-i\infty}^{c+i\infty} \frac{dz}{z} g(z) x^z \quad (85)$$

where  $g(z) = -\partial_z \log \zeta(z)$  and  $c > 1$ . The line of integration can be made into a closed contour by closing at infinity with  $\Re(z) \leq c$ . Now

$$g(z) = -\partial_z \left( \sum_{\rho} \log(z - \rho) + \sum_{\rho'} \log(z - \rho') - \log(z - 1) \right) \quad (86)$$

where  $\rho$  are zeros of  $\zeta(z)$  on the critical strip and  $\rho'$  are the trivial zeros on the negative real axis at  $\rho' = -2n$ . The  $-\log(z - 1)$  is due to the pole at  $z = 1$ . The sum of the residues gives

$$\psi(x) = x - \sum_{\rho} \frac{x^{\rho}}{\rho} - \sum_{\rho'} \frac{x^{\rho'}}{\rho'} + g(0). \quad (87)$$

The first term comes from the  $z = 1$  pole and  $g(0) = -\log(2\pi)$  comes from the  $z = 0$  pole. Finally

$$\sum_{\rho'} \frac{x^{\rho'}}{\rho'} = - \sum_{n=1}^{\infty} \frac{x^{-2n}}{2n} = \frac{1}{2} \log(1 - 1/x^2) \quad (88)$$

and this gives the result (79).

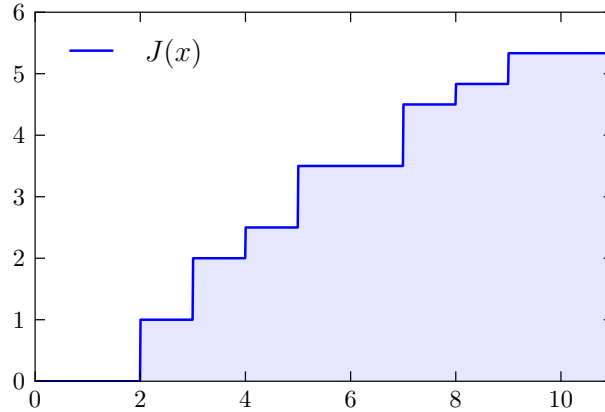


FIG. 7. The number theoretic function  $J(x)$  for  $x < 11$ .

### C. $\pi(x)$ and the Riemann zeros

Let us first explain the relation (74) between  $\pi(x)$  and  $J(x)$  involving the Möbius  $\mu$  function. By definition,  $J(x) = 0$  for  $x < 2$ . It jumps by  $1/n$  at each  $x = p^n$  where  $p$  is a prime. The expression (74) is always a finite sum since for  $n$  large enough  $x^{1/n} < 2$ . Consider for instance the range  $x \leq 10$ .  $J(x)$  in this range is plotted in Figure 7.

Since  $10^{1/4} < 2$ , the formula (74) gives

$$\pi(x) = J(x) - \frac{1}{2}J(x^{1/2}) - \frac{1}{3}J(x^{1/3}). \quad (89)$$

One easily sees that the two subtractions remove from  $J(x)$  the jumps by  $1/2$  at  $x = 2^2, 3^2$  and the jump by  $1/3$  at  $x = 2^3$  leaving only the jumps by one at the primes 2, 3, 5, 7.

Let us now derive (76). Comparing definitions, one has

$$dJ(x) = \frac{1}{\log x} d\psi(x). \quad (90)$$

Integrating this

$$J(x) = \int_0^x \frac{dt}{\log t} \frac{d\psi(t)}{dt} = \int_0^x \frac{dt}{\log t} \left( 1 - \sum_{\rho} t^{\rho-1} - \frac{1}{t(t^2-1)} \right). \quad (91)$$

Making the change of variables  $y = t^\rho$ ,

$$\int_0^x \frac{dt}{\log t} t^{\rho-1} = \int_0^{x^\rho} \frac{dy}{\log y} = \text{Li}(x^\rho). \quad (92)$$

Finally using

$$\int_0^x \frac{dt}{\log t} \frac{1}{(t^2 - 1)t} + \int_x^\infty \frac{dt}{\log t} \frac{1}{(t^2 - 1)t} = \log 2 \quad (93)$$

one obtains the form (76).

## VI. AN ELECTROSTATIC ANALOGY

A complex function is difficult to visualize since it is a hypersurface in a 4-dimensional space. In this section we construct an electric field and electric potential and use them to visualize the RH through a single real scalar field over the 2-dimensional  $(x, y)$ -plane, where  $z = x + iy$ .

### A. The electric field

Let us remove the  $z = 1$  pole in  $\chi(z)$  while maintaining its symmetry under  $z \rightarrow 1 - z$  by defining the function

$$\xi(z) \equiv \frac{1}{2}z(z-1)\chi(z) = \frac{1}{2}z(z-1)\pi^{-z/2}\Gamma(z/2)\zeta(z) \quad (94)$$

which satisfies

$$\xi(z) = \xi(1-z). \quad (95)$$

Let us define the real and imaginary parts of  $\xi(z)$  as

$$\xi(z) = u(x, y) + i v(x, y) \quad (96)$$

The Cauchy-Riemann equations

$$\partial_x u = \partial_y v, \quad \partial_y u = -\partial_x v \quad (97)$$

are satisfied everywhere since  $\xi$  is an entire function. Consequently, both  $u$  and  $v$  are harmonic functions, i.e. solutions of the Laplace equation  $\vec{\nabla}^2 u = (\partial_x^2 + \partial_y^2)u = 0$  and  $\vec{\nabla}^2 v = 0$ , although they are not completely independent. Let us define  $u$  or  $v$  contours as the curves in the  $x$ - $y$  plane corresponding to  $u$  or  $v$  equal to a constant, respectively. The critical line is a  $v = 0$  contour since  $\xi$  is real along it. As a consequence of the Cauchy-Riemann equations we have

$$\vec{\nabla} u \cdot \vec{\nabla} v = 0. \quad (98)$$

Thus where the  $u$  and  $v$  contours intersect, they are necessarily perpendicular, and this is one aspect of their dependency. A Riemann zero occurs wherever the  $u = 0$  and  $v = 0$  contours intersect, as illustrated in Figure 8.

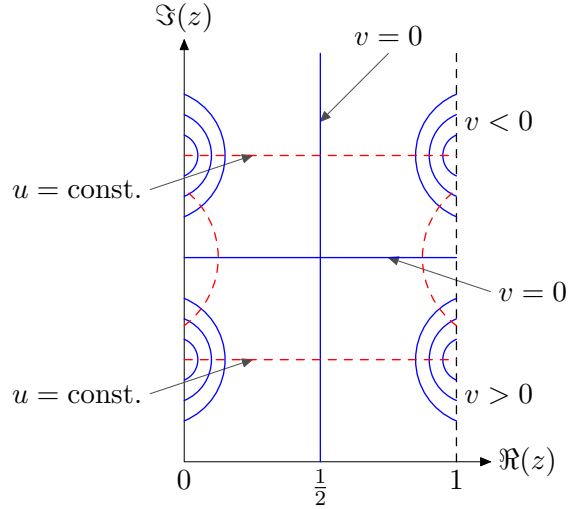


FIG. 8.  $u$  contours are dashed (red) lines and  $v$  contours are solid (blue) lines. A Riemann zero occurs where a  $u = 0$  contour spans the entire strip and passes through the zero on the critical line which is a  $v = 0$  contour.

From the symmetry (95) and  $\xi(z)^* = \xi(z^*)$  it follows that

$$u(x, y) = u(1 - x, y), \quad v(x, y) = -v(1 - x, y). \quad (99)$$

This implies that the  $v$  contours do not cross the critical line except for  $v = 0$ . All the  $u$  contours on the other hand are allowed to cross it by the above symmetry. Away from the  $v = 0$  points on the line  $\Re(z) = 1$ , since the  $u$  and  $v$  contours are perpendicular, the  $u$  contours generally cross the critical line and span the whole strip due to the symmetry (99). The  $u$  contours that do not cross the critical line must be in the vicinity of the  $v = 0$  contours, again by the perpendicularity of their intersections. Figure 8 depicts the behavior of the  $u$  and  $v$  contours in regions of the critical strip with no zeros off of the line.

Introduce the vector field

$$\vec{E} = E_x \hat{x} + E_y \hat{y} \equiv u(x, y) \hat{x} - v(x, y) \hat{y} \quad (100)$$

where  $\hat{x}$  and  $\hat{y}$  are unit vectors in the  $x$  and  $y$  directions. This field has zero divergence and curl as a consequence of the Cauchy-Riemann equations,

$$\vec{\nabla} \cdot \vec{E} = 0, \quad \vec{\nabla} \times \vec{E} = 0, \quad (101)$$

which are defined everywhere since  $\xi$  is entire. Thus it satisfies the conditions of a static electric field with no charged sources. We are only interested in the electric field on the critical strip.  $\vec{E}$  is not a physically realized electric field here, in that we do not need to specify what kind of charge distribution would give rise to such a field. All of our subsequent arguments will be based only on the mathematical identities expressed in equation (101), and

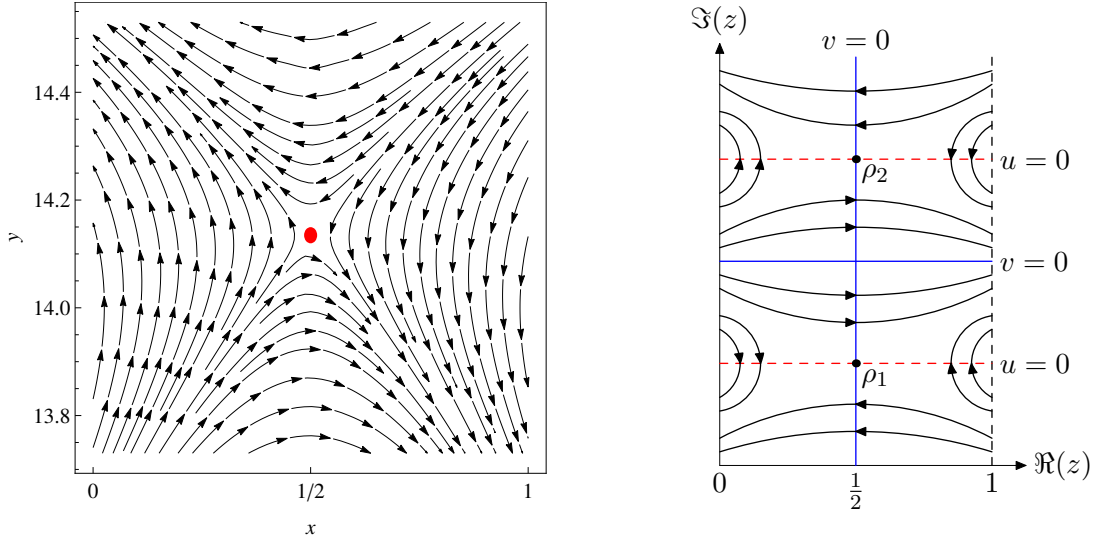


FIG. 9. *Left:* field lines of  $\vec{E}(x, y)$ , equation (100), in the vicinity of the first Riemann zero. *Right:* illustration of the field  $\vec{E}(x, y)$  in the vicinity of two consecutive Riemann zeros  $\rho_1$  and  $\rho_2$  on the critical line.

our reference to electrostatics is simply a useful analogy. Since the divergence of  $\vec{E}$  equals zero everywhere, the hypothetical electric charge distribution that gives rise to  $\vec{E}$  should be thought of as existing at infinity. Alternatively, since  $u$  and  $v$  are harmonic functions, one can view them as being determined by their values on the boundary of the critical strip.

As we now argue, the main properties of the above  $\vec{E}$  field on the critical strip are determined by its behavior near the Riemann zeros on the critical line combined with the behavior near  $\Re(z) = 1$ . In particular, electric field lines do not cross. Any Riemann zero on the critical line arises from a  $u = 0$  contour that crosses the full width of the strip and thus intersects the vertical  $v = 0$  contour. On the  $u = 0$  contour,  $E_x = 0$ , whereas on the  $v = 0$  contour of the critical line itself,  $E_y = 0$ . Furthermore,  $E_y$  changes direction as one crosses the critical line. Finally, taking into account that  $\vec{E}$  has zero curl, one can easily see that there are only two ways that all these conditions can be satisfied near the Riemann zero. One is shown in Figure 9 (left), the second has the direction of all arrows reversed. In short, Riemann zeros on the critical strip are manifestly consistent with the necessary properties of  $\vec{E}$ .

We now turn to the global properties of  $\vec{E}$  along the entire critical strip. The electric field must alternate in sign from one zero to the next, otherwise the curl of  $\vec{E}$  would not be zero in a region between two consecutive zeros. Thus there is a form of quasi-periodicity along the critical line, in the sense that zeros alternate between being even and odd, like the integers, and also analogous to the zeros of  $\sin x$  at  $x = \pi n$  where  $e^{i\pi n} = (-1)^n$ . Also, along the nearly horizontal  $v = 0$  contours that cross the critical line,  $\vec{E}$  is in the  $x$  direction. This leads to the pattern in Figure 9 (right). One aspect of the rendition of this pattern is that it implicitly assumes that the  $v = 0$  and  $u = 0$  points along the line  $\Re(z) = 1$  alternate,

namely, between two consecutive  $v = 0$  points along this line, there is only one  $u = 0$  point, which is consistent with the knowledge that there are no zeros of  $\xi$  along the line  $\Re(z) = 1$ . This fact will be clearer when we reformulate our argument in terms of the potential  $\Phi$  below.

### B. The electric potential $\Phi$

A mathematically integrated version of the above arguments, which has the advantage of making manifest the dependency of  $u$  and  $v$ , can be formulated in terms of the electric potential  $\Phi$  which is a single real function, defined to satisfy  $\vec{E} = -\vec{\nabla}\Phi$ . Although it contains the same information as the above argument, it is more economical.

By virtue of  $\vec{\nabla} \cdot \vec{E} = 0$ ,  $\Phi$  is also a solution of Laplace's equation  $\partial_z \partial_{\bar{z}} \Phi = 0$  where we denote  $\bar{z} = z^*$ . The general solution is that  $\Phi$  is the sum of a function of  $z$  and another function of  $\bar{z}$ . Since  $\Phi$  must be real,

$$\vec{E} = -\vec{\nabla}\Phi, \quad \Phi(x, y) = \frac{1}{2} (\varphi(z) + \bar{\varphi}(\bar{z})) \quad (102)$$

where  $\bar{\varphi}(\bar{z}) = (\varphi(z))^*$ . Clearly  $\Phi$  is not analytic, whereas  $\varphi$  is; it is useful to work with  $\Phi$  since we only have to deal with one real function. Comparing the definitions of  $\vec{E}$  and  $\xi$  in terms of  $u$  and  $v$ , one finds

$$u = -\frac{1}{2} (\partial_z \varphi + \partial_{\bar{z}} \bar{\varphi}), \quad v = -\frac{i}{2} (\partial_{\bar{z}} \bar{\varphi} - \partial_z \varphi). \quad (103)$$

This implies

$$\xi(z) = -\frac{\partial \varphi(z)}{\partial z} \quad (104)$$

This equation can be integrated because  $\xi$  is entire. Riemann's original paper gave the following integral representation

$$\xi(z) = 4 \int_1^\infty dt G(t) \cosh \left[ \left( z - \frac{1}{2} \right) \log(t) / 2 \right] \quad (105)$$

where

$$G(t) = t^{-1/4} \partial_t (t^{3/2} \partial_t g), \quad g(t) = \frac{1}{2} (\vartheta_3(0, e^{-\pi t}) - 1) = \sum_{n=1}^{\infty} e^{-n^2 \pi t}. \quad (106)$$

Here,  $\vartheta_3$  is one of the four elliptic theta functions. Note that the  $z \rightarrow 1 - z$  symmetry is manifest in this expression. Using this, then up to an irrelevant additive constant

$$\varphi(z) = -8 \int_1^\infty \frac{dt}{\log t} G(t) \sinh \left[ \frac{1}{2} \left( z - \frac{1}{2} \right) \log t \right]. \quad (107)$$

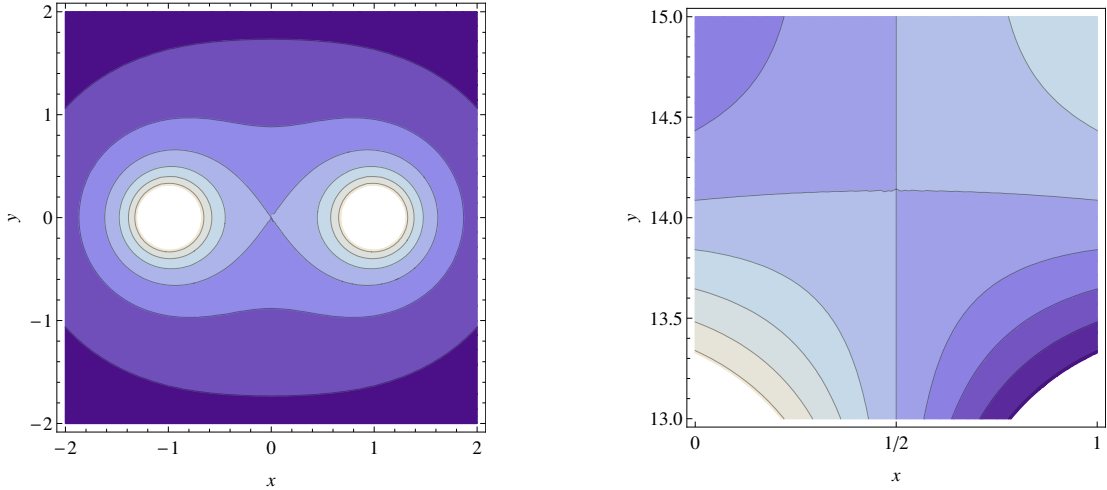


FIG. 10. *Left:* the electric potential of two equal point charges. *Right:* contour plot of the potential  $\Phi$  in the vicinity of the first Riemann zero at  $\rho = 1/2 + (14.1347\dots)i$ . The horizontal (vertical) direction is the  $x$  ( $y$ ) direction, where  $z = x + iy$ . The critical line and nearly horizontal line are  $\Phi = 0$  contours and they intersect at the zero.

Let us now consider the  $\Phi = \text{const.}$  contours in the critical strip. Using the integral representation (107), one finds the symmetry  $\Phi(x, y) = -\Phi(1 - x, y)$ . One sees then that the  $\Phi \neq 0$  contours do not cross the critical line, whereas the  $\Phi = 0$  contours can and do. Since  $\varphi$  is imaginary along the critical line, the latter is also a  $\Phi = 0$  contour.

All Riemann zeros  $\rho$  necessarily occur at isolated points, which is a property of entire functions. This is clear from the factorization formula  $\xi(z) = \xi(0) \prod_{\rho} (1 - z/\rho)$ , conjectured by Riemann, and later proved by Hadamard. Where are these zeros located in terms of  $\Phi$ ? At  $\rho$ ,  $\vec{\nabla}\Phi = 0$ . Thus, such isolated zeros occur when two  $\Phi$  contours *intersect*, which can only occur if the two contours correspond to the same value of  $\Phi$  since  $\Phi$  is single-valued. A useful analogy is the electric potential for equal point charges. The electric field vanishes halfway between them, and this is the unique point where the equi-potential contours vanish. The argument is simple:  $\vec{\nabla}\Phi$  is perpendicular to the  $\Phi$  contours, however as one approaches  $\rho$  along one contour, one sees that it is not in the same direction as inferred from the approach from the other contour. The only way this could be consistent is if  $\vec{\nabla}\Phi = 0$  at  $\rho$ . For purposes of illustration, we show the electric potential contours for two equal point charges in Figure 10 (left). Here, the electric field is only zero halfway between the charges, and indeed this is where two  $\Phi$  contours intersect.

With these properties of  $\Phi$ , we can now begin to understand the location of the known Riemann zeros. Since the  $\Phi = 0$  contours intersect the critical line, which itself is also a  $\Phi = 0$  contour, a zero exists at each such intersection, and we know there are an infinite number of them. The contour plot in Figure 10 (right) for the actual function  $\Phi$  constructed above verify these statements. We emphasize that there is nothing special about the value  $\Phi = 0$ , since  $\Phi$  can be shifted by an arbitrary constant without changing  $\vec{E}$ ; we defined it

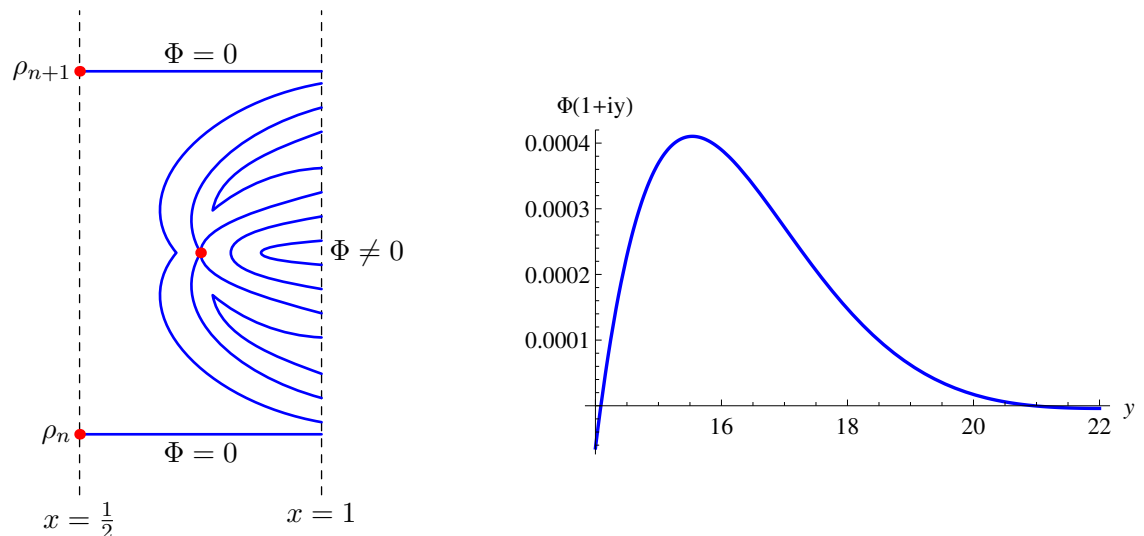


FIG. 11. *Left:* a sketch of the contour plot of the potential  $\Phi$  in the vicinity of a *hypothetical* Riemann zero off of the critical line. Such a zero occurs where the contours intersect.  $\rho_n$  and  $\rho_{n+1}$  are consecutive zeros on the line. *Right:* the electric potential between zeros on the boundary of the critical strip  $\Re(z) = 1$ .

such that the critical line corresponds to  $\Phi = 0$ .

A hypothetical Riemann zero off of the critical line would then necessarily correspond to an intersection of two  $\Phi \neq 0$  contours. For simplicity, let us assume that only two such contours intersect, since our arguments can be easily extended to more of such intersections. Such a situation is depicted in Figure 11 (left).

This figure implies that on the line  $\Re(z) = 1$ , specifically  $z = 1 + iy$ ,  $\Phi$  takes on the same non-zero value at four different values of  $y$  between consecutive zeros, i.e. roots of the equation  $f(y) = 0$ , where

$$f(y) \equiv \Phi(1, y) = \Re(\varphi(1 + iy)). \quad (108)$$

Thus, the real function  $f(y)$  would have to have 3 extrema between two consecutive zeros. Figure 11 (right) suggests that this does not occur. In order to attempt to prove it, let us define a “regular alternating” real function  $h(y)$  of a real variable  $y$  as a function that alternates between positive and negative values in the most regular manner possible: between two consecutive zeros  $h(y)$  has only one maximum, or minimum. For example, the  $\sin(y)$  function is obviously regular alternating. By the above argument, if  $f(y)$  is regular alternating, then two  $\Phi \neq 0$  contours cannot intersect and there are no Riemann zeros off the critical line. In Figure 11 (right) we plot  $f(y)$  for low values of  $y$  in the vicinity of the first two zeros, and as expected, it is regular alternating in this region.

To summarize, based on the symmetry (95), and the existence of the known infinity of Riemann zeros along the critical line, we have argued that  $\vec{E}$  and  $\Phi$  satisfy a regular repeating pattern all along the critical strip, and the RH would follow from such a repeating



pattern. In order to go further, one obviously needs to investigate the detailed properties of the function  $\xi$ , in particular its large  $y$  asymptotic behavior, and attempt to establish this repetitive behavior, more specifically, that  $f(y)$  defined above is a regular alternating function.

### C. Analysis

In this subsection, we attempt to establish that  $f(y)$  of the last section is a regular alternating function, however our results will not be conclusive. If  $f(y)$  is a regular alternating function, then so is  $\partial_y f(y)$ :

$$\partial_y f(y) = \Im [\xi(1 + iy)]. \quad (109)$$

Thus, one only needs to show that  $f'(y)$  is regular alternating. Using the summation formula for  $g(t)$ , one can show

$$\begin{aligned} \xi(z) &= \lim_{N \rightarrow \infty} \xi^{(N)}(z) = \lim_{N \rightarrow \infty} \sum_{n=1}^N \xi_n(z), \\ \xi_n(z) &= n^2 \pi \left[ 4e^{-\pi n^2} - z E_{\frac{z-1}{2}}(\pi n^2) + (z-1) E_{-\frac{z}{2}}(\pi n^2) \right]. \end{aligned} \quad (110)$$

where  $E_\nu(r)$  is an incomplete  $\Gamma$  function

$$E_\nu(r) = \int_1^\infty dt e^{-rt} t^{-\nu} = r^{\nu-1} \Gamma(1 - \nu, r). \quad (111)$$

It is sometimes referred to as the generalized exponential-integral function. In obtaining the above equation we have used the identity

$$r E_\nu(r) = e^{-r} - \nu E_{\nu+1}(r). \quad (112)$$

The nature of this approximation is that the roots  $\rho$  of  $\xi^{(N)}(\rho) = 0$  provide a very good approximation to the smaller Riemann zeros for large enough  $N$ . However small values of  $N$  are actually sufficient to a good degree of accuracy for small  $y$ . For instance, the first root for  $\xi^{(3)}$  coincides with the first Riemann zero to 15 digits, and its sixth root is correct to 8 digits. Furthermore  $\xi_{n+1}$  is smaller than  $\xi_n$  because of the  $e^{-n^2 \pi t}$  suppression in the integrand for  $E_\nu(\pi n^2)$ .

For  $\nu$  large, one has the series

$$\begin{aligned} E_\nu(r) &= \sqrt{\frac{\pi}{2}} r^{\nu-1} \csc[(1-\nu)\pi] e^{-(\nu-1/2) \log \nu + \nu - 1/12\nu + O(1/\nu^3)} \\ &+ \frac{e^{-r}}{\nu} \left\{ 1 - \frac{(r-1)}{\nu} + \frac{(r^2 - 3r + 1)}{\nu^2} + O((r/\nu)^3) \right\}. \end{aligned} \quad (113)$$

Using this, the leading term for large  $y$  is

$$\Im [\xi_n(1 + iy)] \approx -\frac{y^2 e^{-\pi y/4}}{\sqrt{2n}} \sin \left[ \frac{y}{2} \log \left( \frac{y}{2\pi n^2 e} \right) \right]. \quad (114)$$

To a reasonably good approximation, for large  $y$ ,  $\Im [\xi(1 + iy)] \approx \Im [\xi_1(1 + iy)]$ , and (114) indeed is a regularly alternating function because the argument of the sin function is monotonic. However we cannot completely rule out that including the other terms in  $\xi^{(N)}$  for  $N > 1$  could spoil this behavior.

## VII. TRANSCENDENTAL EQUATIONS FOR ZEROS OF THE $\zeta$ -FUNCTION

The main new result presented in the next few sections are transcendental equations satisfied by individual zeros of some  $L$ -functions. For simplicity we first consider the Riemann  $\zeta$ -function, which is the simplest Dirichlet  $L$ -function. Moreover, we first consider the asymptotic equation (131), first proposed in [6], since it involves more familiar functions. This asymptotic equation follows trivially from the exact equation (138), presented later.

### A. Asymptotic equation satisfied by the $n$ -th zero on the critical line

As above, let us define the function

$$\chi(z) \equiv \pi^{-z/2} \Gamma(z/2) \zeta(z). \quad (115)$$

which satisfies the functional equation

$$\chi(z) = \chi(1 - z). \quad (116)$$

Now consider Stirling's approximation

$$\Gamma(z) = \sqrt{2\pi} z^{z-1/2} e^{-z} (1 + O(z^{-1})) \quad (117)$$

where  $z = x + iy$ , which is valid for large  $y$ . Under this condition we also have

$$z^z = \exp \left( i \left( y \log y + \frac{\pi x}{2} \right) + x \log y - \frac{\pi y}{2} + x + O(y^{-1}) \right). \quad (118)$$

Therefore, using the polar representation

$$\zeta = |\zeta| e^{i \arg \zeta} \quad (119)$$

and the above expansions, we can write

$$\chi(z) = A e^{i\theta}$$

where

$$A(x, y) = \sqrt{2\pi} \pi^{-x/2} \left(\frac{y}{2}\right)^{(x-1)/2} e^{-\pi y/4} |\zeta(x + iy)| (1 + O(z^{-1})), \quad (120)$$

$$\theta(x, y) = \frac{y}{2} \log\left(\frac{y}{2\pi e}\right) + \frac{\pi}{4}(x-1) + \arg \zeta(x + iy) + O(y^{-1}). \quad (121)$$

The above approximation is very accurate. For  $y$  as low as 100, it evaluates  $\chi\left(\frac{1}{2} + iy\right)$  correctly to one part in  $10^6$ . Above we are assuming  $y > 0$ . The results for  $y < 0$  follows trivially from the relation  $(\chi(z))^* = \chi(z^*)$ .

We will need the result that the argument on the principle branch,  $\text{Arg } f(z)$ , of an analytic function  $f(z)$  has a well defined limit at a zero  $\rho$  where  $f(\rho) = 0$ . Let  $\mathcal{C}$  be a curve in the  $z$ -plane such that  $z(\mathcal{C})$  approaches the zero  $\rho$  in a smooth manner, namely,  $z(\mathcal{C})$  has a well-defined tangent at  $\rho$ . Without loss of generality, let  $\rho = 0$ . If the zero is of order  $k$ , then near zero

$$f(z) = a_k z^k + a_{k+1} z^{k+1} + \dots \quad (122)$$

Then  $\text{Arg}(f(z)/z^k)$  converges to  $\text{Arg } a_k$  along the curve  $\mathcal{C}$ . Since  $z(\mathcal{C})$  has a tangent at 0,  $\text{Arg } z(\mathcal{C})$  converges to a limit  $t$  as  $\mathcal{C}$  approaches  $\rho$ , so that  $\text{Arg } f(z) \rightarrow \text{Arg}(a_k) + kt$  as  $\mathcal{C} \rightarrow \rho$ .

Now let  $\rho = x + iy$  be a Riemann zero. Then  $\text{Arg } \zeta(\rho)$  can be well-defined by the limit

$$\text{Arg } \zeta(\rho) \equiv \lim_{\delta \rightarrow 0^+} \text{Arg } \zeta(x + \delta + iy). \quad (123)$$

For reasons that are explained below, it is important that  $0 < \delta \ll 1$ . This limit in general is not zero. For instance, for the first Riemann zero at  $\rho = \frac{1}{2} + iy_1$ , where  $y_1 = 14.1347\dots$ ,

$$\text{Arg } \zeta\left(\frac{1}{2} + iy_1\right) \approx 0.157873919880941213041945. \quad (124)$$

On the critical line  $z = \frac{1}{2} + iy$ , if  $y$  does not correspond to the imaginary part of a zero, the well-known function

$$S(y) = \frac{1}{\pi} \arg \zeta\left(\frac{1}{2} + iy\right) \quad (125)$$

is defined by continuous variation along the straight lines starting from 2, then up to  $2 + iy$  and finally to  $\frac{1}{2} + iy$ , where  $\arg \zeta(2) = 0$  (see (B13)). The function  $S(y)$  is discussed in greater detail below in section VIII. On a zero, the standard way to define this term is through the limit  $S(\rho) = \frac{1}{2} \lim_{\epsilon \rightarrow 0} (S(\rho + i\epsilon) + S(\rho - i\epsilon))$ . We have checked numerically that for several zeros on the line, our definition (123) gives the same result as the standard piecewise integration definition, *so long as  $S(y)$  is on the principal branch, which is almost always true for low enough, but relatively large  $y$ .* (See section VIII for more discussion on

this important point.)

From (115) it follows that  $\zeta(z)$  and  $\chi(z)$  have the same zeros on the critical strip, so it is enough to consider the zeros of  $\chi(z)$ . Let us now consider approaching a zero  $\rho = x + iy$  through the  $\delta \rightarrow 0^+$  limit in  $\arg \zeta$ . Consider first the simple zeros along the critical line. Later we will argue that all such zeros are in fact simple. As we now show, these zeros are in one-to-one correspondence with the zeros of the cosine,

$$\lim_{\delta \rightarrow 0^+} \cos \theta = 0. \quad (126)$$

The argument goes as follows.<sup>8</sup> On the critical line  $z = \frac{1}{2} + iy$ , the functional equation (116) implies  $\chi(z) = A(\cos \theta + i \sin \theta)$  is real, thus for  $y$  *not* the ordinate of a zero,  $\sin \theta = 0$  and  $\cos \theta = \pm 1$ . Thus  $\cos \theta$  is a discontinuous function. Now let  $y_\bullet$  be the ordinate of a *simple* zero. Then close to such a zero we define

$$c(y) \equiv \frac{\chi(\frac{1}{2} + iy)}{|\chi(\frac{1}{2} + iy)|} = \frac{y - y_\bullet}{|y - y_\bullet|}. \quad (127)$$

For  $y > y_\bullet$  then  $c(y) = 1$ , and for  $y < y_\bullet$  then  $c(y) = -1$ . Thus  $c(y)$  is discontinuous precisely at a zero. In the above polar representation, formally  $c(y) = \cos \theta(\frac{1}{2}, y)$ . Therefore, by identifying zeros as the solutions to  $\cos \theta = 0$ , we are simply defining the value of the function  $c(y)$  at the discontinuity as  $c(y_\bullet) = 0$ . As explained above, the argument  $\theta$  of  $\chi(z)$  is well defined on a zero so this leads to equations satisfied by the zeros.

The small shift by  $\delta$  in (131) is essential since it smooths out  $S(y)$ , which is known to jump discontinuously at each zero. As is well known,  $S(y)$  is a piecewise continuous function, but rapidly oscillates around zero with discontinuous jumps, as shown in Figure 12 (left). However, when this term is added to the smooth part of  $N_0(T)$  (see equations (132) and (133)), one obtains an accurate staircase function, which jumps by one at each zero on the line; see Figure 12 (right). The function  $S(y)$  is further discussed in section VIII. Note that  $N_0(T)$  and  $N(T)$  are necessarily monotonically increasing functions.

The reason  $\delta$  needs to be positive in (138) is the following. Near a zero  $\rho_n$ ,

$$\zeta(z) \approx (z - \rho_n) \zeta'(\rho_n) = (\delta + i(y - y_n)) \zeta'(\rho_n). \quad (128)$$

This gives

$$\arg \zeta(z) \approx \arctan((y - y_n)/\delta) + \arg \zeta'(\rho_n). \quad (129)$$

Thus, with  $\delta > 0$ , as one passes through a zero from below,  $S(y)$  *increases by one*, as it should based on its role in the counting formula  $N(T)$ . On the other hand, if  $\delta < 0$  then  $S(y)$  would decrease by one instead.

We can now obtain a precise equation for the location of the zeros on the critical line.

---

<sup>8</sup>A more streamlined argument was presented in [14].

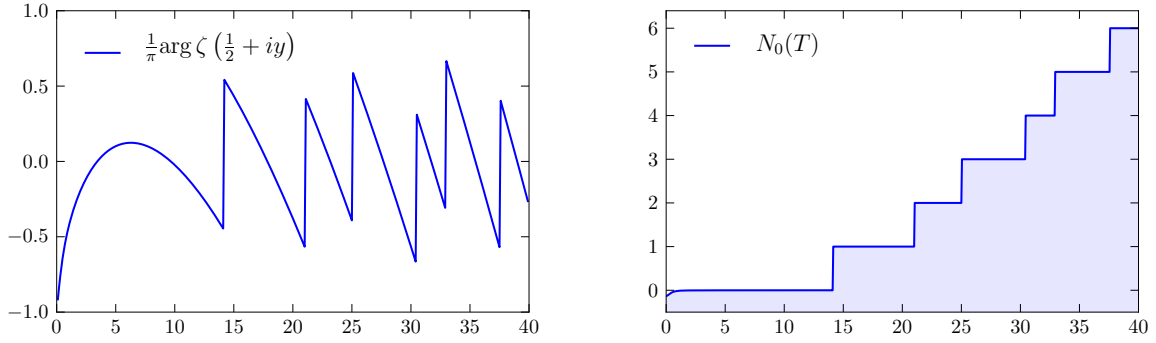


FIG. 12. *Left:*  $\frac{1}{\pi} \arg \zeta \left( \frac{1}{2} + iy \right)$  versus  $y$ , showing its rapid oscillation. The jumps occur on a Riemann zero. *Right:*  $N_0(T)$  versus  $T$  in (132), which is indistinguishable from a manual counting of zeros.

The equation (126), implies  $\lim_{\delta \rightarrow 0^+} \theta \left( \frac{1}{2} + \delta, y \right) = \left( n + \frac{1}{2} \right) \pi$ , for  $n = 0, \pm 1, \pm 2, \dots$ , hence

$$n = \frac{y}{2\pi} \log \left( \frac{y}{2\pi e} \right) - \frac{5}{8} + \lim_{\delta \rightarrow 0^+} \frac{1}{\pi} \arg \zeta \left( \frac{1}{2} + \delta + iy \right). \quad (130)$$

A closer inspection shows that the RHS of the above equation has a minimum in the interval  $(-2, -1)$ , thus  $n$  is bounded from below, i.e.  $n \geq -1$ . Establishing the *convention* that zeros are labeled by positive integers,  $\rho_n = \frac{1}{2} + iy_n$  where  $n = 1, 2, \dots$ , we must replace  $n \rightarrow n - 2$  in (130). Therefore, the imaginary parts of these zeros satisfy the transcendental equation

$$\frac{y_n}{2\pi} \log \left( \frac{y_n}{2\pi e} \right) + \lim_{\delta \rightarrow 0^+} \frac{1}{\pi} \arg \zeta \left( \frac{1}{2} + \delta + iy_n \right) = n - \frac{11}{8} \quad (n = 1, 2, \dots). \quad (131)$$

In summary, we have shown that, asymptotically for now, there are an infinite number of zeros on the critical line whose ordinates can be determined by solving (131). This equation was first proposed in [6]. This equation determines the zeros on the upper half of the critical line. The zeros on the lower half are symmetrically distributed; if  $\rho_n = \frac{1}{2} + iy_n$  is a zero, so is  $\rho_n^* = \frac{1}{2} - iy_n$ .

The LHS of (131) is a monotonically increasing function of  $y$ , and the leading term is a smooth function. This is clear since the same terms appear in the staircase function  $N(T)$  described below. Possible discontinuities can only come from  $\frac{1}{\pi} \arg \zeta \left( \frac{1}{2} + iy \right)$ , and in fact, it has a jump discontinuity by one whenever  $y$  corresponds to a zero on the line. However, if  $\lim_{\delta \rightarrow 0^+} \arg \zeta \left( \frac{1}{2} + \delta + iy \right)$  is well defined for every  $y$ , then the left hand side of equation (131) is well defined for any  $y$ , and due to its monotonicity, there must be a unique solution for every  $n$ . Under this assumption, the number of solutions of equation (131), up to height

$T$ , is given by

$$N_0(T) = \frac{T}{2\pi} \log \left( \frac{T}{2\pi e} \right) + \frac{7}{8} + \frac{1}{\pi} \arg \zeta \left( \frac{1}{2} + iT \right) + O(T^{-1}). \quad (132)$$

This is so because the zeros are already numbered in (131), but the left hand side jumps by one at each zero, with values  $-\frac{1}{2}$  to the left and  $+\frac{1}{2}$  to the right of the zero. Thus we can replace  $n \rightarrow N_0 + \frac{1}{2}$  and  $y_n \rightarrow T$ , such that the jumps correspond to integer values. In this way  $T$  will not correspond to the ordinate of a zero and  $\delta$  can be eliminated.

Using Cauchy's argument principle (see Appendix B) one can derive the Riemann-von Mangoldt formula, which gives the number of zeros in the region  $\{0 < x < 1, 0 < y < T\}$  inside the *critical strip*. This formula is standard [2, 20]:

$$N(T) = \frac{T}{2\pi} \log \left( \frac{T}{2\pi e} \right) + \frac{7}{8} + S(T) + O(T^{-1}). \quad (133)$$

The leading  $T \log T$  term was already in Riemann's original paper. Note that it has the same form as the counting formula on the *critical line* that we have just found (132). Thus, under the assumptions we have described, we conclude that  $N_0(T) = N(T)$  asymptotically. This means that our particular solution (150), leading to equation (131), already saturates the counting formula on the whole strip and there are no additional zeros from  $A = 0$  in (145) nor from the more general equation  $\theta + \theta' = (2n + 1)\pi$  described below. This strongly suggests that (131) describes all non-trivial zeros of  $\zeta(z)$ , which must then lie on the critical line.

## B. Exact equation satisfied by the $n$ -th zero on the critical line

Let us now repeat the previous analysis but without considering an asymptotic expansion. The exact versions of (120) and (121) are

$$A(x, y) = \pi^{-x/2} |\Gamma(\frac{1}{2}(x + iy))| |\zeta(x + iy)|, \quad (134)$$

$$\theta(x, y) = \arg \Gamma(\frac{1}{2}(x + iy)) - \frac{y}{2} \log \pi + \arg \zeta(x + iy), \quad (135)$$

Then, as before, zeros are described by  $\lim_{\delta \rightarrow 0^+} \cos \theta = 0$ , equivalent to  $\lim_{\delta \rightarrow 0^+} \theta(\frac{1}{2} + \delta, y) = (n + \frac{1}{2})\pi$ , and upon replacing  $n \rightarrow n - 2$  the imaginary parts of these zeros must satisfy the exact equation

$$\arg \Gamma\left(\frac{1}{4} + \frac{iy_n}{2}\right) - y_n \log \sqrt{\pi} + \lim_{\delta \rightarrow 0^+} \arg \zeta\left(\frac{1}{2} + \delta + iy_n\right) = \left(n - \frac{3}{2}\right)\pi. \quad (136)$$

The Riemann-Siegel  $\vartheta$  function is defined by

$$\vartheta(y) \equiv \arg \Gamma\left(\frac{1}{4} + \frac{i}{2}y\right) - y \log \sqrt{\pi}, \quad (137)$$

where the argument is defined such that this function is continuous and  $\vartheta(0) = 0$ . This can be done through the relation  $\arg \Gamma = \Im \log \Gamma$ , and numerically one can use the implementation of the “logGamma” function. This is equivalent to the analytic multivalued  $\log(\Gamma)$  function, but it simplifies its complicated branch cut structure. Therefore, there are an infinite number of zeros in the form  $\rho_n = \frac{1}{2} + iy_n$ , where  $n = 1, 2, \dots$ , whose imaginary parts *exactly* satisfy the following equation:

$$\vartheta(y_n) + \lim_{\delta \rightarrow 0^+} \arg \zeta\left(\frac{1}{2} + \delta + iy_n\right) = \left(n - \frac{3}{2}\right) \pi \quad (n = 1, 2, \dots). \quad (138)$$

Expanding the  $\Gamma$ -function in (137) through Stirling’s formula

$$\vartheta(y) = \frac{y}{2} \log\left(\frac{y}{2\pi e}\right) - \frac{\pi}{8} + O(1/y) \quad (139)$$

one recovers the asymptotic equation (131).

Again, as discussed after (131), the first term in (138) is smooth and the whole left hand side is a monotonically increasing function. If  $\lim_{\delta \rightarrow 0^+} \zeta\left(\frac{1}{2} + \delta + iy\right)$  is well defined for every  $y$ , then equation (138) must have a unique solution for every  $n$ . Under this condition it is valid to replace  $y_n \rightarrow T$  and  $n \rightarrow N_0 + \frac{1}{2}$ , and then the number of solutions of (138) is given by

$$N_0(T) = \frac{1}{\pi} \vartheta(T) + 1 + \frac{1}{\pi} \arg \zeta\left(\frac{1}{2} + iT\right). \quad (140)$$

The exact Backlund counting formula (see Appendix B), which gives the number of zeros on the critical strip with  $0 < \Im(\rho) < T$ , is given by [2]

$$N(T) = \frac{1}{\pi} \vartheta(T) + 1 + S(T). \quad (141)$$

Therefore, comparing (140) with the exact counting formula on the *entire critical strip* (141), we have  $N_0(T) = N(T)$  exactly. This indicates that our particular solution, leading to equation (138), captures all the zeros on the strip *assuming there is a solution for every  $n$* , indicating that they should all be on the critical line.

In summary, if (138) has a unique solution for each  $n$ , then this saturates the counting formula for the entire critical strip and this would establish the validity of the RH.

### C. A more general equation

The above equation (138) was first obtained by us with a different, and less rigorous, argument [6, 7]. It is a particular solution of a more general formula which we now present.

We will need the following. From (115) we have  $(\chi(z))^* = \chi(z^*)$ , thus  $A(x, -y) = A(x, y)$  and  $\theta(x, -y) = -\theta(x, y)$ . Denoting

$$\chi(1 - z) = A' e^{-i\theta'} \quad (142)$$

we then have

$$A'(x, y) = A(1 - x, y), \quad \theta'(x, y) = \theta(1 - x, y). \quad (143)$$

From (116) we also have  $|\chi(z)| = |\chi(1 - z)|$ , therefore

$$A(x, y) = A'(x, y) \quad (144)$$

for *any*  $z$  on the critical strip.

From (116) we see that if  $\rho$  is a zero so is  $1 - \rho$ . Then we clearly have

$$\lim_{z \rightarrow \rho} \{\chi(z) + \chi(1 - z)\} = \lim_{z \rightarrow \rho} A(x, y) B(x, y) = 0, \quad (145)$$

where we have defined

$$B(x, y) = e^{i\theta(x, y)} + e^{-i\theta'(x, y)}. \quad (146)$$

The second equality in (145) follows from (144). For now, we do not specify the precise curve  $\mathcal{C}$  through which we approach the zero.

The above equation (145) is identically satisfied on a zero  $\rho$  since  $\lim_{z \rightarrow \rho} A \sim |\zeta(\rho)| = 0$ , independently of  $B$ . However, this by itself does not provide any more detailed information on the zeros. There is much more information in the phases  $\theta$  and  $\theta'$ . Consider instead taking the limits in  $A$  and  $B$  separately,

$$\lim_{z' \rightarrow \rho} \lim_{z \rightarrow \rho} A(x', y') B(x, y) = 0, \quad (147)$$

where  $z' = x' + iy'$ . Taking  $z \rightarrow \rho$  first, a potential zero occurs when

$$\lim_{z \rightarrow \rho} B(x, y) = \lim_{z \rightarrow \rho} \left( e^{i\theta} + e^{-i\theta'} \right) = 0. \quad (148)$$

We propose that Riemann zeros satisfy (148). The equation  $B = 0$  provides more information on the location of zeros than  $A = 0$  since the phases  $\theta$  and  $\theta'$  can be well defined at a zero through an appropriate limit. We emphasize that we have not yet assumed the RH, and the above analysis is valid on the entire complex plane, except at  $z = 1$  due to the simple pole of  $\chi$ . We will provide ample evidence that the equation (148) is evidently correct even



for the example of the Davenport-Heilbronn function, which has zeros off the critical line, and the RH fails. Clearly a more rigorous derivation would be desirable, the delicacy being the limits involved, but let us proceed.

The linear combination in (145) was chosen to be manifestly symmetric under  $z \rightarrow 1 - z$ . Had we taken a different linear combination in (145), such as  $\chi(\rho) + b\chi(1 - \rho)$ , then  $B = e^{i\theta} + be^{-i\theta'}$  for some constant  $b$ . Setting the real and imaginary parts of  $B$  to zero gives the two equations  $\cos \theta + b \cos \theta' = 0$  and  $\sin \theta - b \sin \theta' = 0$ . Summing the squares of these equations one obtains  $\cos(\theta + \theta') = -(b + 1/b)/2$ . However, since  $b + 1/b > 1$ , there are no solutions except for  $b = 1$ .

The general solution of (148) is given by

$$\theta + \theta' = (2n + 1)\pi. \quad (149)$$

Note that  $\chi(z) = \chi(1 - z)$  implies  $\theta + \theta' = 2\pi n$  for  $z \neq \rho$ . This together with (149) is analogous to the previous discussion where  $\cos \theta = 1$  for  $z \neq \rho$  and  $\cos \theta = 0$  for  $z = \rho$ . All zeros satisfying (149) are simple since there are in correspondence with zeros of the cosine or sine function.

The zeros on the *critical line* correspond to the particular solution

$$\theta = \theta' = (n + \frac{1}{2})\pi, \quad (150)$$

which is equivalent to (126) and (138).

In fact, the trivial zeros along the negative  $x$  axis also satisfy (149), which again strongly supports its validity. One can show this as follows. For  $x < 0$ ,  $\theta'(x, 0) = 0$ . Since we are on the real line, we approach the zero through the path  $z = \rho - i\epsilon$ , with  $0 < \epsilon \ll 1$ . This path smooths out the  $\arg \zeta$  term in the same way as the  $\delta \rightarrow 0^+$  for zeros on the critical line. Then from (149) we are left with

$$\frac{1}{\pi}\theta(x, 0) = \frac{1}{\pi}\Im [\log \Gamma(x/2)] + \frac{1}{\pi} \lim_{\epsilon \rightarrow 0^+} \text{Arg} \zeta(x - i\epsilon) + 2k = 2n + 1. \quad (151)$$

Note that we write  $\arg \zeta(x - i\epsilon) = \text{Arg} \zeta(x - i\epsilon) + 2\pi k$ , where we have the principal value  $\text{Arg} \zeta(x) \in \{0, \pm\pi\}$  for  $x < 0$ . The changes in branch are accounted for by  $k$ , and depends on  $x$ . If we take these changes correctly into account we obtain Figure 13, showing the trivial zeros as solutions to (151). The first term in (151), i.e.  $\frac{1}{\pi}\Im [\log \Gamma(x/2)]$ , is already a staircase function with jumps by 1 at every negative even  $x$ . The other two terms,  $\frac{1}{\pi}\text{Arg} \zeta(x - i\epsilon) + 2k$ , just shift the function by a constant, such that these jumps coincide with odd integers  $(2n+1)$  in such a way that (151) is satisfied exactly at a zero. Thus, remarkably, the equation (149) characterizes all known zeros of  $\zeta$ .

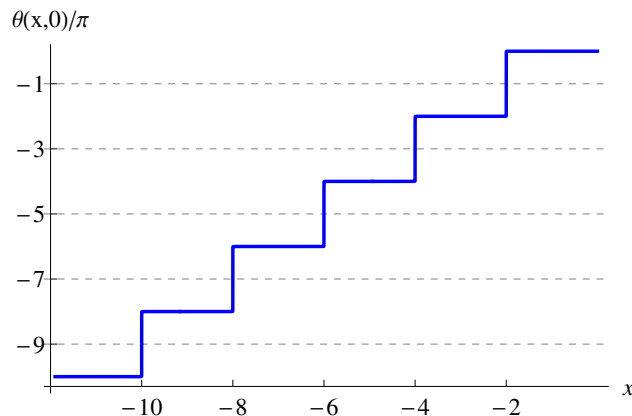


FIG. 13. Plot of equation (151). Note the jumps occurring at  $2n + 1$  corresponding to the trivial zeros of the  $\zeta$ -function.

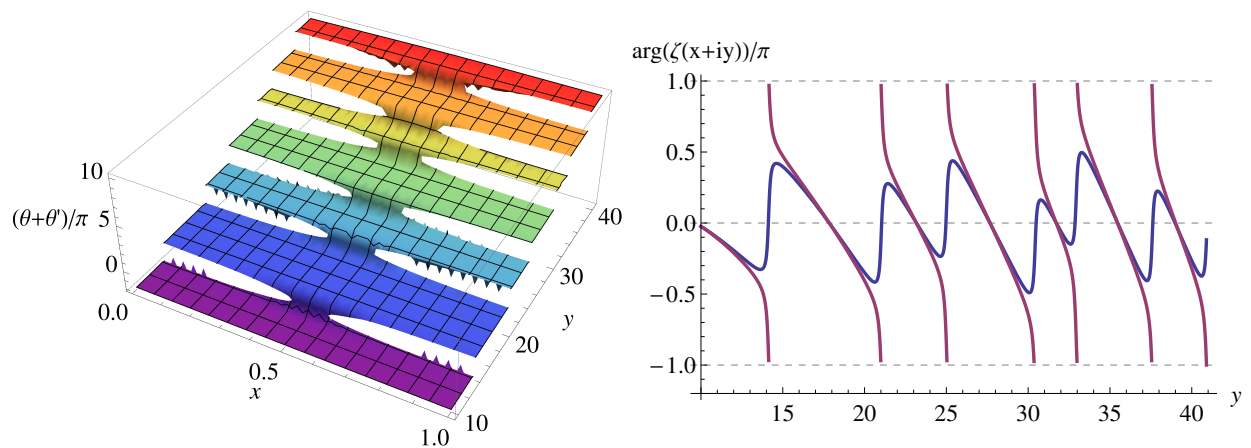


FIG. 14. *Left:* 3D plot of  $\frac{1}{\pi} [\theta(x, y) + \theta'(x, y)]$ . The function does not vary with  $x$  on each plateau, but it is only well defined between jumps very close to the critical line. *Right:*  $\frac{1}{\pi} \arg \zeta(x + iy)$  for  $x = 1/2 + 0.1$  (blue) and  $x = 1/2 - 0.1$  (purple) as a function of  $y$ .

#### D. On possible zeros off of the line

Suppose one looks for solutions to (149) off the line. In Figure 14 (left) we plot the RHS of (149) divided by  $\pi$  for a region on the critical strip. One clearly sees that precisely where a solution requires that this equals an odd integer, the function is not well-defined. On the other hand, for  $x = 1/2$  with the  $\delta$ -prescription it is well-defined and has a unique solution.

The fact that the RHS of (149) is not well defined for  $x > 1/2$  is due to the very different properties of  $\arg \zeta(x + iy)$  for  $x > 1/2$  versus  $x < 1/2$ . In Figure 14 (right) we plot  $\arg \zeta(x + iy)$  for  $x = 1/2 \pm 0.1$  as a function of  $y$ . One sees that for  $x < 1/2$  there are severe changes of branch where the function is not defined, whereas for  $x > 1/2$  it is smooth. Since the RHS of (149) involves both  $\theta$  and  $\theta'$ , the  $\theta'$  term is ill-defined for  $x > 1/2$  and thus neither is the RHS. Only on the critical line where  $\theta = \theta'$  and  $x = 1/2 + \delta$  with  $\delta \rightarrow 0^+$  is

the RHS well-defined.

There is another very interesting aspect of Figure 14 (left). On each plateau the function is mainly constant with respect to  $x$ . This formally follows from

$$\partial_x [\theta(x, y) + \theta'(x, y)] = 0 \quad (152)$$

if one assumes  $\theta$  is differentiable at  $x$ . This leads to the following suggestion. Suppose that the dependence on  $x$  for  $1/2 < x \leq 1$  is weak enough that  $\theta + \theta'$  is very well approximated by the curve at  $x = 1$ . Recall that it is known that there are no zeros along the line  $x = 1$ . If the curve for  $1/2 < x < 1$  is a smooth and very small deformation of the one at  $x = 1$ , then there are no solutions to (149) off of the line, and if the latter captures all zeros, then there are no zeros off the line. As in section VI, the RH would then be related to the non-existence of zeros at  $x = 1$ , which is equivalent to the prime number theorem. The main problem with this argument is that at a zero off the line, probably the above derivative is not well defined.

One sees that the particular solution (150) of the more general  $B = 0$  is a consequence of the direction in which the zero on the line is approached. Let  $\zeta(z) = u(x, y) + iv(x, y)$  as in section VI. The  $u, v = \text{const.}$  contours are sketched in Figure 8. In the transcendental equation (136) the  $\delta \rightarrow 0^+$  limit approaches the zero on the critical line along  $u = 0$  contours that are nearly in the  $x$  direction. For potential zeros off of the line where  $u, v = 0$  contours intersect perpendicularly, one does not expect that the directions of these contours at the zeros is always the same, in contrast to those of the zeros on the critical line. Thus, for zeros off of the line, we expect  $B = 0$  will be satisfied, i.e. (149), but not the particular solution  $\cos \theta = 0$ .

In section XIX we will study an example of an  $L$ -series that does not satisfy the RH, the Davenport-Heilbronn function. We will show that the zeros off the line indeed satisfy (149).

### E. Further remarks

It is possible to introduce a new function  $\zeta(z) \rightarrow \tilde{\zeta}(z) = f(z)\zeta(z)$  that also satisfies the functional equation (116), i.e.  $\tilde{\chi}(z) = \tilde{\chi}(1-z)$ , but has zeros off of the critical line due to the zeros of  $f(z)$ . In such a case the corresponding functional equation will hold if and only if  $f(z) = f(1-z)$  for any  $z$ , and this is a trivial condition on  $f(z)$ , which could have been canceled in the first place. Moreover, if  $f(z)$  and  $\zeta(z)$  have different zeros, the analog of equation (145) has a factor  $f(z)$ , i.e.  $\tilde{\chi}(\rho + \delta) + \tilde{\chi}(1 - \rho - \delta) = f(\rho + \delta) [\chi(\rho + \delta) + \chi(1 - \rho - \delta)] = 0$ , implying (145) again where  $\chi(z)$  is the original (115). Therefore, the previous analysis eliminates  $f(z)$  automatically and only finds the zeros of  $\chi(z)$ . The analysis is non-trivial precisely because  $\zeta(z)$  satisfies the functional equation but  $\zeta(z) \neq \zeta(1-z)$ . Furthermore, it is a well known theorem that the only function which satisfies the functional equation (116) and has the same characteristics of  $\zeta(z)$ , is  $\zeta(z)$  itself.

In other words, if  $\tilde{\zeta}(z)$  is required to have the same properties of  $\zeta(z)$ , then  $\tilde{\zeta}(z) = C\zeta(z)$ , where  $C$  is a constant [20, pg. 31].

Although equations (138) and (141) have an obvious resemblance, it is impossible to derive the former from the later, since the later is just a counting formula valid on the entire strip, and it is assumed that  $T$  is *not* the ordinate of a zero. Moreover, this would require the assumption of the validity of the RH, contrary to our approach, where we derived equations (138) and (131) on the critical line, without assuming the RH. Despite our best efforts, we were not able to find equations (131) and (138) in the literature. Furthermore, the counting formulas (132) and (141) have never been proven to be valid on the critical line [2].

### VIII. THE ARGUMENT OF THE RIEMANN $\zeta$ -FUNCTION

Let us recall the definition used in section VII in conjunction with the França-LeClair equation (138), namely

$$S(y) = \lim_{\delta \rightarrow 0^+} \frac{1}{\pi} \arg \zeta \left( \frac{1}{2} + \delta + iy \right) = \lim_{\delta \rightarrow 0^+} \frac{1}{\pi} \Im \left[ \log \zeta \left( \frac{1}{2} + \delta + iy \right) \right]. \quad (153)$$

Previously, we argued that  $S(y_n)$  is well defined at a zero  $\rho = \frac{1}{2} + iy_n$  in the non-zero  $\delta \rightarrow 0^+$  limit. A proper understanding of this function is essential in any theory of the Riemann zeros because of its role in the counting function  $N(T)$ , and in our equation (138) satisfied by individual zeros. It is the fluctuations in  $S(y)$  that “knows” about the actual zeros. As stated above, if the equation (138) has a unique solution for every  $n$ , then the RH would follow since then  $N_0(T) = N(T)$ . In this section we describe some important properties of  $S(y)$  in connection with the equation (138). However this will still not be sufficient to prove that there is indeed a unique solution to this equation. All of these properties are essentially already known (see for instance [28]).

The conventional way to define  $S(y)$  is by piecewise integration of  $\zeta'/\zeta$  from  $z = 2$  to  $2 + iy$ , then to  $1/2 + iy$ . Namely  $\arg \zeta(\frac{1}{2} + iy) = \arg \zeta(2 + iy) + \Delta$ , where  $\Delta = \arg \zeta(\frac{1}{2} + iy) - \arg \zeta(2 + iy)$ . The integration to arbitrarily high  $y$  along  $\Re(z) = 2$  is bounded and gives something relatively small on the principal branch. This can be seen from the Euler product. For  $x > 1$ ,

$$\arg \zeta(x + iy) = \Im \log \zeta(x + iy) = \frac{1}{2i} \sum_p \log \left( \frac{1 - p^{-x+iy}}{1 - p^{-x-iy}} \right) \approx - \sum_p \frac{1}{p^x} \sin(y \log p). \quad (154)$$

For  $x = 2$ ,

$$|\arg \zeta(2 + iy)| < \sum_p \frac{1}{p^2} = 0.452235 \dots \quad (155)$$

The above sum obviously converges since it is less than  $\zeta(2) = \pi^2/6 = 1.645$ .

It is known that  $S(y)$  is unbounded, which implies that the logs in (154), which are Arg's, can accumulate. The roughest estimate is the known fact that  $S(y) = O(\log y)$ , which actually was not written explicitly in Riemann's paper, but only later by von Mangoldt. Such a logarithmic growth apparently should come from the short integration that gives  $\Delta$  of the last paragraph. Assuming the RH, the current best bound is given by [29] (see also [30])

$$|S(y)| \leq \left( \frac{1}{4} + o(1) \right) \frac{\log y}{\log \log y}$$

for  $y \rightarrow \infty$ . It is important to bear in mind that these are upper bounds, and that  $S(y)$  may actually be much smaller.

The first three properties of  $S(y)$  listed below are well-known [2, 20, 28]:

1. At each zero  $\rho = x + iy$  in the critical strip,  $S(y)$  jumps by the multiplicity  $m$  of the zero. This simply follows from the role of  $S(T)$  in the counting formula  $N(T)$  in (141). For instance, simple zeros on the critical line have  $m = 1$ , whereas double zeros on the line have  $m = 2$ . Since zeros off the line at a given height  $y$  always occurs in pairs, i.e.  $\rho$  and  $1 - \rho^*$ , if one of such zeros has multiplicity  $m$ , then  $S(y)$  has to jump by  $2m$  at this height  $y$ . It is believed that all the Riemann zeros are simple, although this is largely a completely open problem.
2. Between zeros, since  $N(y)$  is constant,

$$S'(y) = \partial_y S(y) = -\frac{1}{\pi} \vartheta'(y) < 0, \quad (156)$$

where the last inequality follows because  $\vartheta(y)$  is a monotonically increasing function.

3. The average  $\langle S \rangle$  of  $S(y)$  is zero [2],

$$\langle S \rangle = \lim_{Y \rightarrow \infty} \frac{1}{Y} \int_0^Y dy S(y) = 0. \quad (157)$$

4. A celebrated theorem of Selberg [31] states that  $S(y)$  over a large interval  $0 < y < T$  satisfies a normal distribution with zero mean and variance

$$\overline{S(y)^2} \equiv \frac{1}{T} \int_0^T S(y)^2 dy = \frac{1}{2\pi^2} \log \log T + O\left(\sqrt{\log \log T}\right). \quad (158)$$

The numerical work performed for these lectures did not go higher than  $y = 10^{10}$ . Over this range the variance of  $S(y)$  is approximately 0.16, which implies it is nearly always on the principal branch. For this reason it is typically OK to compute  $\text{Arg}\zeta(\frac{1}{2} + iy)/\pi$  in solving (138) since it almost always equals  $S(y)$ , especially near the zeros. One must bear this in mind when trying to solve (138) and treat this issue with some

care, however for the ranges of  $t$  numerically considered here this did not present any difficulty. For much much higher  $y$ , one needs to keep track of branches to determine the actual arg.

5. Let

$$\Delta S_n \equiv S(y_n) - S(y_{n+1}) = \frac{1}{\pi} (\vartheta(y_{n+1}) - \vartheta(y_n)) \quad (159)$$

where the equality follows from (156). Then, if the RH is true,  $\Delta S_n$  has to compensate the jumps by 1 at each simple zero, and since  $\langle S \rangle = 0$ , one expects

$$\langle \Delta S_n \rangle = 1. \quad (160)$$

There is one more property we will need, which is a precise statement of the fact that the real part of  $\zeta(\frac{1}{2} + iy)$  is *almost always* positive. Let  $y_n^{(+)}$  and  $y_n^{(-)}$ , where  $n = 1, 2, \dots$ , denote the points where either the imaginary or real part, respectively, of  $\zeta(\frac{1}{2} + iy)$  are zero, but not both. These points are easy to find since they do not depend on the fluctuating  $S(y)$ . We have

$$\zeta(\frac{1}{2} - iy) = \zeta(\frac{1}{2} + iy) G(y), \quad G(y) = e^{2i\vartheta(y)} \quad (161)$$

where  $\vartheta(y)$  is the smooth Riemann-Siegel function (137). Since the real and imaginary parts are not both zero, at  $y_n^{(+)}$  then  $G = 1$ , whereas at  $y_n^{(-)}$  then  $G = -1$ . Thus

$$\Im [\zeta(\frac{1}{2} + iy_n^{(+)})] = 0 \quad \text{for } \vartheta(y_n^{(+)}) = (n-1)\pi, \quad (162)$$

$$\Re [\zeta(\frac{1}{2} + iy_n^{(-)})] = 0 \quad \text{for } \vartheta(y_n^{(-)}) = (n - \frac{1}{2})\pi. \quad (163)$$

Our convention is  $n = 1$  for the first point where this occurs for  $y > 0$ . Using the approximation (139), equations (162) and (163) can be written in the form  $\frac{y}{2\pi} \log\left(\frac{y}{2\pi e}\right) = A_n$ , which through the transformation  $y \rightarrow 2\pi A_n x^{-1}$  can be solved in terms of the Lambert  $W$ -function (see section XII). The result is

$$y_n^{(+)} \approx \frac{2\pi(n - 7/8)}{W[e^{-1}(n - 7/8)]}, \quad y_n^{(-)} \approx \frac{2\pi(n - 3/8)}{W[e^{-1}(n - 3/8)]}, \quad (164)$$

where above  $n = 1, 2, \dots$  and  $W$  denotes the principal branch  $W_0$ . The  $y_n^{(+)}$  are actually the Gram points. From (164) we can see that these points are ordered in a regular manner,

$$y_1^{(+)} < y_1^{(-)} < y_2^{(+)} < y_2^{(-)} < y_3^{(+)} < y_3^{(-)} < \dots \quad (165)$$

as illustrated in Figure 15 (left).

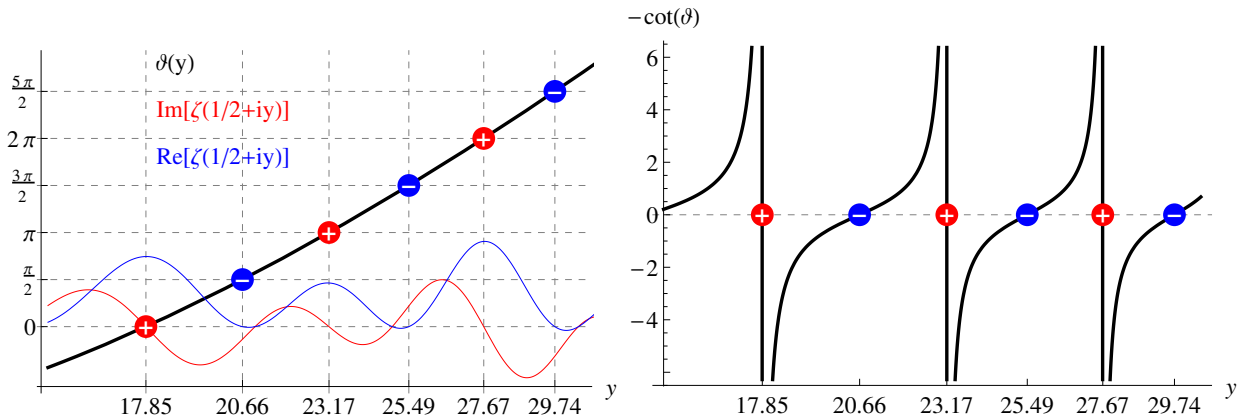


FIG. 15. *Left:* the  $y_n^{(+)}$  (red balls) are the Gram points, where  $\Im [\zeta (\frac{1}{2} + iy)] = 0$ , and  $y_n^{(-)}$  (blue balls) are the points where  $\Re [\zeta (\frac{1}{2} + iy)] = 0$ . These points are determined approximately from formulas (164). *Right:* A plot of (166) indicating the points (164).

The ratio

$$\frac{\Re [\zeta (\frac{1}{2} + iy)]}{\Im [\zeta (\frac{1}{2} + iy)]} = -\cot \vartheta(y) \quad (166)$$

has a regular repeating pattern, as can be seen in Figure 15 (right), thus the signs of the real and imaginary parts are related in a specific manner. From this figure one sees that when the imaginary part is negative the real part is positive.

6. The statement we need about the real part being mainly positive concerns the average value of the real part at the points  $y_n^{(+)}$ . The average of the real part of  $\zeta (\frac{1}{2} + iy)$  at the Gram points  $y_n^{(+)}$  is [20]

$$\lim_{N \rightarrow \infty} \frac{1}{N} \sum_{n=1}^N \Re [\zeta (\frac{1}{2} + iy_n^{(+)})] = 2. \quad (167)$$

Now, let us consider the behavior of  $S(y)$  starting from the first zero. At the first zero, in the jump by 1,  $S(y)$  passes through zero and remains on the principle branch (see Figure 12). The branch cut in the  $z$ -plane is along the negative  $x$ -axis, thus on the principle branch  $-1 < S(y) \leq 1$ . At the points  $y_n^{(+)}$ , where the imaginary part is zero, the vast majority of them have  $\Re [\zeta (\frac{1}{2} + iy_n^{(+)})] > 0$  according to item 6 above, and thus for the most part  $S(y_n^{(+)}) = 0$ . Thus  $S(y) = 0$  at infinitely many points  $y_n^{(+)}$  between zeros, consistent with  $\langle S \rangle = 0$ .

At the relatively rare points  $y_n^{(+)}$  where  $\Re [\zeta (\frac{1}{2} + iy_n^{(+)})] < 0$ ,  $S(y)$  crosses one of the lines  $S(y) = \pm 1$ . Taking into account the properties and 5 and 6, one expects that  $S(y)$  primarily stays in the principle branch, i.e. it can pass to another branch, it has to otherwise it cannot grow as  $\log y$ , but it must return to the principal branch in order for  $\langle S \rangle = 0$ . An example where this occurs is close to the point  $y_{127}^{(+)} = 282.455$ . The function starts to change branch,

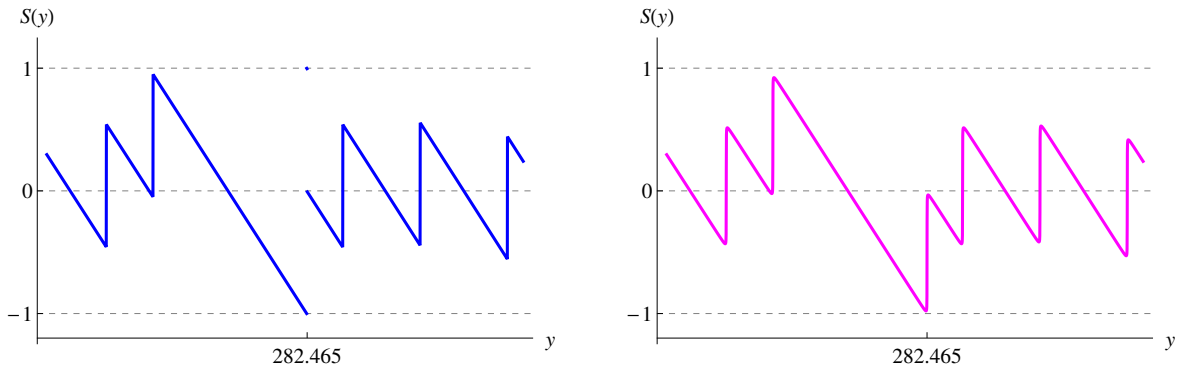


FIG. 16. *Left:*  $S(y)$  in the vicinity of the first point where  $|S(y)| > 1$ , at  $y_{127}^{(+)} = 282.455$ . There is a zero at  $y_{127} = 282.465$ . *Right:* by adding a  $\delta$  in  $S(y) = \frac{1}{\pi} \arg \zeta\left(\frac{1}{2} + \delta + iy\right)$  we can smooth out the curve such that it stays in the principal branch.

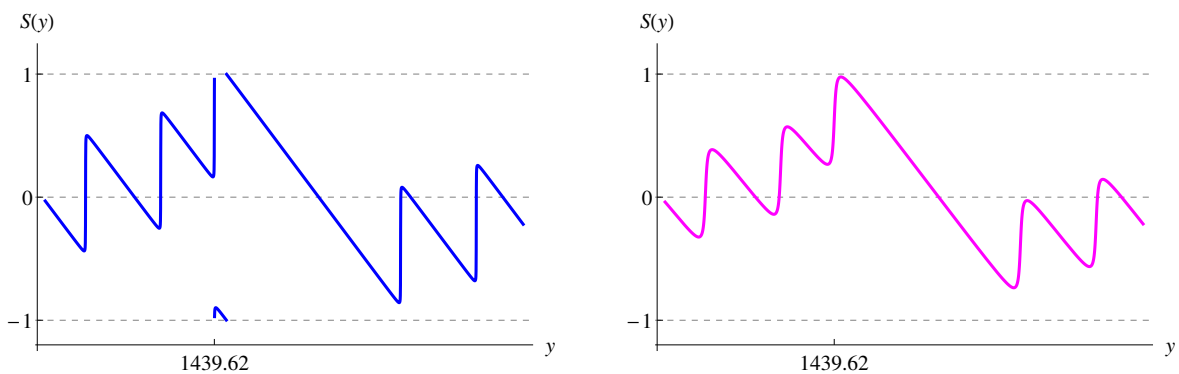


FIG. 17. *Left:*  $S(y)$  on the principle branch in the vicinity of  $y_{1017}^{(+)} = 1439.778$  where  $S(y) > 1$ . *Right:* we have included a non-zero  $\delta$  to smooth out the function, and it stays in the principal branch.

and as soon as it crosses the branch cut, there is a Riemann zero at  $y_{127} = 282.465$  so  $S(y)$  jumps by 1 coming back to the principal branch again. This behavior is shown Figure 16 and one sees that  $S(y)$  just barely touches  $-1$ .

In Figure 17 (left) we plot  $S(y)$  on the principle branch in the vicinity of another point where  $S(y)$  passes to another branch. This time it passes to another branch while jumping at the zero  $y_{1018} = 1439.623$ . The real part is negative for  $y_{1017}^{(+)} = 1439.778$ . Since  $S'(y) < 0$  it comes back to the principal branch pretty quickly. The interpretation of this figure is that  $S(y)$  has changed branch: the dangling part of the curve at the bottom should be shifted by 2 to make  $S(y)$  continuous. By including a  $\delta$  we can smooth out the curve to make it continuous and to stay in the principal branch, as shown in Figure 17 (right), and this is a better rendition of the actual behavior.

Note that at the rare points where  $|S(y)| \geq 1$ , it strays off the principle branch but quickly returns to it. In Figure 18 (left) we plot  $S(y)$  around the  $10^5$ -th zero, and one sees that it is still on the principle branch.

There is a well-known counter example to the RH based on the Davenport-Heilbronn



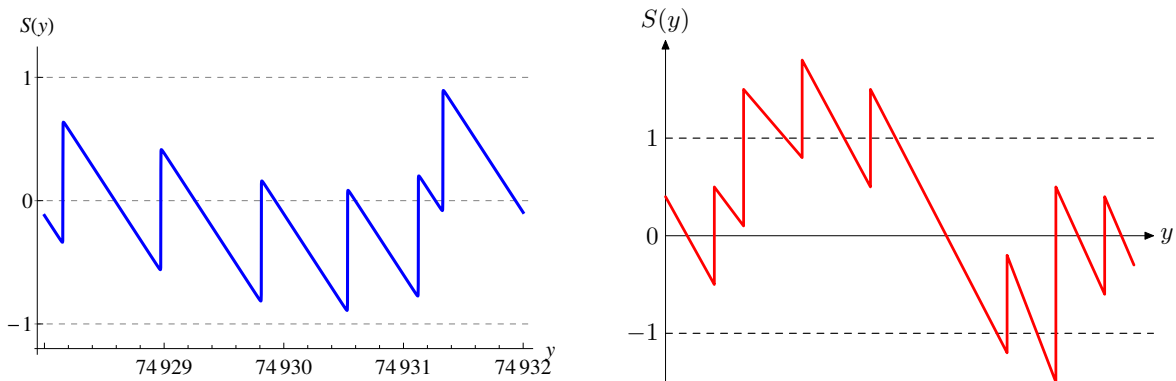


FIG. 18. *Left:* behavior of  $S(y)$  around the  $10^5$ -th zero. *Right:* hypothetical, potentially more dramatic behavior of  $S(y)$  although we have not observed this numerically in the range of  $y$  we have explored.

function. It has a functional equation like  $\zeta$ , but is known to have zeros off of the critical line. We will study this function in section XIX, and explain how the properties of  $S(y)$  described in this section are violated. In short, at a zero off of the line there is a change of branch in such a manner that the analog of  $S(y)$  is ill defined, and there is thus no solution to the transcendental equation at these points, so the argument that  $N_0(T) = N(T)$  fails.

## IX. ZEROS OF DIRICHLET $L$ -FUNCTIONS

### A. Some properties of Dirichlet $L$ -functions

We now consider the generalization of the previous results for the  $\zeta$ -function to Dirichlet  $L$ -functions. The main arguments are the same as for  $\zeta$ , thus we do not repeat all of the statements in section VII.

Much less is known about the zeros of  $L$ -functions in comparison with the  $\zeta$ -function, however let us mention a few works. Selberg [32] obtained the analog of Riemann-von Mangoldt counting formula (133) for Dirichlet  $L$ -functions. Based on this result, Fujii [33] gave an estimate for the number of zeros on the critical strip with the ordinate between  $[T + H, T]$ . The distribution of low lying zeros of  $L$ -functions near and at the critical line was examined in [34], assuming the *generalized Riemann hypothesis* (GRH). The statistics of the zeros, i.e. the analog of the Montgomery-Odlyzko conjecture, were studied in [35, 36]. It is also known that more than half of the non-trivial zeros of Dirichlet  $L$ -functions are on the critical line [37]. For a more detailed introduction to  $L$ -functions see [38].

Let us first introduce the basic ingredients and definitions regarding this class of functions, which are all well known [8]. Dirichlet  $L$ -series are defined as

$$L(z, \chi) = \sum_{n=1}^{\infty} \frac{\chi(n)}{n^z} \quad (\Re(z) > 1) \quad (168)$$

where the arithmetic function  $\chi(n)$  is a Dirichlet character. They enjoy an Euler product formula

$$L(z, \chi) = \prod_p \frac{1}{1 - \chi(p) p^{-z}} \quad (\operatorname{Re}(z) > 1). \quad (169)$$

They can all be analytically continued to the entire complex plane, except for a simple pole at  $z = 1$ , and are then referred to as Dirichlet  $L$ -functions.

There are an infinite number of distinct Dirichlet characters which are primarily characterized by their modulus  $k$ , which determines their periodicity. They can be defined axiomatically, which leads to specific properties, some of which we now describe. Consider a Dirichlet character  $\chi \pmod{k}$ , and let the symbol  $(n, k)$  denote the greatest common divisor of the two integers  $n$  and  $k$ . Then  $\chi$  has the following properties:

1.  $\chi(n + k) = \chi(n)$ .
2.  $\chi(1) = 1$  and  $\chi(0) = 0$ .
3.  $\chi(nm) = \chi(n)\chi(m)$ .
4.  $\chi(n) = 0$  if  $(n, k) > 1$  and  $\chi(n) \neq 0$  if  $(n, k) = 1$ .
5. If  $(n, k) = 1$  then  $\chi(n)^{\varphi(k)} = 1$ , where  $\varphi(k)$  is the Euler totient arithmetic function. This implies that  $\chi(n)$  are roots of unity.
6. If  $\chi$  is a Dirichlet character so is the complex conjugate  $\chi^*$ .

For a given modulus  $k$  there are  $\varphi(k)$  distinct Dirichlet characters, which essentially follows from property 5 above. They can thus be labeled as  $\chi_{k,j}$  where  $j = 1, 2, \dots, \varphi(k)$  denotes an arbitrary ordering. If  $k = 1$  we have the *trivial* character where  $\chi(n) = 1$  for every  $n$ , and (168) reduces to the Riemann  $\zeta$ -function. The *principal* character, usually denoted by  $\chi_1$ , is defined as  $\chi_1(n) = 1$  if  $(n, k) = 1$  and zero otherwise. In the above notation the principal character is always  $\chi_{k,1}$ .

Characters can be classified as *primitive* or *non-primitive*. Consider the Gauss sum

$$G(\chi) = \sum_{m=1}^k \chi(m) e^{2\pi i m/k}. \quad (170)$$

If the character  $\chi \pmod{k}$  is primitive, then

$$|G(\chi)|^2 = k. \quad (171)$$

This is no longer valid for a non-primitive character. Consider a non-primitive character  $\bar{\chi} \pmod{\bar{k}}$ . Then it can be expressed in terms of a primitive character of smaller modulus as  $\bar{\chi}(n) = \bar{\chi}_1(n)\chi(n)$ , where  $\bar{\chi}_1$  is the principal character  $\pmod{\bar{k}}$  and  $\chi$  is a primitive

character mod  $k < \bar{k}$ , where  $k$  is a divisor of  $\bar{k}$ . More precisely,  $k$  must be the *conductor* of  $\bar{\chi}$  (see [8] for further details). In this case the two  $L$ -functions are related as  $L(z, \bar{\chi}) = L(z, \chi) \prod_{p|\bar{k}} (1 - \chi(p)/p^z)$ . Thus  $L(z, \bar{\chi})$  has the same zeros as  $L(z, \chi)$ . The principal character is only primitive when  $k = 1$ , which yields the  $\zeta$ -function. The simplest example of non-primitive characters are all the principal ones for  $k \geq 2$ , whose zeros are the same as the  $\zeta$ -function. Let us consider another example with  $\bar{k} = 6$ , where  $\varphi(6) = 2$ , namely  $\bar{\chi}_{6,2}$ , whose components are<sup>9</sup>

$$\begin{array}{c|cccccc} n & 1 & 2 & 3 & 4 & 5 & 6 \\ \hline \bar{\chi}_{6,2}(n) & 1 & 0 & 0 & 0 & -1 & 0 \end{array} \quad (172)$$

In this case, the only divisors are 2 and 3. Since  $\chi_1 \bmod 2$  is non-primitive, it is excluded. We are left with  $k = 3$  which is the conductor of  $\bar{\chi}_{6,2}$ . Then we have two options;  $\chi_{3,1}$  which is the non-primitive principal character mod 3, thus excluded, and  $\chi_{3,2}$  which is primitive. Its components are

$$\begin{array}{c|ccc} n & 1 & 2 & 3 \\ \hline \chi_{3,2}(n) & 1 & -1 & 0 \end{array} \quad (173)$$

Note that  $|G(\chi_{6,2})|^2 = 3 \neq 6$  and  $|G(\chi_{3,2})|^2 = 3$ . In fact one can check that  $\bar{\chi}_{6,2}(n) = \bar{\chi}_{6,1}(n)\chi_{3,2}(n)$ , where  $\bar{\chi}_{6,1}$  is the principal character mod  $\bar{k} = 6$ . Thus the zeros of  $L(z, \bar{\chi}_{6,2})$  are the same as those of  $L(z, \chi_{3,2})$ . Therefore, it suffices to consider primitive characters, and we will henceforth do so.

We will need the functional equation satisfied by  $L(z, \chi)$ . Let  $\chi$  be a *primitive* character. Define its *order*  $a$  such that

$$a \equiv \begin{cases} 1 & \text{if } \chi(-1) = -1 \text{ (odd),} \\ 0 & \text{if } \chi(-1) = 1 \text{ (even).} \end{cases} \quad (174)$$

Let us define the meromorphic function

$$\Lambda(z, \chi) \equiv \left(\frac{k}{\pi}\right)^{\frac{z+a}{2}} \Gamma\left(\frac{z+a}{2}\right) L(z, \chi). \quad (175)$$

Then  $\Lambda$  satisfies the well known functional equation [8]

$$\Lambda(z, \chi) = \frac{i^{-a} G(\chi)}{\sqrt{k}} \Lambda(1-z, \chi^*). \quad (176)$$

The above equation is only valid for primitive characters.

---

<sup>9</sup>Our enumeration convention for the  $j$ -index of  $\chi_{k,j}$  is taken from Mathematica.

### B. Exact equation for the $n$ -th zero

For a primitive character, since  $|G(\chi)| = \sqrt{k}$ , the factor on the right hand side of (176) is a phase. It is thus possible to obtain a more symmetric form through a new function defined as

$$\xi(z, \chi) \equiv \frac{i^{a/2} k^{1/4}}{\sqrt{G(\chi)}} \Lambda(z, \chi). \quad (177)$$

It then satisfies

$$\xi(z, \chi) = \xi^*(1 - z, \chi) \equiv (\xi(1 - z^*, \chi))^*. \quad (178)$$

Above, the function  $\xi^*$  of  $z$  is defined as the complex conjugation of all coefficients that define  $\xi$ , namely  $\chi$  and the  $i^{a/2}$  factor, evaluated at a non-conjugated  $z$ .

Note that  $(\Lambda(z, \chi))^* = \Lambda(z^*, \chi^*)$ . Using the well known result

$$G(\chi^*) = \chi(-1) (G(\chi))^* \quad (179)$$

we conclude that

$$(\xi(z, \chi))^* = \xi(z^*, \chi^*). \quad (180)$$

This implies that if the character is real, then if  $\rho$  is a zero of  $\xi$  so is  $\rho^*$ , and one needs only consider  $\rho$  with positive imaginary part. On the other hand if  $\chi \neq \chi^*$ , then the zeros with negative imaginary part are different than  $\rho^*$ . For the trivial character where  $k = 1$  and  $a = 0$ , implying  $\chi(n) = 1$  for any  $n$ , then  $L(z, \chi)$  reduces to the Riemann  $\zeta$ -function and (178) yields the well known functional equation (116).

Let  $z = x + iy$ . Then the function (177) can be written as

$$\xi(z, \chi) = Ae^{i\theta} \quad (181)$$

where

$$A(x, y, \chi) = \left(\frac{k}{\pi}\right)^{\frac{x+a}{2}} \left| \Gamma\left(\frac{x+a+iy}{2}\right) \right| |L(x+iy, \chi)|, \quad (182)$$

$$\theta(x, y, \chi) = \arg \Gamma\left(\frac{x+a+iy}{2}\right) - \frac{y}{2} \log\left(\frac{\pi}{k}\right) - \frac{1}{2} \arg G(\chi) + \arg L(x+iy, \chi) + \frac{\pi a}{4}. \quad (183)$$

From (180) we also conclude that  $A(x, y, \chi) = A(x, -y, \chi^*)$  and  $\theta(x, y, \chi) = -\theta(x, -y, \chi^*)$ . Denoting

$$\xi^*(1 - z, \chi) = A'e^{-i\theta'} \quad (184)$$

we have

$$A'(x, y, \chi) = A(1 - x, y, \chi), \quad \theta'(x, y, \chi) = \theta(1 - x, y, \chi). \quad (185)$$

Taking the modulus of (178) we also have that  $A(x, y, \chi) = A'(x, y, \chi)$  for any  $z$ .

On the critical strip, the functions  $L(z, \chi)$  and  $\xi(z, \chi)$  have the same zeros. Thus on a zero we clearly have

$$\lim_{z \rightarrow \rho} \{\xi(z, \chi) + \xi^*(1 - z, \chi)\} = 0. \quad (186)$$

Let us define

$$B(x, y, \chi) \equiv e^{i\theta(x, y, \chi)} + e^{-i\theta'(x, y, \chi)}. \quad (187)$$

Since  $A = A'$  everywhere, and taking separate limits in (186) we therefore have

$$\lim_{z' \rightarrow \rho} \lim_{z \rightarrow \rho} A(x', y', \chi) B(x, y, \chi) = 0. \quad (188)$$

Considering the  $z \rightarrow \rho$  limit, a potential zero occurs when

$$\lim_{z \rightarrow \rho} B(x, y, \chi) = 0. \quad (189)$$

The general solution of this equation is thus given by

$$\theta + \theta' = (2n + 1)\pi. \quad (190)$$

Until now, the path to approach the zero  $z \rightarrow \rho$  was not specified. Now we put ourselves on the critical line  $x = 1/2$ , and the path will be chosen as  $z = \rho + \delta$  with  $0 < \delta \ll 1$ . Then  $\theta = \theta'$  and (190) yields

$$\lim_{\delta \rightarrow 0^+} \theta\left(\frac{1}{2} + \delta, y\right) = \left(n + \frac{1}{2}\right)\pi. \quad (191)$$

Let us define the function

$$\vartheta_{k,a}(y) \equiv \Im \left[ \log \Gamma \left( \frac{1}{4} + \frac{a}{2} + i \frac{y}{2} \right) \right] - \frac{y}{2} \log \left( \frac{\pi}{k} \right). \quad (192)$$

When  $k = 1$  and  $a = 0$ , the function (192) is just the usual Riemann-Siegel  $\vartheta$  function (137). Thus (191) gives the equation

$$\vartheta_{k,a}(y_n) + \lim_{\delta \rightarrow 0^+} \arg L\left(\frac{1}{2} + \delta + iy_n, \chi\right) - \frac{1}{2} \arg G(\chi) + \frac{\pi a}{4} = \left(n + \frac{1}{2}\right)\pi. \quad (193)$$

Analyzing the left hand side of (193) we can see that it has a minimum, thus we shift  $n \rightarrow n - (n_0 + 1)$  for a given  $n_0$ , to label the zeros according to the convention that the first positive zero is labelled by  $n = 1$ . Thus the upper half of the critical line will have the zeros labelled by  $n = 1, 2, \dots$  corresponding to positive  $y_n$ , while the lower half will have the negative values  $y_n$  labelled by  $n = 0, -1, \dots$ . The integer  $n_0$  depends on  $k$ ,  $a$  and  $\chi$ , and should be chosen according to each specific case. In the cases we analyze below  $n_0 = 0$ , whereas for the trivial character  $n_0 = 1$ . In practice, the value of  $n_0$  can always be determined by plotting (193) with  $n = 1$ , passing all terms to its left hand side. Then it is

trivial to adjust the integer  $n_0$  such that the graph passes through the point  $(y_1, 0)$  for the first jump, corresponding to the first positive solution. Henceforth we will *omit* the integer  $n_0$  in the equations, since all cases analyzed in the following have  $n_0 = 0$ . Nevertheless, the reader should bear in mind that for other cases, it may be necessary to replace  $n \rightarrow n - n_0$  in the following equations.

In summary, these zeros have the form  $\rho_n = \frac{1}{2} + iy_n$ , where for a given  $n \in \mathbb{Z}$ , the imaginary part  $y_n$  is the solution of the equation

$$\vartheta_{k,a}(y_n) + \lim_{\delta \rightarrow 0^+} \arg L\left(\frac{1}{2} + \delta + iy_n, \chi\right) - \frac{1}{2} \arg G(\chi) = \left(n - \frac{1}{2} - \frac{a}{4}\right) \pi. \quad (194)$$

### C. Asymptotic equation for the $n$ -th zero

From Stirling's formula we have the following asymptotic form for  $y \rightarrow \pm\infty$ :

$$\vartheta_{k,a}(y) = \operatorname{sgn}(y) \left( \frac{|y|}{2} \log \left( \frac{k|y|}{2\pi e} \right) + \frac{2a-1}{8} \pi + O(1/y) \right). \quad (195)$$

The first order approximation of (194), i.e. neglecting terms of  $O(1/y)$ , is given by

$$\sigma_n \frac{|y_n|}{2\pi} \log \left( \frac{k|y_n|}{2\pi e} \right) + \frac{1}{\pi} \lim_{\delta \rightarrow 0^+} \arg L\left(\frac{1}{2} + \delta + i\sigma_n |y_n|, \chi\right) - \frac{1}{2\pi} \arg G(\chi) = \alpha_n, \quad (196)$$

where

$$\alpha_n = n + \frac{\sigma_n - 4 - 2a(1 + \sigma_n)}{8}. \quad (197)$$

Above  $\sigma_n = 1$  if  $n > 0$  and  $\sigma_n = -1$  if  $n \leq 0$ . For  $n > 0$  we have  $y_n = |y_n|$  and for  $n \leq 0$   $y_n = -|y_n|$ .

### D. Counting formulas

Let us define  $N_0^+(T, \chi)$  as the number of zeros on the critical line with  $0 < \Im(\rho) < T$  and  $N_0^-(T, \chi)$  as the number of zeros with  $-T < \Im(\rho) < 0$ . As explained before,  $N_0^+(T, \chi) \neq N_0^-(T, \chi)$  if the characters are complex numbers, since the zeros are not symmetrically distributed between the upper and lower half of the critical line.

The counting formula  $N_0^+(T, \chi)$  is obtained from (194) by replacing  $y_n \rightarrow T$  and  $n \rightarrow N_0^+ + 1/2$ , therefore

$$N_0^+(T, \chi) = \frac{1}{\pi} \vartheta_{k,a}(T) + \frac{1}{\pi} \arg L\left(\frac{1}{2} + iT, \chi\right) - \frac{1}{2\pi} \arg G(\chi) + \frac{a}{4}. \quad (198)$$

The passage from (194) to (198) is justified under the assumptions already discussed in connection with (132) and (140), i.e. assuming that (194) has a unique solution for every  $n$ .

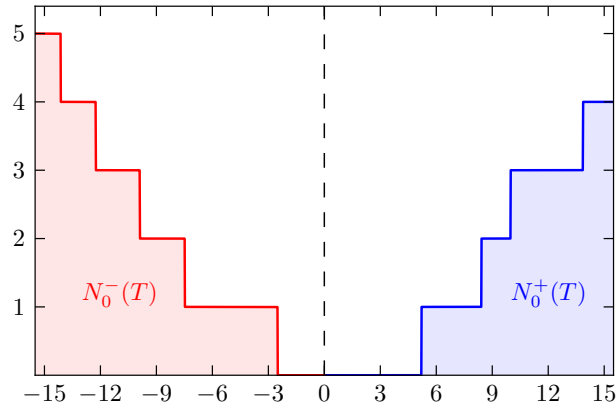


FIG. 19. Exact counting formulae (198) and (199). Note that they are not symmetric with respect to the origin, since the  $L$ -zeros for complex  $\chi$  are not complex conjugates. We used  $\chi = \chi_{7,2}$  (235).

Analogously, the counting formula on the lower half line is given by

$$N_0^-(T, \chi) = \frac{1}{\pi} \vartheta_{k,a}(T) - \frac{1}{\pi} \arg L\left(\frac{1}{2} - iT, \chi\right) + \frac{1}{2\pi} \arg G(\chi) - \frac{a}{4}. \quad (199)$$

Note that in (198) and (199)  $T$  is positive. Both cases are plotted in Figure 19 for the character  $\chi_{7,2}$  shown in (235). One can notice that they are precisely staircase functions, jumping by one at each zero. Note also that the functions are not symmetric about the origin, since for a complex  $\chi$  the zeros on upper and lower half lines are not simply complex conjugates.

From (195) we also have the first order approximation for  $T \rightarrow \infty$ ,

$$N_0^+(T, \chi) = \frac{T}{2\pi} \log\left(\frac{kT}{2\pi e}\right) + \frac{1}{\pi} \arg L\left(\frac{1}{2} + iT, \chi\right) - \frac{1}{2\pi} \arg G(\chi) - \frac{1}{8} + \frac{a}{2}. \quad (200)$$

Analogously, for the lower half line we have

$$N_0^-(T, \chi) = \frac{T}{2\pi} \log\left(\frac{kT}{2\pi e}\right) - \frac{1}{\pi} \arg L\left(\frac{1}{2} - iT, \chi\right) + \frac{1}{2\pi} \arg G(\chi) - \frac{1}{8}. \quad (201)$$

As in (194), again we are omitting  $n_0$  since in the cases below  $n_0 = 0$ , but for other cases one may need to include  $\pm n_0$  on the right hand side of  $N_0^\pm$ , respectively.

It is known that the number of zeros on the *entire critical strip* up to height  $T$ , i.e. in the region  $\{0 < x < 1, 0 < y < T\}$ , is given by [39]

$$N^+(T, \chi) = \frac{1}{\pi} \vartheta_{k,a}(T) + \frac{1}{\pi} \arg L\left(\frac{1}{2} + iT, \chi\right) - \frac{1}{\pi} \arg L\left(\frac{1}{2}, \chi\right). \quad (202)$$

This formula follows from a straightforward generalization of the method shown in Ap-

pendix B for the  $\zeta$ -function. From Stirling's approximation and using

$$2a - 1 = -\chi(-1), \quad (203)$$

for  $T \rightarrow \infty$  we obtain the asymptotic approximation [32, 39]

$$N^+(T, \chi) = \frac{T}{2\pi} \log \left( \frac{kT}{2\pi e} \right) + \frac{1}{\pi} \arg L \left( \frac{1}{2} + iT, \chi \right) - \frac{1}{\pi} \arg L \left( \frac{1}{2}, \chi \right) - \frac{\chi(-1)}{8} + O(1/T). \quad (204)$$

Both formulas (202) and (204) are exactly the same as (198) and (200), respectively. This can be seen as follows. From (178) we conclude that  $\xi$  is real on the critical line. Thus

$$\arg \xi \left( \frac{1}{2} \right) = 0 = -\frac{1}{2} \arg G(\chi) + \arg L \left( \frac{1}{2}, \chi \right) + \frac{\pi a}{4}. \quad (205)$$

Then, replacing  $\arg G$  in (194) we obtain

$$\vartheta_{k,a}(y_n) + \lim_{\delta \rightarrow 0^+} \arg L \left( \frac{1}{2} + \delta + iy_n, \chi \right) - \arg L \left( \frac{1}{2}, \chi \right) = \left( n - \frac{1}{2} \right) \pi. \quad (206)$$

Replacing  $y_n \rightarrow T$  and  $n \rightarrow N_0^+ + 1/2$  in (206) we have precisely the expression (202), and also (204) for  $T \rightarrow \infty$ . Therefore, we conclude that  $N_0^+(T, \chi) = N^+(T, \chi)$  exactly. From (180) we see that negative zeros for character  $\chi$  correspond to positive zeros for character  $\chi^*$ . Then for  $-T < \Im(\rho) < 0$  the counting on the strip also coincides with the counting on the line, since  $N_0^-(T, \chi) = N_0^+(T, \chi^*)$  and  $N^-(T, \chi) = N^+(T, \chi^*)$ . Therefore, the number of zeros on the whole *critical strip* is the same as the number of zeros on the *critical line* obtained as solutions of (194). This is valid under the assumption that (194) has a unique solution for every  $n$ .

## X. ZEROS OF $L$ -FUNCTIONS BASED ON MODULAR FORMS

Let us generalize the previous results to  $L$ -functions based on level one modular forms. We first recall some basic definitions and properties. The *modular group* can be represented by the set of  $2 \times 2$  integer matrices

$$SL_2(\mathbb{Z}) = \left\{ A = \begin{pmatrix} a & b \\ c & d \end{pmatrix} \mid a, b, c, d \in \mathbb{Z}, \det A = 1 \right\}, \quad (207)$$

provided each matrix  $A$  is identified with  $-A$ , i.e.  $\pm A$  are regarded as the same transformation. Thus for  $\tau$  in the upper half complex plane, it transforms as

$$\tau \mapsto A\tau = \frac{a\tau + b}{c\tau + d}$$



under the action of the modular group. A *modular form*  $f$  of weight  $k$  is a function that is analytic in the upper half complex plane which satisfies the functional relation [40]

$$f\left(\frac{a\tau + b}{c\tau + d}\right) = (c\tau + d)^k f(\tau). \quad (208)$$

If the above equation is satisfied for all of  $SL_2(\mathbb{Z})$ , then  $f$  is referred to as being of *level one*. It is possible to define higher level modular forms which satisfy the above equation for a subgroup of  $SL_2(\mathbb{Z})$ . Since our results are easily generalized to the higher level case, henceforth we will only consider level one forms.

For the  $SL_2(\mathbb{Z})$  element  $\begin{pmatrix} 1 & 1 \\ 0 & 1 \end{pmatrix}$ , the above implies the periodicity  $f(\tau) = f(\tau + 1)$ , thus it has a Fourier series

$$f(\tau) = \sum_{n=0}^{\infty} a_f(n) q^n, \quad q \equiv e^{2\pi i\tau}. \quad (209)$$

If  $a_f(0) = 0$  then  $f$  is called a *cusp form*.

From the Fourier coefficients, one can define the Dirichlet series

$$L_f(z) = \sum_{n=1}^{\infty} \frac{a_f(n)}{n^z}. \quad (210)$$

The functional equation relates  $L_f(z)$  to  $L_f(k - z)$ , so that the critical line is  $\Re(z) = k/2$ , where  $k \geq 4$  is an even integer. One can always shift the critical line to  $1/2$  by replacing  $a_f(n) \rightarrow a_f(n)/n^{(k-1)/2}$ , however we will not do this here. Let us define

$$\Lambda_f(z) \equiv (2\pi)^{-z} \Gamma(z) L_f(z). \quad (211)$$

Then the functional equation is given by [40]

$$\Lambda_f(z) = (-1)^{k/2} \Lambda_f(k - z). \quad (212)$$

There are only two cases to consider since  $k/2$  can be an even or an odd integer. As in (177) we can absorb the extra minus sign factor for the odd case. Thus we define  $\xi_f(z) \equiv \Lambda_f(z)$  for  $k/2$  even, and we have  $\xi_f(z) = \xi_f(k - z)$ , and  $\xi_f(z) \equiv e^{-i\pi/2} \Lambda_f(z)$  for  $k/2$  odd, implying  $\xi_f(z) = \xi_f^*(k - z)$ . Representing  $\xi_f(z) = |\xi_f| e^{i\theta}$  where  $z = x + iy$ , we follow exactly the same steps as in the previous sections. From the solution (190) we conclude that there are infinite zeros on the critical line  $\Re(\rho) = k/2$  determined by  $\lim_{\delta \rightarrow 0^+} \theta\left(\frac{k}{2} + \delta, y, \chi\right) = \left(n - \frac{1}{2}\right) \pi$ . Therefore, these zeros have the form  $\rho_n = \frac{k}{2} + iy_n$ , where  $y_n$  is the solution of the equation

$$\vartheta_k(y_n) + \lim_{\delta \rightarrow 0^+} \arg L_f\left(\frac{k}{2} + \delta + iy_n\right) = \left(n - \frac{1 + (-1)^{k/2}}{4}\right) \pi \quad (213)$$

for  $n = 1, 2, \dots$ , and we have defined

$$\vartheta_k(y) \equiv \Im [\log \Gamma (\frac{k}{2} + iy)] - y \log 2\pi. \quad (214)$$

This implies that the number of solutions of (213) with  $0 < y < T$  is given by

$$N_0(T) = \frac{1}{\pi} \vartheta_k(T) + \frac{1}{\pi} \arg L_f (\frac{k}{2} + iT) - \frac{1 - (-1)^{k/2}}{4}. \quad (215)$$

In the limit of large  $y_n$ , neglecting terms of  $O(1/y)$ , the equation (213) becomes

$$y_n \log \left( \frac{y_n}{2\pi e} \right) + \lim_{\delta \rightarrow 0^+} \arg L_f \left( \frac{k}{2} + \delta + iy_n \right) = \left( n - \frac{k + (-1)^{k/2}}{4} \right) \pi. \quad (216)$$

## XI. THE LAMBERT W-FUNCTION

The following section, and even more, section XX, will involve the Lambert- $W$  function, thus we review its most important properties in this section. The basic facts about the  $W$ -function that we present, including some history, are essentially based on [41], where the reader can also find more details.

In 1758 Lambert solved the equation  $x = q + x^m$ , expressing  $x$ , and also powers  $x^\alpha$ , as power series in  $q$ . A few years later Euler considered a more symmetric version of this equation through the substitution  $x \rightarrow x^{-\beta}$ ,  $q \rightarrow (\alpha - \beta)v$  and  $m \rightarrow \frac{\alpha}{\beta}$ . Then taking the limit  $\beta \rightarrow \alpha$  one obtains  $\log x = vx^\alpha$ . This equation can be written in the form  $\log x = vx$  through  $x^\alpha \rightarrow x$  and  $\alpha v \rightarrow v$ . Thus, exponentiating the last equation and introducing the variables  $z = -v$  and  $W(z) = -vx$ , we obtain the equation

$$W(z) e^{W(z)} = z. \quad (217)$$

$W(z)$  is called the *Lambert function*, and (217) is its defining equation. Although its power series approximation was considered for the first time by Lambert and Euler, this function only started to be effectively studied during the past 20 years. The  $W$ -function should be considered as a new elementary function, since it cannot be expressed in terms of the other known elementary functions.

Johan Heinrich Lambert was born in Mulhouse (a French city bordering with Switzerland and Germany) in 1728, and died in Berlin in 1777. Lambert was a self educated mathematician having a broad range of scientific interests. He contributed to number theory, geometry, statistics, astronomy, cosmology and philosophy, just to name a few areas. He is responsible for the modern notation of hyperbolic functions, and was the first one to prove the irrationality of  $\pi$ . When Euler considered the solution to equation  $\log x = vx$ , he gave credit to Lambert. The translation of his paper's title is "On a series of Lambert and some

of its significant properties". It seems that Euler learned about Lambert's result from a conversation between both when Lambert was travelling from Zürich to Berlin. Euler described his excitement in a letter to Goldbach in 1764.

Leaving history aside, let us now consider the  $W$ -function defined through (217) over a complex field,  $z \in \mathbb{C}$ .  $W(z)$  is not a single-valued function, so we need to introduce its branch structure. This is done following the same branch structure of  $\log z$ , that we now recall. If  $u = \log z$  then for every  $z$  we have  $e^u = z$ . However, note that  $u$  is not uniquely defined since  $u \rightarrow u + 2\pi ki$  for  $k \in \mathbb{Z}$  will give the same  $z$ . Thus it is necessary to divide the complex  $u$ -plane in regions which are single-valued related to the  $z$ -plane. Each of these regions is called a *branch* and is labelled by  $k$ . The way one partitions the  $u$ -plane is a convention. The most convenient way is to define the  $k$ -th branch as the region on the  $u$ -plane limited by

$$(2k - 1)\pi < \Im(u) \leq (2k + 1)\pi, \quad k \in \mathbb{Z}. \quad (218)$$

Each boundary in (218) is mapped on the negative real line  $(-\infty, 0]$  of the  $z$ -plane. The line  $(-\infty, 0]$  is called the *branch cut* and  $z = 0$  is the *branch point*. We adopt the counterclockwise direction such that the branch cut closes on top, i.e. for  $z = re^{i\theta}$ ,  $-\pi < \theta \leq \pi$  then  $\log z$ , for each branch  $k$ , is a continuous function of  $z$ .

Now let us turn back to  $W(z)$ . We refer to the  $W$ -plane and the  $z$ -plane, and denote

$$W = u + iv, \quad z = x + iy. \quad (219)$$

From the defining equation (217) we have

$$x = e^u (u \cos v - v \sin v), \quad y = e^u (u \sin v + v \cos v). \quad (220)$$

We require the branch cut of  $W(z)$  to be similar to  $\log z$ , thus we define the branch cut on the  $z$ -plane to be the line  $(-\infty, 0]$ . Imposing  $y = 0$  and  $x \leq 0$  on relations (220) we obtain the boundaries and regions shown in Figure 20 (left). Thus the boundaries of each branch are given by the curves which are contained in the shaded regions, which are shown in Figure 20 (right). Each of these lines are mapped to the branch cut  $(-\infty, 0]$  in the  $z$ -plane. For each branch  $k$  the lower boundary is open, and not included, while the upper boundary is closed, and included, in its defining region. From now on we denote  $W(z)$  by  $W_k(z)$  when referring to the specific  $k$ -th branch. Note that the boundary lines are asymptotic to  $W = n\pi i$ .

The branches  $W_k$  for  $k = \pm 2, \pm 3, \dots$  in Figure 20 (right) are mapped into the  $z$ -plane according to Figure 21 (left). The curve in the  $W$ -plane separating  $W_k$  from  $W_{k+1}$  for  $k = 1, 2, \dots$  is given by  $\{-v \cot v + iv \mid 2k\pi < v < (2k + 1)\pi\}$ , and the curve separating  $W_k$  from  $W_{k-1}$  for  $k = -1, -2, \dots$  is given by  $\{-v \cot v + iv \mid (2k - 1)\pi < v < 2k\pi\}$ .

The branch structure for  $W_0$  and  $W_{\pm 1}$  is different from above. The curves shown in Figure 20 (right), separating  $W_0$  from  $W_{\pm 1}$  are given by  $\{-v \cot v + iv \mid -\pi < v < \pi\}$ . The point  $W = -1$ , corresponding to  $z = -1/e$ , is a double branch point, linking  $W_0$  and

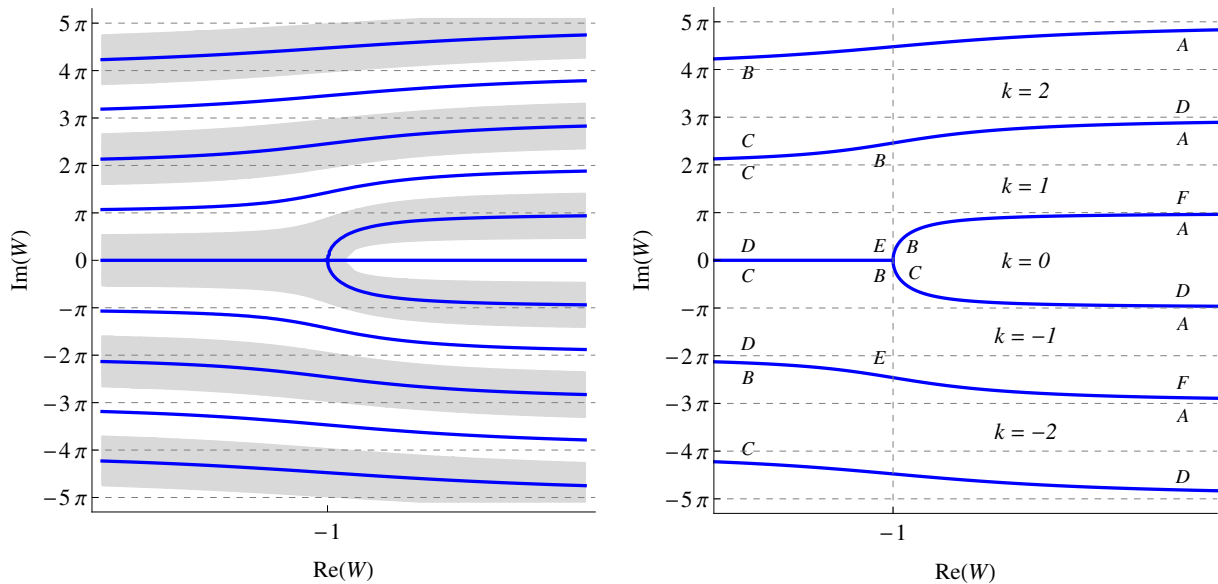


FIG. 20. *Left:* the solid (blue) lines correspond to the condition  $y = 0$  in (220) and the shaded (gray) regions to  $x \leq 0$ . *Right:* the boundaries of each branch are given by the lines which are contained in the shaded regions. This is the branch structure of  $W(z)$  viewed from the  $W$ -plane.

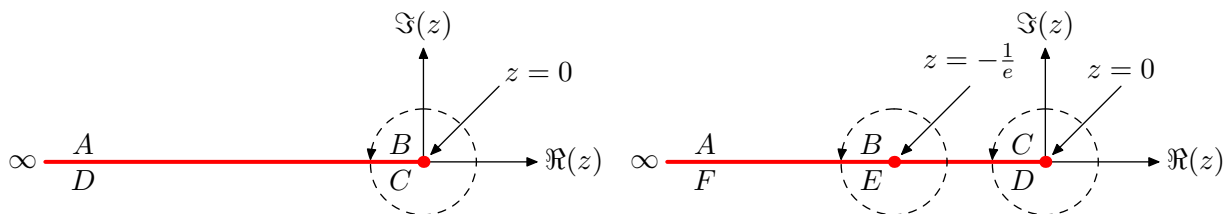


FIG. 21. *Left:* Mapping from  $W_k$  for  $k = \pm 2, \pm 3, \dots$  (Figure 20 (right)) into the  $z$ -plane. Note how the points A, B, C and D are mapped. We close the contour on top, i.e.  $z = re^{i\theta}$  where  $-\pi < \theta \leq \pi$ , and  $W_k(z)$  is a continuous single-valued function. *Right:* The branch cuts for  $W_{\pm 1}$ .

$W_{\pm 1}$ . The curve separating  $W_1$  and  $W_{-1}$  is  $(-\infty, -1]$ . Note that  $W_1$  does not include the real line, since the lower boundary is not included in its region. The branches  $W_0$  and  $W_{-1}$  are special in the sense that they are the only ones which include part of the real line. Thus only  $W_0$  and  $W_{-1}$  can yield real values.

The branches  $W_1$  and  $W_{-1}$  have a double branch cut in the  $z$ -plane. One is the line  $(-\infty, 0]$  and the other is  $(-\infty, -1/e]$ . Both branches are mapped into the  $z$ -plane according to Figure 21 (right). Note how the points A, B, ... F are related.

The branch  $W_0$  has only one branch cut which is  $(-\infty, -1/e]$ . It is exactly like in Figure 21 (left) but with the point  $z = 0$  replaced by  $z = -1/e$ . For real values of  $z \in [-1/e, \infty)$  we see from (217) that  $W_0(-1/e) = -1$ ,  $W_0(0) = 0$  and  $W_0(\infty) = \infty$ . For the branch  $W_{-1}$  we see that the function is real for  $z \in [-1/e, 0)$ , having the values  $W_{-1}(-1/e) = -1$  and  $W_{-1}(0) = -\infty$ . Thus for real  $z$  we have the picture shown in Figure 22. Sometimes the

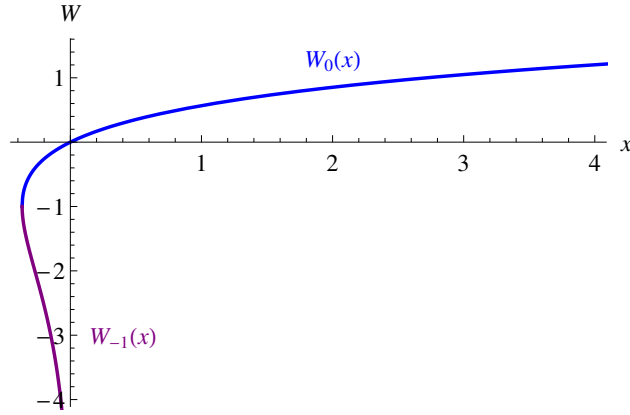


FIG. 22. The two branches  $W_0(x)$  and  $W_{-1}(x)$  for real  $x$ . These are the only branches giving real values. The domain of  $W_0(x)$  is  $x \in [-1/e, \infty)$  and the domain of  $W_{-1}(x)$  is  $x \in [-1/e, 0)$ .

principal branch  $W_0$  is denoted simply by  $W$  for short, when there is no chance of confusion.

Now it only remains to show that each branch maps bijectively into the  $z$ -plane. This will be true provided the Jacobian determinant of the transformation (220) does not vanish. We therefore have

$$J = \frac{\partial(x, y)}{\partial(u, v)} = e^u \begin{pmatrix} \cos v + u \cos v - v \sin v & -v \cos v - \sin v - u \sin v \\ \sin v + v \cos v + u \sin v & \cos v + u \cos v - v \sin v \end{pmatrix}. \quad (221)$$

Then,  $\det J = e^{2u} (v^2 + (1 + u)^2)$ . This can only be zero if  $u = -1$  and  $v = 0$ , which correspond exactly to the double branch point. Thus for every branch  $W_k$  we have  $\det J > 0$ .

Except on the branch cut we have the symmetry

$$(W_k(z))^* = W_{-k}(z^*). \quad (222)$$

This can easily be seen from Figure 20 (right), where the branches are symmetric by  $v \rightarrow -v$ , and analyzing how the points are mapped into the  $z$ -plane by complex conjugation on the  $W$ -plane.

## XII. APPROXIMATE ZEROS IN TERMS OF THE LAMBERT $W$ -FUNCTION

### A. Explicit formula

We now show that it is possible to obtain an approximate solution to the previous transcendental equations with an explicit formula. Let us start with the zeros of the  $\zeta$ -function, described by equation (131). Consider its leading order approximation, or equivalently its

average since  $\langle \arg \zeta \left( \frac{1}{2} + iy \right) \rangle = 0$ . Then we have the transcendental equation

$$\frac{\tilde{y}_n}{2\pi} \log \left( \frac{\tilde{y}_n}{2\pi e} \right) = n - \frac{11}{8}. \quad (223)$$

Through the transformation

$$\tilde{y}_n = 2\pi \left( n - \frac{11}{8} \right) \frac{1}{x_n} \quad (224)$$

the equation (223) can be written as

$$x_n e^{x_n} = \frac{n - \frac{11}{8}}{e}. \quad (225)$$

Comparing with (217) we thus we obtain

$$\tilde{y}_n = \frac{2\pi \left( n - \frac{11}{8} \right)}{W \left[ e^{-1} \left( n - \frac{11}{8} \right) \right]} \quad (226)$$

for  $n = 1, 2, \dots$ , where above  $W$  denotes the principal branch  $W_0$ .

Although the inversion from (223) to (226) is rather simple, it is very convenient since it is indeed an explicit formula depending only on  $n$ , and  $W$  is included in most numerical packages. It gives an approximate solution for the ordinates of the Riemann zeros in closed form. The values computed from (226) are much closer to the Riemann zeros than Gram points, and one does not have to deal with violations of Gram's law (see below).

Analogously, for Dirichlet  $L$ -functions, after neglecting the  $\arg L$  term, the equation (196) yields a transcendental equation which can be solved explicitly as

$$\tilde{y}_n = \frac{2\pi \sigma_n A_n(\chi)}{W [k e^{-1} A_n(\chi)]} \quad (227)$$

for  $n = 0, \pm 1, \pm 2, \dots$  and where

$$A_n(\chi) = \sigma_n \left( n + \frac{1}{2\pi} \arg G(\chi) \right) + \frac{1 - 4\sigma_n - 2a(\sigma_n + 1)}{8}. \quad (228)$$

In the above formula  $n = 1, 2, \dots$  correspond to positive  $y_n$  solutions, while  $n = 0, -1, \dots$  correspond to negative  $y_n$  solutions. Contrary to the  $\zeta$ -function, in general, the zeros are not conjugate related along the critical line.

In the same way, ignoring the small  $\arg L_f$  term in (216), the approximate solution for the imaginary part of the zeros of  $L$ -functions based on level one modular forms is given by

$$\tilde{y}_n = \frac{A_n \pi}{W [(2e)^{-1} A_n]} \quad (229)$$

$n$	$\tilde{y}_n$
$10^{22} + 1$	$1.370919909931995308226770 \times 10^{21}$
$10^{50}$	$5.741532903784313725642221053588442131126693322343461 \times 10^{48}$
$10^{100}$	$2.80690383842894069903195445838256400084548030162846045192360059224930$ $922349073043060335653109252473234 \times 10^{98}$
$10^{200}$	$1.38579222214678934084546680546715919012340245153870708183286835248393$ $8909689796343076797639408172610028651791994879400728026863298840958091$ $288304951600695814960962282888090054696215023267048447330585768 \times 10^{198}$

TABLE I. Formula (226) can easily estimate very high Riemann zeros. The results are expected to be correct up to the decimal point, i.e. to the number of digits in the integer part. The numbers are shown with three digits beyond the integer part.

where  $n = 1, 2, \dots$  and

$$A_n = n - \frac{k + (-1)^{k/2}}{4}. \quad (230)$$

## B. Further remarks

Let us focus on the approximation (226) regarding zeros of the  $\zeta$ -function. Obviously the same arguments apply to the zeros of the other classes of functions, based on formulas (227) and (229).

The estimates given by (226) can be calculated to high accuracy for arbitrarily large  $n$ , since  $W$  is a standard elementary function. Of course, the  $\tilde{y}_n$  are not as accurate as the solutions  $y_n$  including the  $\arg \zeta$  term, as we will see in section XIII. Nevertheless, it is indeed a good estimate, especially if one considers very high zeros, where traditional methods have not previously estimated such high values. For instance, formula (226) can easily estimate the zeros shown in Table I, and much higher if desirable.

The numbers in this table are accurate approximations to the  $n$ -th zero to the number of digits shown, which is approximately the number of digits in the integer part. For instance, the approximation to the  $10^{100}$  zero is correct to 100 digits. With Mathematica we easily calculated the first million digits of the  $10^{10^6}$  zero.<sup>10</sup>

Using the asymptotic behaviour  $W(x) \sim \log x$  for large  $x$ , the  $n$ -th zero is approximately  $\tilde{y}_n \approx 2\pi n / \log n$ , as already known [20]. The distance between consecutive zeros is  $2\pi / \log n$ , which tends to zero when  $n \rightarrow \infty$ .

The solutions (226) are reminiscent of the so-called Gram points  $g_n$ , which are solutions to  $\vartheta(g_n) = n\pi$  where  $\vartheta$  is given by (137). Gram's law is the tendency for Riemann zeros to lie between consecutive Gram points, but it is known to fail for about 1/4 of all Gram intervals. Our  $\tilde{y}_n$  are intrinsically different from Gram points. It is an approximate solution

<sup>10</sup>The result is 200 pages long and available at <http://www.lepp.cornell.edu/~leclair/10106zero.pdf>.

for the ordinate of the zero itself. In particular, the Gram point  $g_0 = 17.8455$  is the closest to the first Riemann zero, whereas  $\tilde{y}_1 = 14.52$  is already much closer to the true zero which is  $y_1 = 14.1347\dots$ . The traditional method to compute the zeros is based on the Riemann-Siegel formula,  $\zeta\left(\frac{1}{2} + iy\right) = Z(y) (\cos \vartheta(y) - i \sin \vartheta(y))$ , and the empirical observation that the real part of this equation is almost always positive, except when Gram's law fails, and  $Z(y)$  has the opposite sign of  $\sin \vartheta$ . Since  $Z(y)$  and  $\zeta\left(\frac{1}{2} + iy\right)$  have the same zeros, one looks for the zeros of  $Z(y)$  between two Gram points, as long as Gram's law holds  $(-1)^n Z(g_n) > 0$ . To verify the RH numerically, the counting formula (141) must also be used, to assure that the number of zeros on the critical line coincide with the number of zeros on the strip. The detailed procedure is thoroughly explained in [2, 20]. Based on this method, amazingly accurate solutions and high zeros on the critical line were computed [42–45]. Nevertheless, our proposal is *fundamentally* different. We claim that (138), or its asymptotic approximation (131), is the equation that determines the Riemann zeros on the critical line. Then, one just needs to find its solution for a given  $n$ . We will compute the Riemann zeros in this way in the next section, just by solving the equation numerically, starting from the approximation given by the explicit formula (226), without using Gram points nor the Riemann-Siegel  $Z$  function. Let us emphasize that our goal is not to provide a more efficient algorithm to compute the zeros [42], although the method described here may very well be, but to justify the validity of equations (131) and (138).

### XIII. NUMERICAL ANALYSIS: $\zeta$ -FUNCTION

Instead of solving the exact equation (138) we will initially consider its first order approximation, which is equation (131). As we will see, this approximation already yields surprisingly accurate values for the Riemann zeros. These approximate solutions will be used to study the GUE statistics and prime number counting function in the next two sections.

Let us first consider how the approximate solution given by (226) is modified by the presence of the  $\arg \zeta$  term in (131). Based on the discussion in section VIII, up to rather high  $y < 10^{10}$ ,  $S(y)$  is almost always on the principal branch, thus we numerically compute  $\arg \zeta$  by taking its principal value. This is not necessarily correct given the growth of  $S(y)$ , thus we check it is indeed a zero to a high number of digits by verifying  $|L(\rho)| = 0$  to this precision. Numerically this prescription of taking the  $\text{Arg}$  rather than the  $\arg$  seems to be better near a zero  $y_n$  than for typical  $y$ .<sup>11</sup> As already discussed, the function  $\arg \zeta\left(\frac{1}{2} + iy\right)$  oscillates around zero, as shown in Figure 12 (left). At a zero it can be well-defined by the limit (123). For example, for the first Riemann zero  $y_1 = 14.1347\dots$ ,

$$\lim_{\delta \rightarrow 0^+} \arg \zeta\left(\frac{1}{2} + \delta + iy_1\right) = 0.157873919880941213041945\dots \quad (231)$$

---

<sup>11</sup>We remind the reader that  $\arg \zeta = \text{Arg} \zeta + 2\pi n$ , with  $-\pi < \text{Arg} \zeta < \pi$ , where  $n$  is an integer.



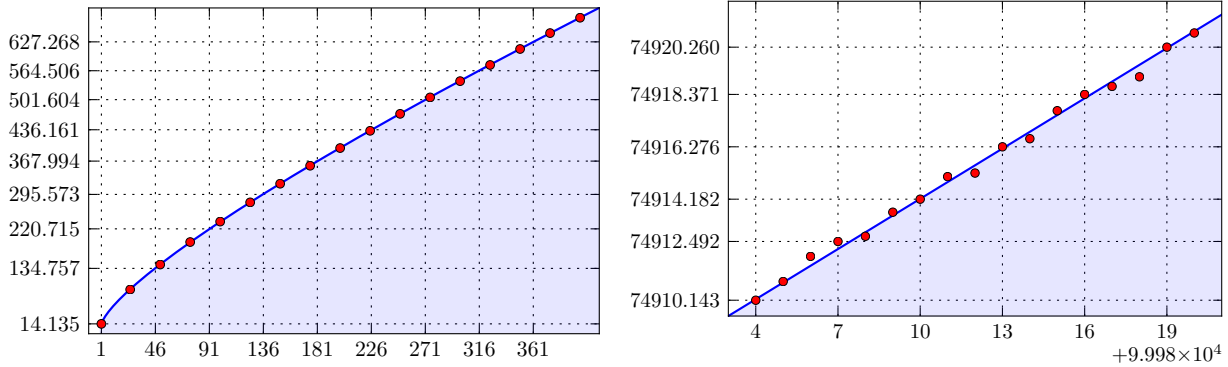


FIG. 23. Comparison of (226) (blue line) and (131) (red dots). We plot  $y_n$  against  $n$ . *Left*: here  $n \in [1, \dots, 400]$ . *Right*: if we focus on a small range we can see the solutions of (131) oscillating around the line (226) due to the fluctuating  $\arg \zeta$  term. Here  $n \in [99984, \dots, 10^5]$ .

$n$	$\tilde{y}_n$	$y_n$	$n$	$y_n$
1	14.52	14.134725142	1	14.13472514173469379045725198356247
10	50.23	49.773832478	2	21.02203963877155499262847959389690
$10^2$	235.99	236.524229666	3	25.01085758014568876321379099256282
$10^3$	1419.52	1419.422480946	4	30.42487612585951321031189753058409
$10^4$	9877.63	9877.782654006	5	32.93506158773918969066236896407490
$10^5$	74920.89	74920.827498994	6	37.58617815882567125721776348070533
$10^6$	600269.64	600269.677012445	7	40.91871901214749518739812691463325
$10^7$	4992381.11	4992381.014003179	8	43.32707328091499951949612216540681
$10^8$	42653549.77	42653549.760951554	9	48.00515088116715972794247274942752
$10^9$	371870204.05	371870203.837028053	10	49.77383247767230218191678467856372
$10^{10}$	3293531632.26	3293531632.397136704	11	52.97032147771446064414729660888099

TABLE II. Numerical solutions of equation (131). *Left*: solutions accurate up to the 9-th decimal place and agree with [43, 46]. *Right*: although it was derived for high  $y$ , it provides accurate numbers even for the lower zeros.

The  $\arg \zeta$  term plays an essential role and indeed improves the estimate of the  $n$ -th zero. This can be seen in Figure 23, where we compare the estimate given by (226) with the numerical solutions of (131).

Since equation (131) typically alternates in sign around a zero, we can apply a root finder method in an appropriate interval, centered around the approximate solution  $\tilde{y}_n$  given by formula (226). Some of the solutions obtained in this way are presented in Table II (left), and are accurate up to the number of decimal places shown. We used only Mathematica or some very simple algorithms to perform these numerical computations, taken from standard open source numerical libraries.

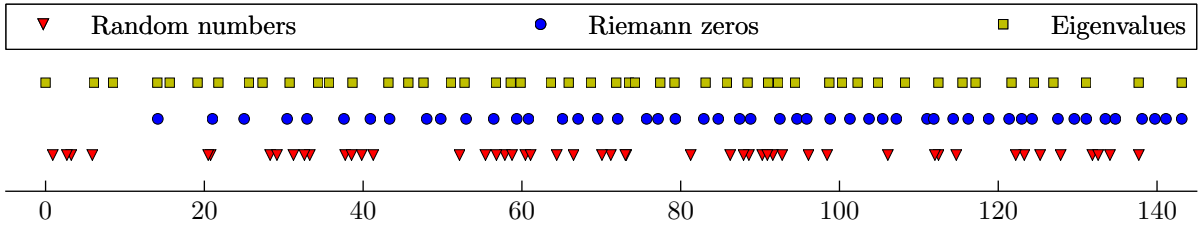


FIG. 24. The first 50 Riemann zeros at  $x = 1/2$ , in comparison with 50 random numbers to the left and the eigenvalues of a random  $50 \times 50$  hermitian matrix.

Although the formula for  $y_n$  was solved for large  $n$ , it is surprisingly accurate even for the lower zeros, as shown in Table II (right). It is actually easier to solve numerically for low zeros since  $\arg \zeta$  is better behaved. These numbers are correct up to the number of digits shown, and the precision was improved simply by decreasing the error tolerance.

#### XIV. GUE STATISTICS

The link between the Riemann zeros and random matrix theory started with the pair correlation of zeros, proposed by Montgomery [39], and the observation of Dyson that it is the same as the 2-point correlation function predicted by the gaussian unitary ensemble (GUE) for large random matrices [47].

The main result of the GUE random matrix theory is that the eigenvalues of a random hermitian matrix are not completely random, for instance there are correlations in the spacings of eigenvalues, commonly referred to as level-repulsion. In Figure 24 we show 3 collections of points: the first 50 Riemann zeros, 50 random real numbers between 0 and the ordinate of the 50-th zero, and the eigenvalues of a  $50 \times 50$  hermitian matrix where each element of the matrix is also random. One clearly sees the statistical resemblance of the statistics of the Riemann zeros and that of the GUE, in contrast to the 50 random numbers.

The main purpose of this section is to test whether our approximation (131) to the zeros is accurate enough to reveal this statistics. Whereas formula (226) is a valid estimate of the zeros, it is not sufficiently accurate to reproduce the GUE statistics, since it does not have the oscillatory  $\arg \zeta$  term. On the other hand, the solutions to equation (131) are accurate enough, which again indicates the importance of the  $\arg \zeta$  term.

Montgomery's pair correlation conjecture can be stated as follows:

$$\frac{1}{N(T)} \sum_{\substack{0 \leq y, y' \leq T \\ \alpha < d(y, y') \leq \beta}} 1 \sim \int_{\alpha}^{\beta} du \left( 1 - \frac{\sin^2(\pi u)}{\pi^2 u^2} \right) \quad (232)$$

where  $d(y, y') = \frac{1}{2\pi} \log \left( \frac{T}{2\pi} \right) (y - y')$ ,  $0 < \alpha < \beta$ ,  $N(T) \sim \frac{T}{2\pi} \log \left( \frac{T}{2\pi} \right)$  according to (133),

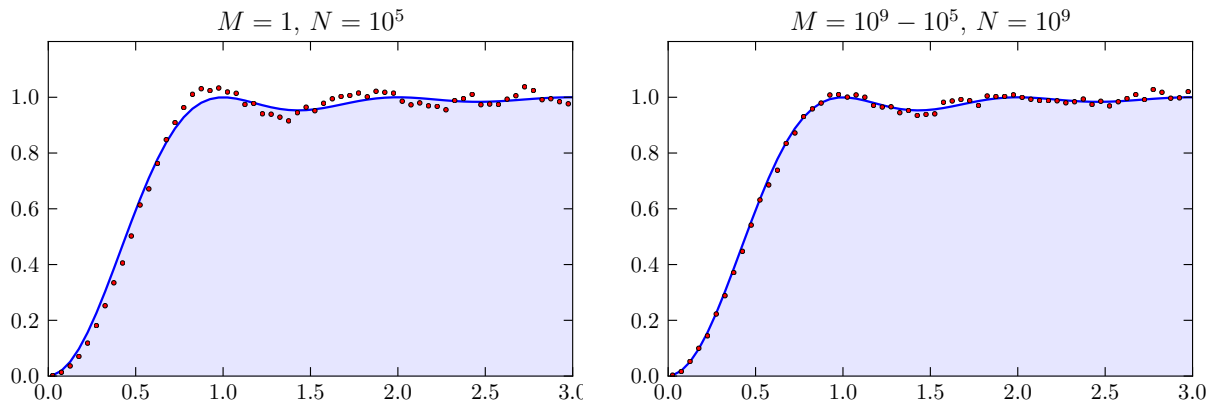


FIG. 25. The solid line represents the RHS of (234) and the dots its LHS, computed from equation (131). The parameters are  $\beta = \alpha + 0.05$ ,  $\alpha = (0, 0.05, \dots, 3)$  and the  $x$ -axis is given by  $x = \frac{1}{2}(\alpha + \beta)$ . *Left*: we use the first  $10^5$  zeros. *Right*: the same parameters but using zeros in the middle of the critical line;  $M = 10^9 - 10^5$  and  $N = 10^9$ .

and the statement is valid in the limit  $T \rightarrow \infty$ . The right hand side of (232) is the 2-point GUE correlation function. The average spacing between consecutive zeros is given by  $\frac{T}{N} \sim 2\pi / \log\left(\frac{T}{2\pi}\right) \rightarrow 0$  as  $T \rightarrow \infty$ . This can also be seen from (226) for very large  $n$ , i.e.  $\tilde{y}_{n+1} - \tilde{y}_n \rightarrow 0$  as  $n \rightarrow \infty$ . Thus  $d(y, y')$  is a normalized distance.

While (232) can be applied if we start from the first zero on the critical line, it is unable to provide a test if we are centered around a given high zero on the line. To deal with such a situation, Odlyzko [44] proposed a stronger version of Montgomery's conjecture, by taking into account the large density of zeros higher on the line. This is done by replacing  $d(y, y')$  in (232) by a sum of normalized distances over consecutive zeros in the form

$$\delta_n = \frac{1}{2\pi} \log\left(\frac{y_n}{2\pi}\right) (y_{n+1} - y_n). \quad (233)$$

Thus (232) is replaced by

$$\frac{1}{(N - M)(\beta - \alpha)} \sum_{\substack{M \leq m, n \leq N \\ \alpha < \sum_{k=1}^n \delta_{m+k} \leq \beta}} 1 \approx \frac{1}{\beta - \alpha} \int_{\alpha}^{\beta} du \left(1 - \frac{\sin^2(\pi u)}{\pi^2 u^2}\right), \quad (234)$$

where  $M$  is the label of a given zero on the line and  $N > M$ . In this sum it is assumed that  $n > m$  also, and we included the correct normalization on both sides. The conjecture (234) is already well supported by extensive numerical analysis [44, 45].

Odlyzko's conjecture (234) is a very strong constraint on the statistics of the zeros. Thus we submit the numerical solutions of equation (131), as discussed in the previous section, to this test. In Figure 25 (left) we can see the result for  $M = 1$  and  $N = 10^5$ , with  $\alpha$  ranging from  $0 \dots 3$  in steps of  $s = 0.05$ , and  $\beta = \alpha + s$  for each value of  $\alpha$ , i.e.  $\alpha = (0.00, 0.05, 0.10, \dots, 3.00)$  and  $\beta = (0.05, 0.10, \dots, 3.05)$ . We compute the left hand

$n$	$y_n$	$n$	$y_n$
$10^5 - 5$	74917.719415828	$10^9 - 5$	371870202.244870467
$10^5 - 4$	74918.370580227	$10^9 - 4$	371870202.673284457
$10^5 - 3$	74918.691433454	$10^9 - 3$	371870203.177729799
$10^5 - 2$	74919.075161121	$10^9 - 2$	371870203.274345928
$10^5 - 1$	74920.259793259	$10^9 - 1$	371870203.802552324
$10^5$	74920.827498994	$10^9$	371870203.837028053

TABLE III. Last numerical solutions to (131) around  $n = 10^5$  and  $n = 10^9$ .

side of (234) for each pair  $(\alpha, \beta)$  and plot the result against  $x = \frac{1}{2}(\alpha + \beta)$ . In Figure 25 (right) we do the same thing but with  $M = 10^9 - 10^5$  and  $N = 10^9$ .

Clearly, the numerical solutions of (131) reproduce the correct statistics. In fact, Figure 25 (left) is identical to the one in [44]. In Table III we provide the solutions to (131) at the end of the ranges considered, so that the reader may compare with [43, 46].

## XV. PRIME NUMBER COUNTING FUNCTION REVISITED

In this section we explore whether our approximations to the Riemann zeros are accurate enough to reconstruct the prime number counting function. In Figure 26 (left) we plot  $\pi(x)$  from equations (74) and (76), computed with the first 50 zeros in the approximation  $\rho_n = \frac{1}{2} + i\tilde{y}_n$  given by (226). Figure 26 (right) shows the same plot with zeros obtained from the numerical solutions of equation (131). Although with the Lambert approximation  $\tilde{y}_n$  the curve is trying to follow the steps in  $\pi(x)$ , once again, one clearly sees the importance of the  $\arg \zeta$  term.

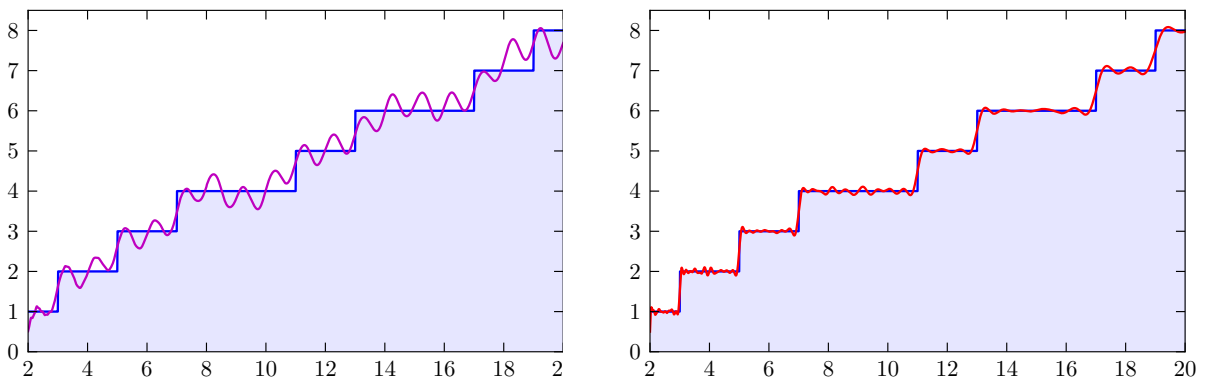


FIG. 26. The prime number counting function  $\pi(x)$  with the first 50 Riemann zeros. *Left:* zeros approximated by the Lambert formula (226). *Right:* zeros obtained from numerical solutions to the equation (131).

$n$	$y_n$
1	14.1347251417346937904572519835624702707842571156992431756855
2	21.0220396387715549926284795938969027773343405249027817546295
3	25.0108575801456887632137909925628218186595496725579966724965
4	30.4248761258595132103118975305840913201815600237154401809621
5	32.9350615877391896906623689640749034888127156035170390092800

TABLE IV. The first few numerical solutions to (138), accurate to 60 digits (58 decimals).

## XVI. SOLUTIONS TO THE EXACT EQUATION

In the previous sections we have computed numerical solutions of (131) showing that, actually, this first order approximation to (138) is very good and already captures some interesting properties of the Riemann zeros, like the GUE statistics and ability to reproduce the prime number counting formula. Nevertheless, by simply solving (138) it is possible to obtain values for the zeros as accurately as desirable. The numerical procedure is performed as follows:

1. We apply a root finder method on (138) looking for the solution in a region centered around the number  $\tilde{y}_n$  provided by (226), with a not so small  $\delta$ , for instance  $\delta \sim 10^{-5}$ .
2. We solve (138) again but now centered around the solution obtained in step 1 above, and we decrease  $\delta$ , for instance  $\delta \sim 10^{-8}$ .
3. We repeat the procedure in step 2 above, decreasing  $\delta$  again.
4. Through successive iterations, and decreasing  $\delta$  each time, it is possible to obtain solutions as accurate as desirable. In carrying this out, it is important to not allow  $\delta$  to be exactly zero.

An actual implementation of the above procedure in Mathematica is shown in Appendix C. The first few zeros computed in this way are shown in Table IV. Through successive iterations it is possible achieve even much higher accuracy than these values.

It is known that the first zero where Gram's law fails is for  $n = 126$ . Applying the same method, like for any other  $n$ , the solution of (138) starting with the approximation (226) does not present any difficulty. We easily found the following number:

$$y_{126} = 279.229250927745189228409880451955359283492637405561293594727$$

Just to illustrate, and to convince the reader that the solutions of (138) can be made arbitrarily precise, we compute the zero  $n = 1000$  accurate up to 500 decimal places, also

using the same simple approach<sup>12</sup>:

$$\begin{aligned}
y_{1000} = & 1419.42248094599568646598903807991681923210060106416601630469081468460 \\
& 86764175930104179113432911792099874809842322605601187413974479526 \\
& 50637067250834288983151845447688252593115944239425195484687708163 \\
& 94625633238145779152841855934315118793290577642799801273605240944 \\
& 61173370418189624947474596756904798398768401428049735900173547413 \\
& 19116293486589463954542313208105699019807193917543029984881490193 \\
& 19367182312642042727635891148784832999646735616085843651542517182 \\
& 417956641495352443292193649483857772253460088
\end{aligned}$$

Substituting precise Riemann zeros into (138) one can check that the equation is identically satisfied. These results corroborate that (138) is an exact equation for the Riemann zeros.

## XVII. NUMERICAL ANALYSIS: DIRICHLET $L$ -FUNCTIONS

We perform exactly the same numerical procedure as described in the previous section XVI, but now with equation (194) and (227) for Dirichlet  $L$ -functions.

We will illustrate our formulas with the primitive characters  $\chi_{7,2}$  and  $\chi_{7,3}$ , since they possess the full generality of  $a = 0$  and  $a = 1$  and complex components. There are actually  $\varphi(7) = 6$  distinct characters mod 7.

**Example  $\chi_{7,2}$ .** Consider  $k = 7$  and  $j = 2$ , i.e. we are computing the Dirichlet character  $\chi_{7,2}(n)$ . For this case  $a = 1$ . Then we have the following components:

$$\begin{array}{c|ccccccc}
n & 1 & 2 & 3 & 4 & 5 & 6 & 7 \\
\hline
\chi_{7,2}(n) & 1 & e^{2\pi i/3} & e^{\pi i/3} & e^{-2\pi i/3} & e^{-\pi i/3} & -1 & 0
\end{array} \quad (235)$$

The first few zeros, positive and negative, obtained by solving (194) are shown in Table V (see Appendix C). The solutions shown are easily obtained with 50 decimal places of accuracy, and agree with the ones in [48], which were computed up to 20 decimal places.

**Example  $\chi_{7,3}$ .** Consider  $k = 7$  and  $j = 3$ , such that  $a = 0$ . In this case the components of  $\chi_{7,3}(n)$  are the following:

$$\begin{array}{c|ccccccc}
n & 1 & 2 & 3 & 4 & 5 & 6 & 7 \\
\hline
\chi_{7,3}(n) & 1 & e^{-2\pi i/3} & e^{2\pi i/3} & e^{2\pi i/3} & e^{-2\pi i/3} & 1 & 0
\end{array} \quad (236)$$

---

<sup>12</sup>Computing this number to 500 digit accuracy took a few minutes on a standard personal laptop computer. It only takes a few seconds to obtain 100 digit accuracy.

$n$	$\tilde{y}_n$	$y_n$
10	25.57	25.68439458577475868571703403827676455384372032540097
9	23.67	24.15466453997877089700472248737944003578203821931614
8	21.73	21.65252506979642618329545373529843196334089625358303
7	19.73	19.65122423323359536954110529158230382437142654926200
6	17.66	17.16141654370607042290552256158565828745960439000612
5	15.50	15.74686940763941532761353888536874657958310887967059
4	13.24	13.85454287448149778875634224346689375234567535103602
3	10.81	9.97989590209139315060581291354262017420478655402522
2	8.14	8.41361099147117759845752355454727442365106861800819
1	4.97	5.19811619946654558608428407430395403442607551643259
0	-3.44	-2.50937455292911971967838452268365746558148671924805
-1	-7.04	-7.48493173971596112913314844807905530366284046079242
-2	-9.85	-9.89354379409772210349418069925221744973779313289503
-3	-12.35	-12.25742488648921665489461478678500208978360618268664
-4	-14.67	-14.13507775903777080989456447454654848575048882728616
-5	-16.86	-17.71409256153115895322699037454043289926793578042465
-6	-18.96	-18.88909760017588073794865307957219593848843485334695
-7	-20.99	-20.60481911491253262583427068994945289180639925014034
-8	-22.95	-22.66635642792466587252079667063882618974425685038326
-9	-24.87	-25.28550752850252321309973718800386160807733038068585

TABLE V. Numerical solutions of (194) starting with the approximation (227), for the character (235). The solutions are accurate to 50 decimal places and verified to  $|L(\frac{1}{2} + iy_n)| \sim 10^{-50}$ .

The first few solutions of (194) are shown in Table VI and are accurate up to 50 decimal places, and agree with the ones obtained in [48].

As stated previously, the solutions to equation (194) can be calculated to any desired level of accuracy. For instance, continuing with the character  $\chi_{7,3}$ , we can easily compute the following number for  $n = 1000$ , accurate to 100 decimal places, i.e. 104 digits:

$$y_{1000} = 1037.56371706920654296560046127698168717112749601359549 \\ 01734503731679747841764715443496546207885576444206$$

We also have been able to solve the equation for high zeros to high accuracy, up to the millionth zero, some of which are listed in Table VII, and were previously unknown.

$n$	$\tilde{y}_n$	$y_n$
10	25.55	26.16994490801983565967242517629313321888238615283992
9	23.65	23.20367246134665537826174805893362248072979160004334
8	21.71	21.31464724410425595182027902594093075251557654412326
7	19.71	20.03055898508203028994206564551578139558919887432101
6	17.64	17.61605319887654241030080166645399190430725521508443
5	15.48	15.93744820468795955688957399890407546316342953223035
4	13.21	12.53254782268627400807230480038783642378927939761728
3	10.79	10.73611998749339311587424153504894305046993275660967
2	8.11	8.78555471449907536558015746317619235911936921514074
1	4.93	4.35640162473628422727957479051551913297149929441224
0	-5.45	-6.20123004275588129466099054628663166500168462793701
-1	-8.53	-7.92743089809203774838798659746549239024181788857305
-2	-11.15	-11.01044486207249042239362741094860371668883190429106
-3	-13.55	-13.82986789986136757061236809479729216775842888684529
-4	-15.80	-16.01372713415040781987211528577709085306698639304444
-5	-17.94	-18.04485754217402476822077016067233558476519398664936
-6	-20.00	-19.11388571948958246184820859785760690560580302023623
-7	-22.00	-22.75640595577430793123629559665860790727892846161121
-8	-23.94	-23.95593843516797851393076448042024914372113079309104
-9	-25.83	-25.72310440610835748550521669187512401719774475488087

TABLE VI. Numerical solutions of (194) starting with the approximation (227), for the character (236). The solutions are accurate to 50 decimal places and verified to  $|L(\frac{1}{2} + iy_n)| \sim 10^{-50}$ .

$n$	$\tilde{y}_n$	$y_n$
$10^3$	1037.61	1037.5637170692065429656004612769816871711127496013595490
$10^4$	7787.18	7787.337916840954922060149425635486826208937584171726906
$10^5$	61951.04	61950.779420880674657842482173403370835983852937763461400
$10^6$	512684.78	512684.856698029779109684519709321053301710419463624401290

TABLE VII. Higher zeros for the Dirichlet character (236). These solutions to (194) are accurate to 50 decimal places.

## XVIII. MODULAR $L$ -FUNCTION BASED ON RAMANUJAN $\tau$

In this section we study an  $L$ -function based on a level one modular form related to the Ramanujan  $\tau$  function, and numerically solve the equations (213) and (229).



### A. Definition of the function

Here we will consider an example of a modular form of weight  $k = 12$ . The simplest example is based on the Dedekind  $\eta$ -function

$$\eta(\tau) = q^{1/24} \prod_{n=1}^{\infty} (1 - q^n). \quad (237)$$

Up to a simple factor,  $\eta$  is the inverse of the chiral partition function of the free boson conformal field theory [49], where  $\tau$  is the modular parameter of the torus. The modular discriminant

$$\Delta(\tau) = \eta(\tau)^{24} = \sum_{n=1}^{\infty} \tau(n) q^n \quad (238)$$

is a weight  $k = 12$  modular form. It is closely related to the inverse of the partition function of the bosonic string in 26 dimensions, where 24 is the number of light-cone degrees of freedom [50]. The Fourier coefficients  $\tau(n)$  correspond to the Ramanujan  $\tau$ -function, and the first few are

$n$	1	2	3	4	5	6	7	8	(239)
$\tau(n)$	1	-24	252	-1472	4830	-6048	-16744	84480	

We then define the Dirichlet series

$$L_{\Delta}(z) = \sum_{n=1}^{\infty} \frac{\tau(n)}{n^z}. \quad (240)$$

Applying (213), the zeros are  $\rho_n = 6 + iy_n$ , where the  $y_n$  satisfy the exact equation

$$\vartheta_{12}(y) + \lim_{\delta \rightarrow 0^+} \arg L_{\Delta}(6 + \delta + iy_n) = \left(n - \frac{1}{2}\right) \pi. \quad (241)$$

The counting function (215) and its asymptotic approximation are

$$N_0(T) = \frac{1}{\pi} \vartheta_{12}(T) + \frac{1}{\pi} \arg L_{\Delta}(6 + iT) \quad (242)$$

$$\approx \frac{T}{\pi} \log \left( \frac{T}{2\pi e} \right) + \frac{1}{\pi} \arg L_{\Delta}(6 + iT) + \frac{11}{4}. \quad (243)$$

A plot of (242) is shown in Figure 27, and we can see that it is a perfect staircase function.

The approximate solution (229) now has the form

$$\tilde{y}_n = \frac{\left(n - \frac{13}{4}\right) \pi}{W \left[ (2e)^{-1} \left(n - \frac{13}{4}\right) \right]} \quad (244)$$

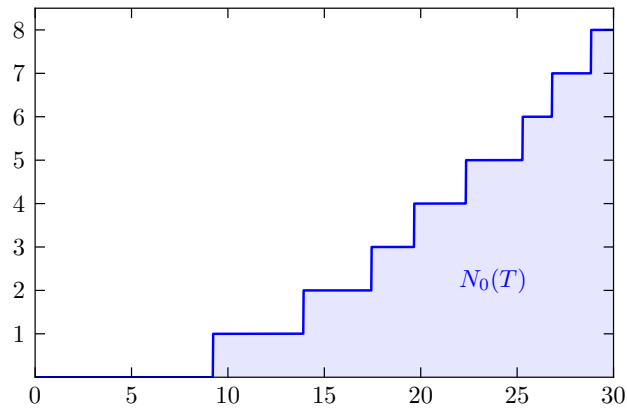


FIG. 27. Exact counting formula (242) based on the Ramanujan  $\tau$ -function.

$n$	$\tilde{y}_n$	$y_n$
1		9.22237939992110252224376719274347813552877062243201
2	12.46	13.90754986139213440644668132877021949175755235351449
3	16.27	17.44277697823447331355152513712726271870886652427527
4	19.30	19.65651314195496100012728175632130280161555091200324
5	21.94	22.33610363720986727568267445923624619245504695246527
6	24.35	25.27463654811236535674532419313346311859592673122941
7	26.60	26.80439115835040303257574923358456474715296800497933
8	28.72	28.83168262418687544502196191298438972569093668609124
9	30.74	31.17820949836025906449218889077405585464551198966267
10	32.68	32.77487538223120744183045567331198999909916163721260
100	143.03	143.08355526347845507373979776964664120256210342087127
200	235.55	235.74710143999213667703807130733621035921210614210694
300	318.61	318.36169446742310747533323741641236307865855919162340

TABLE VIII. Non-trivial zeros of the modular  $L$ -function based on the Ramanujan  $\tau$ -function, obtained from (241) starting with the approximation (244). These solutions are accurate to 50 decimal places.

for  $n = 2, 3, \dots$ . Note that the above equation is valid for  $n > 1$ , since  $W(x)$  is not defined for  $x < -1/e$ .

## B. Numerical analysis

We follow the same procedure, previously discussed in section XVI and implemented in Appendix C, to solve the equation (241) starting with the approximation provided by (244). Some of these solutions are shown in Table VIII and are accurate to 50 decimal places.

### XIX. COUNTEREXAMPLE OF DAVENPORT-HEILBRONN

The *Davenport-Heilbronn* function has almost all the same properties of  $\zeta$ , such as a functional equation, except that it has no Euler product formula. It is well known that such a function has zeros in the region  $\Re(z) > 1$  and zeros in the critical strip  $0 \leq \Re(z) \leq 1$ , of which infinitely many of them lie on *the critical line*  $\Re(z) = 1/2$ , but it also *has zeros off of the critical line*, thus violating the RH. Whether this is due to the absence of an Euler product is not understood, although this is likely to be the reason. It is very interesting to apply the formalism of the previous sections to this function and to understand clearly why the RH fails here. Such an exercise sharpens our understanding of the RH. For a detailed study of this function and numerical computation of the zeros see [51].

This function is somewhat contrived since it is linear combination of Dirichlet  $L$ -functions, engineered to satisfy a functional equation. It is defined by

$$\mathcal{D}(z) \equiv \frac{(1 - i\kappa)}{2} L(z, \chi_{5,2}) + \frac{(1 + i\kappa)}{2} L(z, \chi_{5,2}^*) \quad (245)$$

with

$$\kappa = \frac{\sqrt{10 - 2\sqrt{5}} - 2}{\sqrt{5} - 1}, \quad (246)$$

and the Dirichlet character is given by

$n$	1	2	3	4	5
$\chi_{5,2}(n)$	1	$i$	$-i$	$-1$	0

(247)

and  $\chi_{5,2}(-1) = -1$  thus  $a = 1$ . This function satisfies the functional equation

$$\xi(z) = \xi(1 - z), \quad \xi(z) \equiv \left(\frac{\pi}{5}\right)^{-z/2} \Gamma\left(\frac{1+z}{2}\right) \mathcal{D}(z). \quad (248)$$

$\mathcal{D}(z)$  has no Euler product because it is a linear combination of functions that do.

Now we repeat the analysis we presented for the Riemann  $\zeta$ -function. We have

$$\xi(z) = Ae^{i\theta}, \quad \xi(1 - z) = A'e^{-i\theta'}, \quad (249)$$

with  $A(x, y) = A'(x, y)$  and  $\theta'(x, y) = \theta(1 - x, y)$ , where

$$\theta(x, y) = \Im \left[ \log \Gamma \left( \frac{1 + x + iy}{2} \right) \right] - \frac{y}{2} \log \left( \frac{\pi}{5} \right) + \arg \mathcal{D}(x + iy). \quad (250)$$

As for previous  $L$ -functions, zeros should be characterized by our equation (149), namely

$$\theta + \theta' = (2n + 1)\pi. \quad (251)$$

The zeros on the critical line correspond to

$$\theta = \theta' \quad \Rightarrow \quad \theta = \left(n + \frac{1}{2}\right) \pi. \quad (252)$$

As before, adopting the convention that the first positive zero is labeled by  $n = 1$ , we shift  $n \rightarrow n - 1$ , then the equation yielding zeros on the critical line is given by

$$\Xi(y_n) + \lim_{\delta \rightarrow 0^+} \arg \mathcal{D} \left( \frac{1}{2} + \delta + iy_n \right) = \left(n - \frac{1}{2}\right) \pi \quad (253)$$

where

$$\Xi(y) \equiv \Im \left[ \log \Gamma \left( \frac{3}{4} + i \frac{y}{2} \right) \right] - \frac{y}{2} \log \left( \frac{\pi}{5} \right). \quad (254)$$

Expanding  $\Gamma(z)$  through Stirling's formula and neglecting the  $\arg \mathcal{D}$  term in (253) it is possible to obtain an explicit approximate solution given by

$$\tilde{y}_n = \frac{2\pi \left(n - \frac{5}{8}\right)}{W \left[ 5e^{-1} \left(n - \frac{5}{8}\right) \right]}, \quad (255)$$

where  $n = 1, 2, \dots$  and  $W$  denotes the principal branch  $W_0$  of the Lambert function (217).

Now we can numerically solve (253) starting with the approximation given by (255). The first few solutions are shown in Table IX (left).

As for the trivial zeros of  $\zeta$  we expect that zeros off of the line also satisfy (251). We indeed verified this. It is more difficult to find these zeros since they are at scattered values of  $x$ , but it is in fact feasible. In Table IX (right) we show some of the lower zeros and the

$n$	$\tilde{y}_n$	$y_n$	$\rho$	$\frac{1}{\pi}\theta$	$\frac{1}{\pi}(\theta + \theta')$
1	5.32	5.094159844584467267	0.8085171825 + $i$ 85.6993484854	44.092	89
2	8.96	8.939914408100472858	0.6508300806 + $i$ 114.1633427308	64.026	127
3	11.93	12.133545425790163309	0.5743560504 + $i$ 166.4793059132	103.023	207
4	14.60	14.404003112292645158	0.7242576946 + $i$ 176.7024612429	111.075	223
5	17.08	17.130239400567288918	0.8695305796 + $i$ 240.4046723514	163.055	325
6	19.43	19.308800174241700381	0.8195495921 + $i$ 320.8764896688	232.106	465
7	21.68	22.159707765035018919	0.7682231236 + $i$ 331.0502594079	241.098	483
8	23.85	23.345370112090190151	0.6285081083 + $i$ 366.6409075762	273.027	545
9	25.95	26.094967346227912542	0.8158736778 + $i$ 411.7967375490	314.133	629
10	28.00	27.923798821611878096	0.7088822242 + $i$ 440.4845107397	341.017	681

TABLE IX. *Left:* first few zeros of (245) on the critical line,  $\rho_n = \frac{1}{2} + iy_n$ , computed from (253) starting with the approximation (255). *Right:* We can see that equation (251) is indeed verified for the first few zeros off of the critical line. Note that  $\frac{1}{\pi}\theta$  can be any real number, while the combination  $\frac{1}{\pi}(\theta + \theta')$  always gives an odd integer at a non-trivial zero.

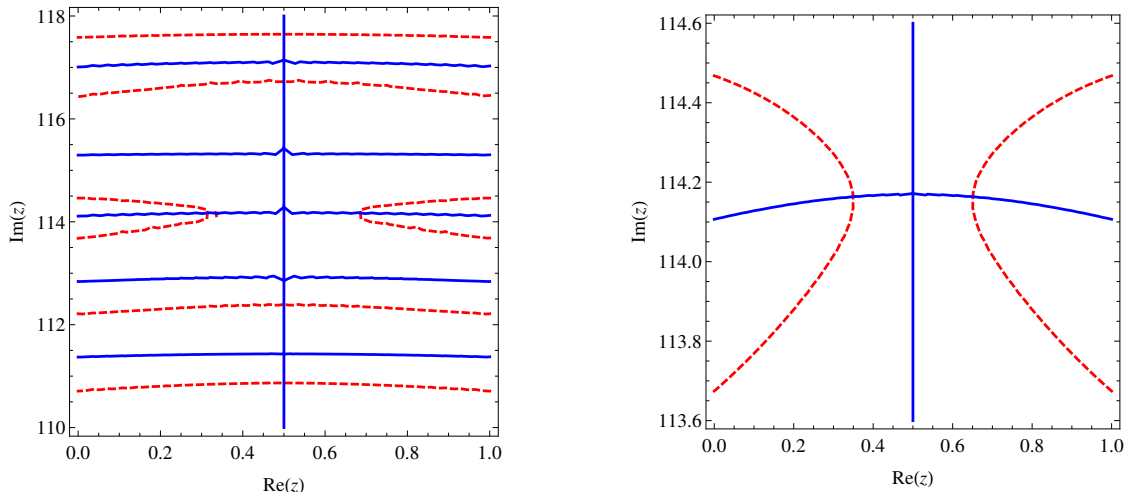


FIG. 28. Contour plot of  $\xi = u + iv$ , equation (248), for  $x = 0 \dots 1$  and  $y = 110 \dots 118$ . Note the zeros off-line for  $y \approx 114.1633$ . The solid (blue) lines correspond to curves  $v = 0$  and the dashed (red) lines to  $u = 0$ .

values of  $\frac{1}{\pi}(\theta + \theta')$ , which are odd integers. In Figure 28 we show the contour lines of (248), i.e.  $\xi(z) = u(x, y) + iv(x, y)$ , and we consider the lines  $u = 0$  and  $v = 0$ . On the critical line  $x = 1/2$  we have a  $v = 0$  contour everywhere, and we approach the zero on a  $u = 0$  contour through the  $\delta$  limit, as shown in equation (253). In this case the  $\delta$  smooths out the discontinuity. However, note how the curves  $u = 0$  are very different in nature for zeros off of the critical line. In this case the  $\delta$  limit does not smooth out the function, since the path to approach the zero is more involved. Nevertheless, equation (251) is still satisfied for these zeros off of the critical line.

If there is a unique solution to (253) for every  $n$ , then as for the  $\zeta$ -function we can determine  $N_0(T)$  which counts zeros on the line. However, the equation (253) *is not defined* for every  $n$ . For instance, for  $n = 44$  and  $n = 45$  this equation has no solution, as illustrated in Figure 29. The same thing happens again for  $n = 64$  and  $n = 65$ , for  $n = 103$  and  $n = 104$ , and so on.

If  $N(T)$  counts zeros on the entire strip, then clearly  $N_0(T) \neq N(T)$ . For these values of  $y$ , corresponding to zeros off the line,  $\lim_{\delta \rightarrow 0^+} \arg \mathcal{D} \left( \frac{1}{2} + \delta + iy \right)$  is not defined, i.e. the  $\delta$  limit *does not smooth out* the function since there is a severe change of branch. This is why the equation (253) is not defined in the vicinity of such  $y$ 's. In Figure 30 (left) we show a plot of  $\frac{1}{\pi} [\theta(x + \delta, y) + \theta'(x + \delta, y)]$  for  $x = 0 \dots 1$  and  $y = 81 \dots 90$ . Note that there are zeros off the line at  $y \approx 85.6993$ . We included a  $\delta \sim 10^{-1}$ . Note how the function can be smoothed on the critical line  $x = 1/2$  if there are only zeros on the line. However, when there are zeros off of the critical line the function cannot be made continuous (note the “big hole” around the critical line).

Finally, in Figure 30 (right) we plot the analog of Figure 14 (right). In the vicinity of the

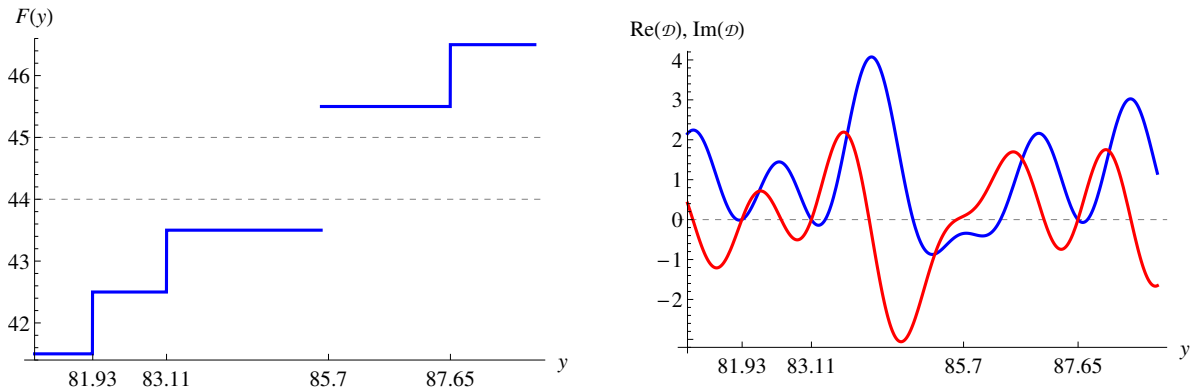


FIG. 29. *Left:*  $F(y) = \frac{1}{\pi} (\Xi(y) + \arg \mathcal{D}(\frac{1}{2} + \delta + iy)) + \frac{1}{2}$  versus  $y$ . Note the discontinuity in the graph for  $y \approx 85.6993$ , corresponding to  $n = 44$  and  $n = 45$ , where the equation (253) has no solution. *Right:* the blue line is  $\Re(\mathcal{D}(\frac{1}{2} + iy))$  and the red line is  $\Im(\mathcal{D}(\frac{1}{2} + iy))$ . Equation (253) is not defined since  $\arg \mathcal{D}(\frac{1}{2} + iy)$  changes branch. Note that  $\Re(\mathcal{D}) < 0$  and  $\Im(\mathcal{D}) = 0$  at  $y \approx 85.6993$ , where there are two zeros off the line at this height.

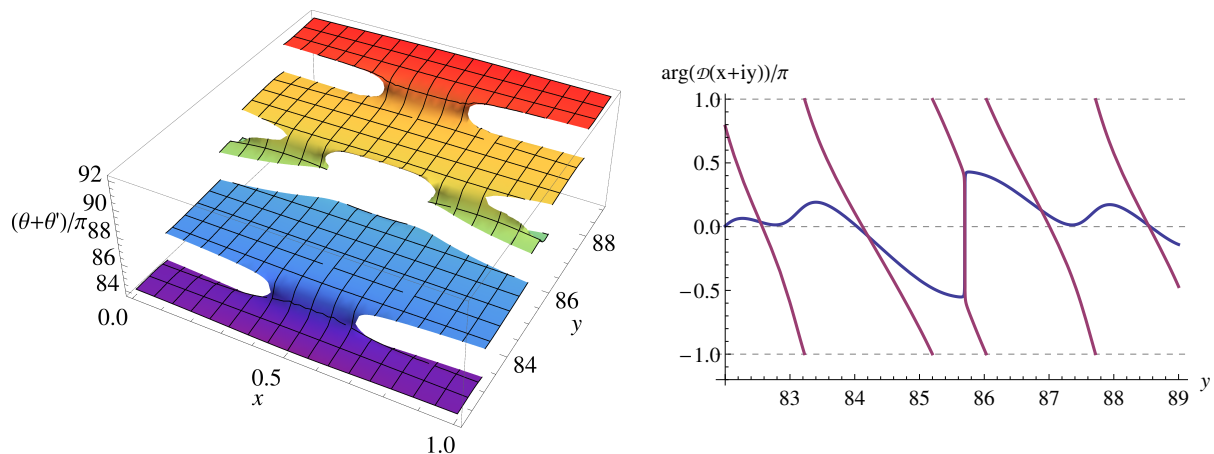


FIG. 30. *Left:* The zeros off-line do not allow the function to be smoothed on the critical line. *Right:* the blue line is  $\frac{1}{\pi} \arg \mathcal{D}(x + iy)/\pi$  versus  $y$ , in the vicinity of the first zero off the line, where  $x \approx 0.8085$ . The purple line is  $\frac{1}{\pi} \arg \mathcal{D}(1 - x + iy)$ .

first zero off the critical line, both  $\theta$  and  $\theta'$  are well-defined and there is a solution to (251).

For Riemann  $\zeta$ , we provided arguments, though not a proof, that there is a unique solution to the analogous equation (138), implying that  $N_0(T) = N(T)$ . If  $\arg \zeta(\frac{1}{2} + iy)$  does not change branch, or if it changes “very little”, the  $\delta$  limit smooths out the function, making the equation well defined. On the other hand, if there is a severe change of branch it is impossible to make this function continuous, which is the case here for the function (245) (see Figures 29 and 30). In the case of the Davenport-Heilbronn function, Karatsuba [52] showed that at least  $T(\log T)^{1/2-\epsilon}$  zeros lie on the critical line.

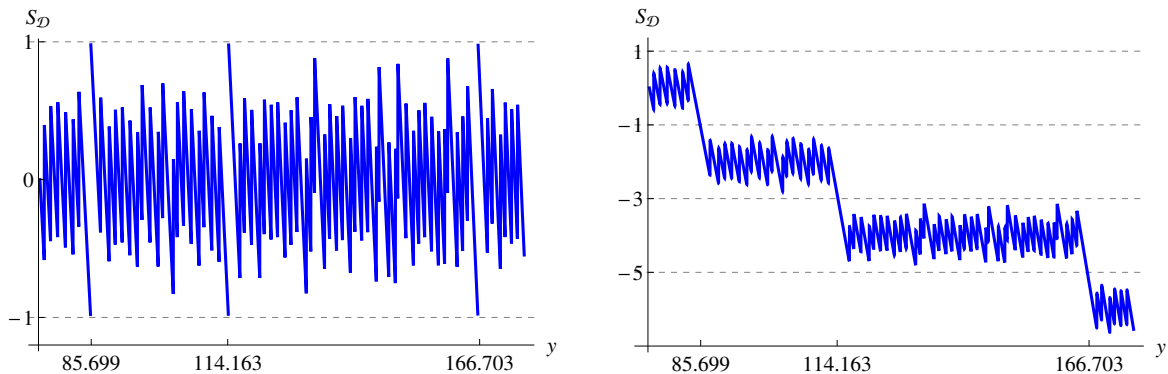


FIG. 31. *Left:*  $S_{\mathcal{D}}$  in the principal branch. *Right:*  $S_{\mathcal{D}}$  explicitly showing the changes in branch.  $\langle S_{\mathcal{D}} \rangle \neq 0$  in this range.

The important difference with  $\zeta$  is that

$$S_{\mathcal{D}}(y) = \lim_{\delta \rightarrow 0^+} \frac{1}{\pi} \arg \mathcal{D} \left( \frac{1}{2} + \delta + y \right) \quad (256)$$

has very different properties in comparison to  $S(y) = \lim_{\delta \rightarrow 0^+} \frac{1}{\pi} \arg \zeta \left( \frac{1}{2} + \delta + iy \right)$  or the argument of the other  $L$ -functions we have considered. The properties conjectured for  $S(y)$  in section VIII should not hold. The repeated changes in branch suggests that  $S_{\mathcal{D}}(y)$  has the behavior sketched in Figure 31, however we have not proven this.

## XX. SADDLE POINT APPROXIMATION

The original aim of the work in this section was to obtain an approximate analytic expression for  $\arg \zeta \left( \frac{1}{2} + iy \right)$  because of its importance to the whole theory of the zeros. For the smooth part,  $\arg \Gamma$ , one has such an expression due to the Stirling's approximation, and we will present something similar for  $\zeta$ .

The saddle-point method, also known as steepest descent method, approximates integrals of the type

$$I(\lambda) = \int_{\mathcal{C}} e^{\lambda f(u)} du \quad (257)$$

for large  $\lambda$ . The saddle-points are solutions to  $f'(u) = 0$ , provided  $f''(u) \neq 0$ , where  $f'$  and  $f''$  are the first and second derivatives of  $f$ . For simplicity let us consider only one saddle point denoted by  $s$ . The contour  $\mathcal{C}$  must be deformed in such a way as to pass through  $u = s$  with  $\Re(u)$  having the steepest descent (hence the name). If  $f(u)$  is an *analytic* function, using  $f(u) \approx f(s) + \frac{1}{2} f''(s)(u - s)^2$  one is left with a gaussian integral and obtains

$$I(\lambda) \approx \sqrt{\frac{2\pi}{-f''(s)}} e^{\lambda f(s)}. \quad (258)$$

Let us consider a very illustrative example, the result of which we will need later. The  $\Gamma$ -function has the integral representation

$$\Gamma(z) = \int_0^{\infty} u^{z-1} e^{-u} du, \quad \Re(z) > 0. \quad (259)$$

Writing the integrand as  $e^{f(u)}$  where  $f(u) = -u + (z-1)\log u$ , then  $f'(u) = 0$  implies  $s = z - 1$ . Then (258) yields

$$\Gamma(z) \approx \sqrt{2\pi}(z-1)^{z-1/2} e^{-(z-1)}. \quad (260)$$

For  $n$  a positive integer,  $\Gamma(n+1) = n! \approx \sqrt{2\pi} n^{n+1/2} e^{-n}$ , which is the very useful Stirling's approximation. Since the above approximation is an analytic function of  $z$ , it is valid in the whole complex plane through analytic continuation. It is very useful for instance to determine the asymptotic expansion of the Riemann-Siegel  $\vartheta$  function,

$$\vartheta(y) = \arg \Gamma\left(\frac{1}{4} + \frac{iy}{2}\right) - y \log \sqrt{\pi} \approx \frac{y}{2} \log\left(\frac{y}{2\pi e}\right) - \frac{\pi}{8} \quad (261)$$

where as usual  $\arg \Gamma = \Im \log \Gamma$ .

Now let us consider the  $\zeta$ -function, which has the well known integral representation

$$\zeta(z) = \frac{1}{\Gamma(z)} \int_0^{\infty} \frac{u^{z-1}}{e^u - 1} du, \quad \Re(z) > 1. \quad (262)$$

If  $z \gg 1$  is real, then the saddle point of the integrand in (262) is far from the origin, and one can approximate  $e^u - 1 \approx e^u$ , then this integral is approximately the same as (259), showing that for real  $z$  then  $\zeta(z) \rightarrow 1$  as  $z \rightarrow \infty$ . The above integral is badly behaved at the origin  $u = 0$ , thus let us introduce a small parameter  $\mu$ , having in mind that we can always take the limit  $\mu \rightarrow 0^+$ . The above integral arises in quantum statistical physics, and  $\mu$  is minus the chemical potential. Thus we introduce

$$\zeta(z) = \lim_{\mu \rightarrow 0^+} \frac{1}{\Gamma(z)} \int_0^{\infty} \frac{u^{z-1}}{e^{u+\mu} - 1} du. \quad (263)$$

We want to estimate this integral through the saddle-point method. For this aim we can write the integrand in the form  $e^{f(u)}$  where

$$f(u) = (z-1)\log u - \log(e^{u+\mu} - 1). \quad (264)$$

The condition  $f'(u) = 0$  yields the transcendental equation

$$\frac{z-1}{u} = \frac{e^{u+\mu}}{e^{u+\mu} - 1}, \quad (265)$$



which can be solved explicitly, determining the saddle points in the following form:

$$s_k(z) = z - 1 + w_k(z), \quad (266)$$

with

$$w_k(z) = W_k \left[ (1 - z)e^{1-z-\mu} \right],$$

where  $W_k$  is the  $k$ -th branch of the multi-valued Lambert  $W$  function (217). Note that setting  $w_k = 0$ , one recovers the saddle point for the  $\Gamma$ -function.

One can easily show that

$$f(s_k) = -s_k - \mu + (z - 2) \log s_k + \log(z - 1) \quad (267)$$

and

$$f''(s_k) = \frac{(1 + w_k)}{(1 - z) \left(1 + \frac{w_k}{z-1}\right)^2}. \quad (268)$$

For real  $z$  (266) yields only one saddle-point given by the principal branch  $k = 0$ . For complex  $z$  we have an infinite number of saddle-points. However, not all of them contribute to the integral (263), since according to the integration path we must choose the ones which satisfy  $\Re(s_k) > 0$ . Using equations (267), (268) and dividing by the Stirling approximation to  $\Gamma(z)$ , equation (260), one then obtains

$$\zeta(z) \approx \sum_k' \zeta_k(z) \quad (269)$$

where

$$\zeta_k(z) = \exp \left\{ (z - 1) \log \left( 1 + \frac{w_k}{(z - 1)} \right) - w_k - \mu - \frac{1}{2} \log(w_k + 1) \right\}. \quad (270)$$

In the above formula (269) the  $\mu \rightarrow 0^+$  is implicit. The sum over integers  $k$  must be taken according to the condition  $\Re(s_k) > 0$ .

In obtaining (269) it is important to note that (264) is *not* an analytic function, since  $\log u$  has branches for  $u \in \mathbb{C}$ . Thus we are taking into account the contribution of each different branch  $k$  for the saddle-points. This goes a little beyond the assumptions of the saddle-point method (258).

For real values of  $z$  there is only one saddle-point corresponding to  $k = 0$  in (269). This approximation describes the  $\zeta(z)$  very well over this range, as shown in Figure 32 (left).

For complex values in the approximation (269) we need to consider the contribution for different branches  $k$ . On the critical line  $z = 1/2 + iy$ , a plot of the absolute value of (269) is shown in Figure 32 (right). The number of saddle points varies with  $y$ . For instance, for  $y \sim 15$  we need  $k = -2, -1, 0$  and for  $y \sim 30$  we need  $k = -4, -3, \dots, 0$ . Thus the sum in (269) ranges differently for each value of  $y$ .

Roughly, the number of branches one needs is  $-|y|/2\pi < k \leq 0$  which can be obtained

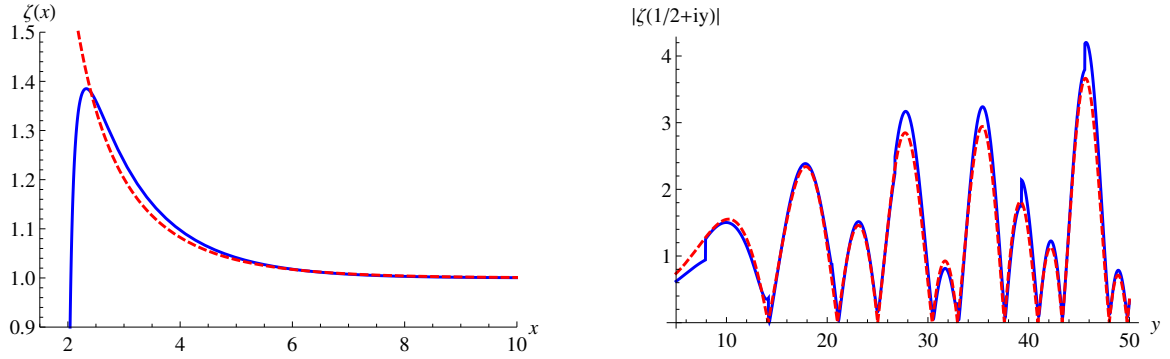


FIG. 32. The dashed (red) line corresponds to the exact  $\zeta(z)$  while the solid (blue) line corresponds to the saddle point approximation (269). *Left*: real values. *Right*: complex values on the critical line.

from the condition  $\Re(s_k) > 0$  (the branches  $k > 0$  can be neglected). This approximation works surprisingly well, as Figure 32 shows; it clearly captures the zeros. However it remains difficult to characterize  $\arg \zeta$  precisely, because of the sum over branches  $k$ .

## XXI. DISCUSSION AND OPEN PROBLEMS

In the second half of these lectures we have provided new insights into the RH. We have actually proposed several concrete strategies towards its proof which are all based on analysis. Let us list some of the main open problems, namely what would be needed to complete this program.

1. Is there a more rigorous derivation of our main equation (149), i.e.  $\theta + \theta' = (2n + 1)\pi$ ? It is a powerful new equation that is valid whether the RH is true or not and contains detailed information about the zeros since they are enumerated by an integer  $n$ . It is evidently correct and captures all zeros, trivial or non-trivial, of the multitude of functions considered in this paper, including functions with zeros off of the critical line, where the RH fails. This seems to be a matter of carefully defining the limit as one approaches a zero.
2. Can one prove there is a unique solution to the transcendental equation (138) for every  $n$ ? As explained, this would imply the RH is true since then  $N_0(T) = N(T)$ . We provided arguments that the  $\delta \rightarrow 0^+$  prescription smooths out the function  $S(y)$  sufficiently so that there is indeed a unique solution. We also showed that it is precisely this property that fails for the Davenport-Heilbronn function, where the RH is false.
3. Can one prove that the real electric potential  $\Phi(x, y)$  is a regular alternating function along the line  $\Re(z) = 1$ ? We showed this asymptotically, but only in a crude

approximation. We argued that this would also establish the RH. Can the latter be proven?

4. Can one prove directly that there are no zeros off of the critical line by proving there are no solutions to  $\theta(x, y) + \theta'(x, y) = (2n + 1)\pi$  for  $x \neq 1/2$ ? We suggested one approach, based on the observation that the left hand side of this equation has very little dependence on  $x$  for  $x > 1/2$  (see Figure 13). Since we know there are no solutions for  $x \geq 1$ , i.e. there are no zeros with  $x \geq 1$ , this suggests that this would imply there are no zeros for  $x > 1/2$ , since the curve for  $x > 1/2$  is essentially the same as at  $x = 1$ , and there we know there are no solutions. Can this argument be made more precise? This is an appealing idea since the RH would then be related to the fact that there are no zeros with  $x \geq 1$ , which follows from the Euler product formula. Functions such as the Davenport-Heilbronn function where the RH fails do not have an Euler product formula.

**Note added 4.** A clearer derivation of the equation (138), referred to as the França-LeClair equation and proposed in [7], was given in [14]. ▲

**Note added 5.** Progress on open questions 2 and 4 above was recently presented in [14, 15], based on defining a quantum mechanical model of a single particle scattering through impurities arranged on a circle, where each impurity is associated with a prime number through a scattering phase based on the Euler product. The quantized energies  $E_n(\sigma)$  are easily calculated from a Bethe-ansatz equation. The quantized energies of this model are exactly the Riemann zeros on the critical line in the limit  $\sigma \rightarrow \frac{1}{2}$  from the right, since they satisfy the França-LeClair equation. In this model, the pseudo-randomness of the primes implies the particle is scattering through an essentially disordered potential, as in Anderson localization, which implies an underlying pseudo-random Hamiltonian. The latter property offers a new perspective on the origin of random matrix (GUE) statistics of the Riemann zeros. Let us mention also that random matrix theory is used extensively in the study of disordered systems and Anderson localization. ▲

**Note added 6.** The spectral flow for the quantized energies  $E_n(\sigma)$  of the model in [14] was studied in [15], where it was argued that the scattering problem necessarily has real eigenvalues since the S-matrix is unitary, and this would imply the Riemann Hypothesis is true. This can be viewed as a scattering version of the Hilbert-Pólya conjecture since the S-matrix is  $S = e^{-iH}$ , where  $H$  is a Hermitian Hamiltonian, and  $S^\dagger S = 1$ .<sup>13</sup> For the RH, to crack this nut, seemingly made of steel, one must first create a suitable tool before thinking about how to crack it precisely into two hemispheres. Cautiously speaking, this recent work [15] may establish the validity of the Riemann Hypothesis based on quantum physics. This work shows that the Hilbert-Pólya conjecture is true if one plucks a Hamiltonian of

---

<sup>13</sup>This is an over simplification: in general, one needs to consider a time-ordered exponential.

the right feather, in particular one that leads to a *scattering problem* rather than a bound state problem (as was presumably implied in the Hilbert-Pólya conjecture). However, it is probably not yet rigorous enough to constitute a pure mathematical proof, although it has all of the expected ingredients towards a proof of the Riemann Hypothesis: functional equation, Euler product formula, and pseudo-randomness of the primes that may induce GUE random matrix statistics. Another nice feature of this approach is that it easily extends to the General Riemann Hypothesis for  $L$ -functions based on Dirichlet characters and those based on cusp forms. On the other hand, the Davenport-Heilbronn counter-example has no such unitary S-matrix since the linear combination of Dirichlet  $L$ -functions does not admit an Euler product, showing why it fails within this framework [15]. ▲

**Note added 7.** Although the Euler product does not converge to the right of the critical line for Dirichlet  $L$ -functions based on principal characters, such as Riemann  $\zeta$  itself which corresponds to the trivial character  $\chi(n) = 1$  for all integer  $n$ , a truncated Euler product can still provide a good approximation. We used this to estimate the  $n = 10^{100}$ -th zero to 103 decimals in [10]: Using only  $10^6$  primes, we found the following  $y_n$ :

$$\begin{aligned} n &= 10^{100}\text{th zero:} \\ y_n &= 280690383842894069903195445838256400084548030162846 \\ &\quad 045192360059224930922349073043060335653109252473.244\dots \end{aligned}$$

Obtaining this number took only a few minutes on a laptop using Mathematica. The integer part is easily calculated using the Lambert approximation described above. We are reasonably confident that the last 3 digits  $\sim .244$  are correct since we checked that they didn't change between using  $10^6$  and  $5 \times 10^6$  primes in the Euler product. Although this needs more detailed investigation, if correct this google-th zero is far beyond what is currently known based on computational mathematics, which are zeros around  $n = 10^{33}$ . ▲

## ACKNOWLEDGMENTS

We wish to thank the organizers Olaf Lechtenfeld and Ulrich Theis for the opportunity to present these lectures. We also thank Denis Bernard and Timothy Healy for useful discussions. GF is supported by CNPq-Brazil. For this updated version, AL thanks Steve Gonek and Ghaith Hiary for discussions, as well as Guilherme França and Giuseppe Mussardo for their subsequent collaboration on this topic.

### Appendix A: The Perron formula

Consider the sum

$$A(x) = \sum'_{n \leq x} a(n) \quad (\text{A1})$$

where  $a(n)$  is an arithmetic function. Here, the prime on the summation indicates that the last term of the sum must be multiplied by  $1/2$  when  $x$  is an integer. One has the following integral:

$$\int_0^\infty A(x)x^{-z-1}dx = \int_0^\infty \left( \sum_{n \leq x} a(n) \right) x^{-z-1}dx = -\frac{1}{z} \int_0^\infty \left( \sum_{n \leq x} a(n) \right) \frac{d}{dx} (x^{-z}) dx. \quad (\text{A2})$$

Since  $A(x)$  is a sequence of step functions, and the derivative of a step function is the Dirac delta-function, one has

$$\frac{d}{dx} \sum_{n \leq x} a(n) = a(x)\delta(x - n)$$

Integrating the above expression by parts one obtains

$$\frac{g(z)}{z} = \int_0^\infty A(x)x^{-z-1}dx. \quad (\text{A3})$$

where

$$g(z) = \sum_{n=1}^\infty \frac{a(n)}{n^z}. \quad (\text{A4})$$

The standard definition of the Mellin transform  $\mathcal{M}f$  of the function  $f$  is

$$(\mathcal{M}f)(s) = \varphi(s) = \int_0^\infty x^{s-1}f(x)dx. \quad (\text{A5})$$

Its inverse is well-known:

$$(\mathcal{M}^{-1}\varphi)(x) = f(x) = \frac{1}{2\pi i} \int_{c-i\infty}^{c+i\infty} x^{-s}\varphi(s)ds. \quad (\text{A6})$$

Identifying  $s = -z$ ,  $\varphi(-z) = g(z)/z$ , and  $f(x) = A(x)$  one obtains (84).

### Appendix B: Counting formula on the entire critical strip

The argument principle enables us to count zeros and poles of a complex function inside a simply connected bounded region. Let us consider two functions  $f(z)$  and  $g(z)$ , such that  $f$  is analytic and  $g$  is meromorphic inside and on a given closed contour  $\mathcal{C}$ . Thus we can

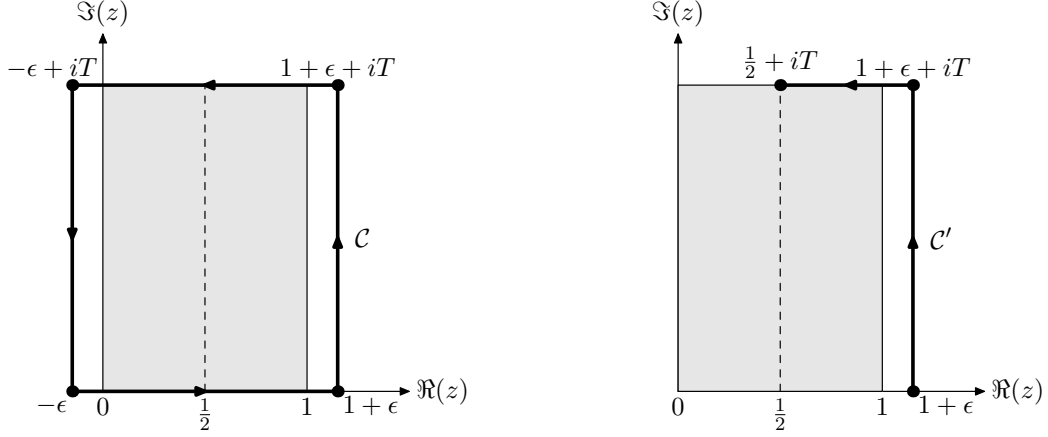


FIG. 33. *Left:* contour  $\mathcal{C}$  for (B7) in the counterclockwise direction. The contour must have no zeros on it. The critical line  $\Re(z) = 1/2$  splits the rectangle in half. *Right:* it is equivalent to consider the contour  $\mathcal{C}'$ .

write

$$g(z) = (z - w_1)^{n_1} (z - w_2)^{n_2} \cdots \frac{1}{(z - \bar{w}_1)^{\bar{n}_1} (z - \bar{w}_2)^{\bar{n}_2} \cdots} h(z) \quad (\text{B1})$$

where  $w_i$  and  $\bar{w}_i$  denotes the zeros and poles, respectively, with its respective multiplicities  $n_i$  and order  $\bar{n}_i$ , and  $h(z)$  is analytic and without zeros or poles in and on  $\mathcal{C}$ . Then we have

$$\frac{g'(z)}{g(z)} = \frac{d}{dz} \log g(z) = \frac{n_1}{z - w_1} + \frac{n_2}{z - w_2} + \cdots - \frac{\bar{n}_1}{z - \bar{w}_1} - \frac{\bar{n}_2}{z - \bar{w}_2} - \cdots + \frac{h'(z)}{h(z)}. \quad (\text{B2})$$

Assuming that  $g(z)$  has no zeros or poles on the contour  $\mathcal{C}$ , we thus have

$$\oint_{\mathcal{C}} f(z) \frac{g'(z)}{g(z)} dz = \sum_i n_i \oint_{\mathcal{C}} \frac{f(z)}{z - w_i} dz - \sum_j \bar{n}_j \oint_{\mathcal{C}} \frac{f(z)}{z - \bar{w}_j} dz + \oint_{\mathcal{C}} f(z) \frac{h'(z)}{h(z)} dz. \quad (\text{B3})$$

Since  $\frac{fh'}{h}$  is analytic, the last integral vanishes by Cauchy's integral theorem. By Cauchy's integral formula we therefore have

$$\frac{1}{2\pi i} \oint_{\mathcal{C}} f(z) \frac{g'(z)}{g(z)} dz = \sum_i n_i f(w_i) - \sum_j \bar{n}_j f(\bar{w}_j). \quad (\text{B4})$$

Now setting  $f(z) = 1$  we have *Cauchy's argument principle*

$$\frac{1}{2\pi i} \oint_{\mathcal{C}} \frac{g'(z)}{g(z)} dz = N - \bar{N}, \quad (\text{B5})$$

where  $N = \sum_i n_i$  is the number of zeros inside  $\mathcal{C}$ , including multiplicities, and  $\bar{N} = \sum_j \bar{n}_j$  is the number of poles, accounting its orders.

Now let us use (B5) to count the zeros of  $\zeta(z)$  inside the region  $0 \leq \Re(z) \leq 1$  and  $0 \leq \Im(z) \leq T$ . Remember that  $\zeta(z)$  and  $\chi(z)$  have the same zeros in this region. Since  $\zeta(z)$  has a simple pole at  $z = 1$ , and so has  $\chi(z)$ , we consider the function

$$\xi(z) \equiv \frac{1}{2}z(z-1)\pi^{-z/2}\Gamma(z/2)\zeta(z), \quad (\text{B6})$$

which is entire and has no poles. Note that  $\zeta(z)$ , and thus  $\xi(z)$ , has no zeros along the positive real line, and according to (B5) we must assume that  $T$  does not correspond to the imaginary part of a zero. Then from (B5) we have

$$N(T) = \frac{1}{2\pi} \Im \left[ \oint_{\mathcal{C}} \frac{\xi'(z)}{\xi(z)} dz \right], \quad (\text{B7})$$

where the contour  $\mathcal{C}$  is chosen to be the boundary of the rectangle with vertices at the points  $z \in \{-\epsilon, 1 + \epsilon, 1 + \epsilon + iT, -\epsilon + iT\}$ , as illustrated in Figure 33 (left). Since  $\xi(z)$  is real on the real line, the integration along the line segment  $[-\epsilon, 1 + \epsilon]$  does not contribute to (B7). Moreover, since  $\xi(z) = \xi(1 - z)$  we can consider just the right half of the rectangle, whose contribution to the integral (B7) comes from line segments  $[1 + \epsilon, 1 + \epsilon + iT]$  and  $[1 + \epsilon + iT, 1/2 + iT]$ . This is the contour  $\mathcal{C}'$  shown in Figure 33 (right). Therefore we have

$$N(T) = \frac{1}{\pi} \Im \int_{\mathcal{C}'} dz \frac{d}{dz} \log \xi(z) \quad (\text{B8})$$

$$= \frac{1}{\pi} \Im \int_{\mathcal{C}'} dz \frac{d}{dz} \left[ \log \left( \frac{1}{2}z(z-1) \right) + \log \left( \pi^{-z/2} \Gamma(z/2) \right) + \log \zeta(z) \right]. \quad (\text{B9})$$

The first term in (B9) gives

$$\frac{1}{\pi} \Im \log \left[ \frac{1}{2}z(z-1) \right] \Big|_{1+\epsilon}^{1/2+iT} = \frac{1}{\pi} \Im \log \left( -\frac{1}{2} \left( T^2 + \frac{1}{4} \right) \right) = 1. \quad (\text{B10})$$

For the second term in (B9), since  $\pi^{-z/2}\Gamma(z/2)$  is analytic and real on  $z = 1 + \epsilon$ , we have the contribution only from the end point of the contour, which gives

$$\frac{1}{\pi} \Im \log \Gamma \left( \frac{1}{4} + i\frac{T}{2} \right) - \frac{T}{2\pi} \log \pi \equiv \frac{1}{\pi} \vartheta(T), \quad (\text{B11})$$

where we have the Riemann-Siegel  $\vartheta$  function. Therefore, the number of zeros in the critical strip up to height  $T$  is given by

$$N(T) = \frac{1}{\pi} \vartheta(T) + 1 + S(T) \quad (\text{B12})$$

where

$$S(T) \equiv \frac{1}{\pi} \Im \int_{\mathcal{C}'} d(\log \zeta(z)) = \frac{1}{\pi} \Delta_{\mathcal{C}'} \arg \zeta(z). \quad (\text{B13})$$

The above formula (B12) is known as the *Backlund counting formula*. Note that  $\Im \log \zeta = \arg \zeta$ . The above result consists in computing the variation of  $\arg \zeta(z)$  through the line segments starting at  $z = 1 + \epsilon$ , where  $\arg \zeta(1 + \epsilon) = 0$ , then up to  $z = 1 + \epsilon + iT$ , then finally to  $z = 1/2 + iT$ . Since the integrand in (B13) is a total derivative, it is tempting to write  $S(T) = \frac{1}{\pi} \Im \log \zeta(1/2 + iT) = \frac{1}{\pi} \arg \zeta(1/2 + iT)$ , corresponding to the end point of the contour  $\mathcal{C}'$ . However, this must be carefully considered since  $\log \zeta(z)$  can not be always in the principal branch along  $\mathcal{C}'$ . Nevertheless, if  $\Re(\zeta) > 0$  for all  $z$  on  $\mathcal{C}'$ , then  $\log \zeta(z)$  is well defined and is always in the principal branch, i.e.  $\log \zeta(z) = \log |\zeta(z)| + i \arg \zeta(z)$  with  $-\pi/2 < \arg \zeta(z) \leq \pi/2$ . In such a case it is valid to set  $S(T) = \frac{1}{\pi} \arg \zeta(1/2 + iT)$ , and we also have  $|S(T)| < 1/2$ .

Let us now consider  $z = x + iy$  for  $x \geq 2$ . From the series  $\zeta(z) = \sum_{n=1}^{\infty} n^{-z}$  we have

$$\Re(\zeta) = 1 + \frac{\cos(y \log 2)}{2^x} + \frac{\cos(y \log 3)}{3^x} + \dots \geq 1 - \left( \frac{1}{2^x} + \frac{1}{3^x} + \dots \right). \quad (\text{B14})$$

Since  $x \geq 2$  we also have

$$\frac{1}{2^x} + \frac{1}{3^x} + \frac{1}{4^x} + \dots \leq \frac{1}{2^2} + \frac{1}{3^2} + \frac{1}{4^2} + \dots = \zeta(2) - 1 = \frac{\pi^2}{6} - 1 \quad (\text{B15})$$

Therefore

$$\Re(\zeta) > \frac{12 - \pi^2}{6} > 0. \quad (\text{B16})$$

For this reason it is often assumed  $\epsilon = 1$  in the contour  $\mathcal{C}'$  appearing in (B13). In this way one only needs to analyze the behaviour of  $\Re(\zeta)$  along the horizontal line joining the points  $2 + iT$  and  $\frac{1}{2} + iT$ .

If one expands  $\Gamma(z)$  in (B11) through Stirling's formula one obtains

$$\vartheta(T) = \frac{T}{2} \log \left( \frac{T}{2\pi e} \right) - \frac{\pi}{8} + O(T^{-1}). \quad (\text{B17})$$

Then (B12) yields the *Riemann-von Mangoldt counting formula*

$$N(T) = \frac{T}{2\pi} \log \left( \frac{T}{2\pi} \right) - \frac{T}{2\pi} + \frac{7}{8} + S(T) + O(T^{-1}). \quad (\text{B18})$$

### Appendix C: Mathematica code

Here we provide a simple Mathematica implementation to compute the zeros of  $L$ -functions based on the previous transcendental equations. We will consider Dirichlet  $L$ -functions, since it involves more ingredients, like the modulus  $k$ , the order  $a$  and the Gauss sum  $G(\tau)$ . For the Riemann  $\zeta$ -function the procedure is trivially adapted, as well as for the Ramanujan  $\tau$ -function of section XVIII.



The function (192) is implemented as follows:

```
RSTheta[y_, a_, k_] := Im[LogGamma[1/4 + a/2 + I*y/2]] - y/2*Log[Pi/k]
```

For the transcendental equation (194) we have

```
ExactEq[n_, y_, s_, a_, k_, j_, G_, n0_] :=
  (RSTheta[y, a, k] + Arg[DirichletL[k, j, 1/2 + s + I*y]] - 1/2*Arg[G])/Pi +
  a/4 + 1/2 - n + n0
```

Above,  $s$  denotes  $0 < \delta \ll 1$ ,  $a$  is the order (174),  $k$  is the modulus,  $j$  specify the Dirichlet character  $\chi_{k,j}$  (as discussed in section IX), and  $G$  is the Gauss sum (170). Note that we also included  $n_0$ , discussed after (193), but we always set  $n_0 = 0$  for the cases analysed in section XVII. The implementation of the approximate solution (227) is

```
Sgn[n_] := Which[n != 0, Sign[n], n == 0, -1]
A[n_, a_, G_, n0_] := Sgn[n]*(n - n0 + 1/2/Pi*Arg[G]) + (1 - 4*Sgn[n] - 2*a*(
  Sgn[n] + 1))/8
yApprox[n_, a_, G_, k_, n0_] := 2*Pi*Sgn[n]*A[n, a, G, n0]/LambertW[k*A[n, a,
  G, n0]/E]
```

One can then obtain the numerical solution of the transcendental equation (194) as follows:

```
FindZero[n_, s_, a_, k_, j_, G_, n0_, y0_, prec_] :=
  y /. FindRoot[ExactEq[n, y, s, a, k, j, G, n0], {y, y0}, PrecisionGoal ->
  prec/2, AccuracyGoal -> prec/2, WorkingPrecision -> prec]
```

Above,  $y_0$  will be given by the approximate solution (227). The variable  $prec$  will be adjusted iteratively. Now the procedure described in section XVI can be implemented as follows:

```
DirichletNZero[n_, order_, digits_, k_, j_, n0_] := (
  chi = DirichletCharacter[k, j, -1];
  a = Which[chi == -1, 1, chi == 1, 0];
  s = 10^(-3);
  prec = 15;
  G = Sum[DirichletCharacter[k, j, 1]*Exp[2*Pi*I*1/k], {1, 1, k}];
  y = N[yApprox[n, a, G, k, n0], 20];
  absvalue = 1;
  While[absvalue > order,
    y = FindZero[n, s, a, k, j, G, n0, y, prec];
    Print[NumberForm[y, digits]];
    s = s/1000;
    prec = prec + 20;
    absvalue = Abs[DirichletL[k, j, 1/2 + I*y]];
  ]
```

```
Print[ScientificForm[absvalue, 5]];
)
```

Above, the variable `order` controls the accuracy of the solution. For instance, if `order = 10-50`, it will iterate until the solution is verified at least to  $|L(\frac{1}{2}) + iy| \sim 10^{-50}$ . The variable `digits` controls the number of decimal places shown in the output.

Let us compute the zero  $n = 1$ , for the character (236), i.e.  $k = 7$  and  $j = 3$ . We will verify the solution to  $\sim 50$  decimal places and print the results with 52 digits. Thus executing

```
DirichletNZero[1, 10-50, 52, 7, 3, 0]
```

the output will be

```
4.35640188194945
...
4.356401624736284227279574790515519132971499551683092
4.356401624736284227279574790515519132971499294412496
4.356401624736284227279574790515519132971499294412239
4.1664*10-55
```

Note how the decimal digits converge in each iteration. By decreasing `order` and increasing `digits` it is possible to obtain highly accurate solutions. Depending on the height of the critical line under consideration, one should adapt the parameters `s` and `prec` appropriately. In Mathematica we were able to compute solutions up to  $n \sim 10^6$  for Dirichlet  $L$ -functions, and up to  $n \sim 10^9$  for the Riemann  $\zeta$ -function without problems. We were unable to go much higher only because Mathematica could not compute the  $argL$  term reliably. To solve the transcendental equations (138) and (194) for very high values on the critical line is a challenging numerical problem. Nevertheless, we believe that it can be done through a more specialized implementation.

- 
- [1] Max Planck, "On the law of distribution of energy in the normal spectrum," *Annalen der Physik* **4**, 553 (1901).
  - [2] H. M. Edwards, *Riemann's Zeta Function* (Dover Publications Inc., 1974).
  - [3] J. B. Conrey, "The Riemann hypothesis," *Notices of the AMS* **42** (2003).
  - [4] P. Sarnak, "Problems of the Millennium: The Riemann hypothesis," Clay Mathematics Institute (2004).
  - [5] E. Bombieri, "Problems of the Millennium: The Riemann hypothesis," Clay Mathematics Institute (2000).
  - [6] A. LeClair, "An electrostatic depiction of the validity of the Riemann hypothesis and a formula for the  $N$ -th zero at large  $N$ ," *Int. J. Mod. Phys. A* **28**, 1350151 (2013).

- [7] G. França and A. LeClair, “Transcendental equations satisfied by the individual zeros of Riemann  $\zeta$ , Dirichlet and modular  $L$ -functions,” *Commun. Number Theor. and Phys.* **9**, 1–50 (2015).
- [8] T. M. Apostol, *Introduction to Analytic Number theory* (Springer-Verlag, New York, 1976).
- [9] G. França and A. LeClair, “Some Riemann hypotheses from random walks over primes,” *Commun. Contemp. Math.* **20**, 1750085 (2018).
- [10] A. LeClair, “Riemann Hypothesis and random walks: the zeta case,” *Symmetry* **13**, 1–13 (2021).
- [11] G. Mussardo and A. LeClair, “Generalized Riemann hypothesis and stochastic time series,” *J. Stat. Mech.* **06**, 063205 (2018).
- [12] A. LeClair and G. Mussardo, “Generalized Riemann hypothesis, time series and normal distributions,” *J. Stat. Mech.* , 023203 (2019).
- [13] G. Mussardo and A. LeClair, “Randomness of möbius coefficients and brownian motion: growth of the mertens function and the riemann hypothesis,” *J. Stat. Mech.* , 113106 (2021).
- [14] A. LeClair and G. Mussardo, “Riemann zeros as quantized energies of scattering with impurities,” *J. High Energ. Phys.* **2024** (2024).
- [15] A. LeClair, “Spectral flow for the Riemann zeros,” arXiv:2406.01828 [math.ph] (2024).
- [16] J.-B. Bost and A. Connes, “Hecke algebras, type iii factors and phase transitions with spontaneous symmetry breaking in number theory”,” *Sel. Math. New Ser.* , 411–457 (1995).
- [17] D. Schumayer and D. A. W. Hutchinson, “Physics of the Riemann hypothesis,” *Rev. Mod. Phys.* **83**, 307–330 (2011).
- [18] M. V. Berry and J. P. Keating, “A compact Hamiltonian with the same asymptotic mean spectral density as the riemann zeros,” *J. Phys. A: Math. Theor.* **44**, 285203 (2011).
- [19] G. Sierra, “The Riemann zeros as spectrum and the Riemann hypothesis,” *Symmetry* **11**, 494 (2019).
- [20] E. C. Titchmarsh, *The Theory of the Riemann Zeta-Function* (Oxford University Press, 1988).
- [21] R. Apéry, “Irrationalité de  $\zeta(2)$  and  $\zeta(3)$ ,” *Astérisque* , 11–13 (1979).
- [22] R. Apéry, “Interpolation de fractions continues et irrationalité de certaines constantes,” *Bulletin de la section des sciences du C.T.H.S* , 37–53 (1981).
- [23] F. Beukers, “A note on the irrationality of  $\zeta(2)$  and  $\zeta(3)$ ,” *Bull. London Math. Soc.* , 268–272 (1979).
- [24] W. Zudilin, “An elementary proof of Apéry’s theorem,” *Intern. J. Math. Computer Sci.* , 9–19 (2009).
- [25] T. Rivoal, “La fonction zêta de Riemann prend une infinité de valeurs irrationnelles aux entiers impairs,” *C. R. Acad. Sci. Paris* , 267–270 (2000).
- [26] W. Kohlen, “Transcendence conjectures about periods of modular forms and rational structures on spaces of modular forms,” *Proc. Indian Acad. Sci. - Math. Sci.* **99**, 231–233 (1989).
- [27] H E Boos, V E Korepin, Y Nishiyama, and M Shiroishi, “Quantum correlations and number

- theory,” *J. Phys. A: Math. Gen.* **35**, 4443 (2002).
- [28] A. A. Karatsuba and M. A. Korolev, “The argument of the Riemann zeta function,” *Russian Math. Surveys* **60**, 433–488 (2005).
- [29] E. Carneiro, V. Chandee, and M. B. Milinovich, “Bounding  $S(t)$  and  $S_1(t)$  on the Riemann hypothesis,” *Mathematische Annalen* **356**, 939–968 (2013).
- [30] D. A. Goldston and S. M. Gonek, “A note on  $S(t)$  and the zeros of the Riemann zeta-function,” *Bull. London Math. Soc.* **39**, 482–486 (2007).
- [31] A. Selberg, “Contributions to the theory of the Riemann zeta-function,” *Arch. Math. Naturvid.* **48**, 89–155 (1946).
- [32] A. Selberg, “Contributions to the theory of Dirichlet’s  $L$ -functions,” *Skr. Norske Vid. Akad. Oslo. I.* **1946**, 2–62 (1946).
- [33] A. Fujii, “On the zeros of Dirichlet  $L$ -functions. I,” *Transactions of the American Math. Soc.* **196**, 225–235 (1974).
- [34] H. Iwaniec, W. Luo, and P. Sarnak, “Low lying zeros of families of  $L$ -functions,” (1999), arXiv:math/9901141 [math.NT].
- [35] J. B. Conrey, “ $L$ -functions and random matrices,” in *Mathematics unlimited—2001 and beyond* (Springer, 2001) pp. 331–352.
- [36] C. P. Hughes and Z. Rudnick, “Linear statistics of low-lying zeros of  $L$ -functions,” *Quart. J. Math.* **54**, 309–333 (2003), arXiv:math/0208230v2 [math.NT].
- [37] J. B. Conrey, H. Iwaniec, and K. Soundararajan, “Critical zeros of Dirichlet  $L$ -functions,” (2011), arXiv:1105.1177 [math.NT].
- [38] E. Bombieri, “The Classical Theory of Zeta and  $L$ -Functions,” *Milan J. of Math.* **78**, 11–59 (2010).
- [39] H. Montgomery, “The pair correlation of zeros of the zeta function,” in *Analytic number theory, Proc. Sympos. Pure Math. XXIV* (Providence, R.I.: AMS, 1973) p. 181D193.
- [40] T. M. Apostol, *Modular Functions and Dirichlet Series in Number Theory* (Springer-Verlag, 1990).
- [41] R.M. Corless, G.H. Gonnet, D.E.G. Hare, D.J. Jeffrey, and D.E. Knuth, “On the Lambert  $W$  function,” *Adv. Comp. Math.* **5**, 329–359 (1996).
- [42] A. M. Odlyzko and A. Schönhage, “Fast algorithms for multiple evaluations of the Riemann zeta function,” *Trans. Amer. Math. Soc.* **309**, 797–809 (1988).
- [43] A. Odlyzko, “Tables of zeros of the riemann zeta function,” .
- [44] A. M. Odlyzko, “On the distribution of spacings between zeros of the zeta function,” *Math. Comp.* **48**, 273–308 (1987).
- [45] X. Gourdon, “The  $10^{13}$  first zeros of the Riemann Zeta function, and zeros computation at very large height,” (2004).
- [46] T. Oliveira e Silva, “Tables of zeros of the Riemann zeta function,” (2010).
- [47] F. J. Dyson, “Correlations between eigenvalues of a random matrix,” *Commun. Math. Phys.*

- 19**, 235–250 (1970).
- [48] T. Oliveira e Silva, “Tables of approximate values of the first zeros on the critical line of some primitive Dirichlet  $L$ -series,” (2007).
- [49] P. Francesco, P. Mathieu, and D. Senechal, *Conformal Field Theory* (Springer, 1999).
- [50] M. B. Green, J. H. Schwarz, and E. Witten, *Superstring Theory: Volume 1* (Cambridge University Press, 1988).
- [51] E. Bombieri and A. Ghosh, “Around the Davenport-Heilbronn function,” *Russian Math. Surveys* **66**, 221–270 (2011).
- [52] A. A. Karatsuba, “On the zeros of the Davenport-Heilbronn function lying on the critical line,” *Math. USSR Izv.* **36**, 311–324 (1991).